

Removal of ferrous and arsenic from contaminated groundwater
by co-precipitation coupling with membrane separation process



A Thesis Submitted in Partial Fulfillment of the Requirements
for the Degree of Master of Engineering in Environmental Engineering
Department of Environmental Engineering
FACULTY OF ENGINEERING
Chulalongkorn University
Academic Year 2021
Copyright of Chulalongkorn University

การกำจัดเฟอร์รัสและสารหนูออกจากน้ำใต้ดินปนเปื้อน โดยกระบวนการเมมเบรนร่วมกับกระบวนการ
ตกตะกอนร่วม



วิทยานิพนธ์นี้เป็นส่วนหนึ่งของการศึกษาตามหลักสูตรปริญญาวิศวกรรมศาสตรมหาบัณฑิต
สาขาวิชาวิศวกรรมสิ่งแวดล้อม ภาควิชาวิศวกรรมสิ่งแวดล้อม
คณะวิศวกรรมศาสตร์ จุฬาลงกรณ์มหาวิทยาลัย
ปีการศึกษา 2564
ลิขสิทธิ์ของจุฬาลงกรณ์มหาวิทยาลัย

Thesis Title	Removal of ferrous and arsenic from contaminated groundwater by co-precipitation coupling with membrane separation process
By	Miss Bonita Pen
Field of Study	Environmental Engineering
Thesis Advisor	Professor PISUT PAINMANAKUL, Ph.D.
Thesis Co Advisor	Pattarasiri Fagkaew

Accepted by the FACULTY OF ENGINEERING, Chulalongkorn University
in Partial Fulfillment of the Requirement for the Master of Engineering

----- Dean of the FACULTY OF
ENGINEERING
(SUPOT TEACHAVORASINSKUN)

THESIS COMMITTEE

----- Chairman
(MANASKORN RACHAKARAKIJ)
----- Thesis Advisor
(Professor PISUT PAINMANAKUL, Ph.D.)
----- Thesis Co-Advisor
(Pattarasiri Fagkaew)
----- Examiner
(KHEMARATH OSATHAPHAN)
----- External Examiner
(Marupatch Jamnongwong)

จุฬาลงกรณ์มหาวิทยาลัย
CHULALONGKORN UNIVERSITY

โบนิตา เพน : การกำจัดเฟอร์รัสและสารหนูออกจากน้ำใต้ดินปนเปื้อนโดยกระบวนการเมมเบรนร่วมกับกระบวนการตกตะกอนร่วม. (Removal of ferrous and arsenic from contaminated groundwater by co-precipitation coupling with membrane separation process) อ.ที่ปรึกษาหลัก : พิสุทธิ เพ็ชรมนกุล, อ.ที่ปรึกษาร่วม : ภรศิริ พักแก้ว

งานวิจัยนี้มีวัตถุประสงค์ในการบำบัดน้ำบาดาลที่ปนเปื้อนด้วยสารหนูและเฟอร์รัสสำหรับการบริโภคด้วยกระบวนการเมมเบรนร่วมกับกระบวนการตกตะกอนร่วมให้มีคุณภาพผ่านมาตรฐานตามคำแนะนำขององค์การอนามัยโลก โดยงานนี้แบ่งการศึกษาออกเป็นสี่ส่วน คือ (1) ศึกษาและเปรียบเทียบผลของชนิดของตัวกลางและเงื่อนไขการทดลองต่อค่าสัมประสิทธิ์การถ่ายเทออกซิเจน (KLa) และตัวแปรทางอุทกพลศาสตร์ของฟองอากาศ โดยชนิดของตัวกลางที่ทำการศึกษา ได้แก่ ฟองน้ำทำความสะอาด เส้นใยสังเคราะห์ทำความสะอาด วงแหวนพลาสติกและแอคติเวทาร์บอนโฟม (2) ศึกษาสภาวะที่เหมาะสมในการกำจัดเฟอร์รัสด้วยกระบวนการออกซิเดชัน โดยการประยุกต์ใช้การออกแบบการทดลองแบบพื้นผิวสะท้อนร่วมกับการทดลองแบบ Central Composite Design (RSM-CCD) (3) ศึกษาสภาวะที่เหมาะสมในการกำจัดสารหนู โดยกระบวนการตกตะกอนร่วมของเฟอร์ริก โดยการประยุกต์ใช้การออกแบบการทดลองแบบพื้นผิวสะท้อนร่วมกับการทดลองแบบ CCD และ (4) ศึกษาการบำบัดน้ำที่ผ่านกระบวนการในข้างต้นด้วยกระบวนการตกตะกอนและกระบวนการเมมเบรน จากผลการวิจัยพบว่าฟองน้ำทำความสะอาดมีประสิทธิภาพมากที่สุดสำหรับทำหน้าที่เป็นตัวกลางในการเพิ่มสัมประสิทธิ์การถ่ายเทออกซิเจนสูงถึงร้อยละ 9 – 80 โดยผลกระทบของความเร็วฟองอากาศที่เพิ่มขึ้นไม่ส่งผลต่อการแตกตัวของฟองอากาศ สำหรับสภาวะที่เหมาะสมในการกำจัดเหล็กจากการออกแบบการทดลอง คือ อัตราการไหลของอากาศเท่ากับ 14 ลิตร/นาที พีเอชเริ่มต้นเท่ากับ 8 ความเข้มข้นเริ่มต้นของเฟอร์รัสเท่ากับ 5 มก./ลิตร ความเข้มข้นของเฟอร์ริก เท่ากับ 25 มก./ลิตร และเวลาในการบำบัดเท่ากับ 25 นาที ส่วนสภาวะที่เหมาะสมในการกำจัดสารหนูจากการออกแบบการทดลอง คือ อัตราการไหลของอากาศเท่ากับ 8 ลิตร/นาที พีเอชเริ่มต้นเท่ากับ 8, ความเข้มข้นเริ่มต้นของเฟอร์รัสเท่ากับ 36 มก./ลิตร, ความเข้มข้นของเฟอร์ริกเท่ากับ 25 มก./ลิตร และเวลาในการบำบัดเท่ากับ 33 นาที นอกจากนี้ยังพบว่ากระบวนการตกตะกอนไม่สามารถบำบัดน้ำให้ผ่านมาตรฐานที่กำหนดไว้ได้ จึงจำเป็นต้องมีการประยุกต์ใช้กระบวนการเมมเบรนร่วมด้วย โดยการบำบัดน้ำที่ผ่านกระบวนการตกตะกอนร่วมด้วยกระบวนการเมมเบรน พบว่าสามารถกำจัดตะกอนของสารหนูและเหล็ก ทำให้ได้น้ำบาดาลที่มีความใสและมีคุณภาพดี ดังนั้นกระบวนการเมมเบรนร่วมกับกระบวนการตกตะกอนร่วมจึงเป็นทางเลือกหนึ่งที่น่าสนใจในการบำบัดน้ำบาดาลที่ปนเปื้อนด้วยสารหนูและเฟอร์รัสสำหรับการบริโภค

จุฬาลงกรณ์มหาวิทยาลัย
CHULALONGKORN UNIVERSITY

สาขาวิชา วิศวกรรมสิ่งแวดล้อม
ปีการศึกษา 2564

ลายมือชื่อนิสิต
ลายมือชื่อ อ.ที่ปรึกษาหลัก
ลายมือชื่อ อ.ที่ปรึกษาร่วม

6272049021 : MAJOR ENVIRONMENTAL ENGINEERING

KEYWOR Arsenic, Ferrous iron, Oxygen mass transfer, Design of Experiment,
D: Co-precipitation, Membrane filtration, Solid media

Bonita Pen : Removal of ferrous and arsenic from contaminated groundwater by co-precipitation coupling with membrane separation process. Advisor: Prof. PISUT PAINMANAKUL, Ph.D. Co-advisor: Pattarasiri Fagkaew

This work aimed to treat contaminated groundwater with arsenic and ferrous iron pollutants to be drinking water standard following by WHO by co-precipitation process and membrane separation process. The relative effect of different solid media types (scouring sponge, scouring pad, plastic ring, and activated carbon foam) and operating conditions on oxygen mass transfer coefficient (K_{La}) and hydrodynamic bubble parameters was studied. The optimization process of ferrous oxidation and arsenic removal was observed by Design of Experiment (DOE) with Central Composition Design of Response Surface Methodology (CCD-RSM). Lastly, separation process was experimented with conventional process and membrane technology, i.e., settling process, different effect of scouring sponge loading on turbidity removal, and impact of settling process on ultra-filtration membrane fouling. The result showed that scouring sponge was the most effective solid media to enhance volumetric oxygen transfer coefficient around 9-80% by impact of bubble rising velocity not breaking up bubble mechanism. The maximum removal of ferrous by optimization process was $Q_g = 14$ LPM, initial pH=8, initial $[Fe^{2+}] = 5$ mg/L, adding $[Fe^{3+}] = 25$ mg/L and operating time 25 min. However, for arsenic removal with co-precipitation process, the optimization process found under condition $Q_g = 8$, initial pH=8, initial $[Fe^{2+}] = 36$ mg/L, adding $[Fe^{3+}] = 25$ mg/L and operating time 33 min. Furthermore, initial pH and ferrous initial concentration was defined as the most significant factor. In separation process, the removal of turbidity by settling process was remaining around 60NTU while the highest scouring sponge loading (10%) was able to remove turbidity around 15% (not pass WHO standard). Finally, ultra-filtration was used to get complete clear and clean drinking water. The result showed that the performance of settling process before membrane filtration could reduce the membrane fouling mechanism. Thus, the combination of settling process and membrane technology could provide more benefits.

Field of Study: Environmental
Engineering

Academic 2021
Year:

Student's Signature

.....

Advisor's Signature

.....

Co-advisor's Signature

.....

ACKNOWLEDGEMENTS

First, I would like to express my gratitude to Prof. Pisut Painmanakul, my adviser, who instructed, encouraged, and supported me throughout the project. I am thankful to Dr. Pattarasiri Fagkaew, my co-advisor, for taking care, correcting, and suggesting me along this hard path. I would like to show my thankfulness to thesis committees: Asst.Prof. Manaskorn Rachakornkij, PhD, Assoc.Prof. Khemarath Osathapha, PhD, and Asst. Prof. Marupath Jamnongwong, PhD, for their insightful comments on this work. I would like to extend my thanks to all the lecturers, department staff, and colleagues in the Department of Environmental Engineering who contributed expertise and laboratory facilities to this project. I want to acknowledge ASEAN and Non-ASEAN scholarships for great opportunity of this scholarship. My deepest gratitude also goes out to my seniors, Dr. Saret Bun, Mr. Phaly Ham, and Ms. Theary Peng and other seniors, for all their kindness, teaching, counseling, advice, and motivation throughout this research. Finally, I would to convey my deep appreciation to my loving family and friends for their love, inspiration, and care.

Bonita Pen

TABLE OF CONTENTS

	Page
ABSTRACT (THAI)	iii
ABSTRACT (ENGLISH).....	iv
ACKNOWLEDGEMENTS	v
TABLE OF CONTENTS.....	vi
LIST OF TABLES	xi
LIST OF FIGURES	xiii
CHAPTER 1 INTRODUCTION	16
1.1 Background.....	16
1.2 Objectives	22
1.3 Scope of study.....	22
1.4 Hypotheses.....	23
1.5 Results Expectation	23
CHAPTER 2 THEORY AND LITERATURE REVIEW	24
2.1 Groundwater in Cambodia.....	24
2.1.1 Groundwater consumption	25
2.1.2 Groundwater quality.....	26
2.2 Iron in groundwater	28
2.2.1 Chemical Property	30
2.2.2 The Solubility and Precipitation.....	31
2.3 Arsenic in groundwater.....	32
2.3.1 Chemical Property	33
2.3.2 Chemistry of precipitation of ferric iron and arsenate.....	36
2.4 Iron treatment method.....	37
2.4.1 Oxidation Process.....	37
2.4.2 Electrocoagulation (EC) method	40

2.4.3 Ion Exchange Process.....	41
2.4.4 Membrane Filtration Process.....	42
2.5 Arsenic treatment method.....	43
2.5.1 Oxidation Process.....	43
2.5.2 Precipitation Process	44
2.5.3 Membrane process.....	45
2.6 Aeration Process	45
2.6.1 Dissolved Oxygen in Water	46
2.6.2 Gas-liquid Transfer.....	47
2.6.3 Oxygen Transfer Rate	49
2.7 Membrane technology	53
2.7.1 Membrane permeability	54
2.7.2 Membrane fouling	55
2.7.3 Membrane cleaning process.....	55
2.8 Design of Experiment (DOE).....	57
2.8.1 Concept of DOE	58
2.8.2 Response surface methodology	58
(A) Central composite design.....	60
(B) Box-Behnken design.....	60
CHAPTER 3 METHODOLOGY.....	61
3.1 Study Overview	61
3.2 Experimental set-up	63
3.2.1 Bubble column reactor (BCR).....	63
3.2.2 Membrane Filtration.....	64
3.3 Chemical reagents and equipment	64
3.3.1 Equipment	64
3.3.2 Chemical reagents	65
3.4 Experimental procedures	66
3.4.1 Groundwater synthesis	67

3.4.2 Effect of solid media addition on mass transfer rate in BCR.....	68
(A) Without solid media addition.....	68
(B) With solid media addition.....	68
3.4.3 Optimization of Ferrous oxidation process	71
3.4.4 Optimization of arsenic and iron removal in co-precipitation process	72
3.4.5 Separation process	74
(A) Settling Process.....	74
(B) Membrane filtration	74
3.5 Analytical Parameters and Method.....	75
3.5.1 Dissolved oxygen concentration	75
3.5.2 Overall volumetric mass transfer coefficient (K_{La})	76
3.5.3 Ferrous ion concentration.....	77
3.5.4 Arsenic concentration.....	78
3.5.5 Removal efficiency.....	78
3.5.6 Membrane permeability	79
3.6 Design of Experiment (DOE)	79
CHAPTER 4 RESULTS AND DISCUSSIONS	82
4.1 Effect of adding solid media on mass transfer rate.....	83
4.1.1 Mass transfer coefficient (K_{La}).....	83
(A) Effect of gas velocity	83
(B) Effect of solid media loading	84
4.1.2 Bubble dynamics	86
(A) Bubble diameter (D_B).....	86
(B) Bubble rising velocity (U_B).....	87
(C) Interfacial area (a)	88
4.1.3 Physical mechanism of solid media	89
4.1.4 Summary	91
4.2 Optimization of process condition for ferrous oxidation.....	92
4.2.1 Experimental design by CCD-RSM	92

4.2.2 Experimental result.....	94
4.2.3 Empirical Model for ferrous oxidation.....	95
4.2.4 Factorial analysis.....	99
4.2.5 Process optimization.....	101
(A) Effect of initial pH.....	101
(B) Effect of ferrous initial concentration.....	103
4.2.6 Summary of prediction and experimental equation.....	104
4.3 Optimization of process condition for arsenic removal.....	104
4.3.1 Experimental Design by CCD-RSD.....	105
4.3.2 Experimental Result.....	106
4.3.3 Empirical model for arsenic removal.....	107
4.3.4 Factorial Analysis.....	111
4.3.5 Process Optimization.....	112
(A) Effect of initial pH.....	113
(B) Effect of initial ferrous concentration.....	114
(C) Effect of initial pH and ferrous initial concentration.....	115
(D) Effect of other factors.....	116
4.3.6 Summary of optimum level.....	117
4.4 Separation process.....	119
4.4.1 Settling process.....	119
4.4.2 Solid Media effect on suspended particles.....	120
4.4.3 Membrane filtration.....	122
4.4.4 Summary work.....	124
CHAPTER 5 CONCLUSION AND RECOMMENDATION.....	129
5.1 Conclusion.....	129
5.2 Recommendation.....	130
REFERENCES.....	132
APPENDIXES.....	139
VITA.....	147



จุฬาลงกรณ์มหาวิทยาลัย
CHULALONGKORN UNIVERSITY

LIST OF TABLES

	Page
Table 2.1 Groundwater Quality in Cambodia.....	26
Table 2.2 Summary groundwater quality in Kandal province, Cambodia from different sources.....	27
Table 2.3 The drinking water standard from WHO, Cambodia, and Maximum real concentration in groundwater	28
Table 2.4 Identity and physicochemical properties of selected arsenic species identifies in water (Nielsen and Larsen, 2014).....	34
Table 2.5 Chemical oxidants for iron oxidation	37
Table 2.6 Water quality and DO content in ppm at 20°C (Bun, 2015).....	46
Table 2.7 The characteristic of application of membrane processes (Pangarkar, Sane, and Guddad, 2011).....	53
Table 2.8 Effects of operating strategies on membrane fouling.....	56
Table 3.1 Term condition of solid media study	70
Table 3.2 The details of physical properties and characteristics of solid media (Sastaravet et al., 2020).....	70
Table 3.3 The influent parameters on ferrous oxidation.....	71
Table 3.4 Condition of each parameter for arsenic removal experiment.....	73
Table 3.5 Condition of membrane filtration for suspended solids removal	75
Table 3.6 Factors designed and its levels for optimizing ferrous oxidation process ...	80
Table 3.7 Factors designed and its levels for optimizing arsenic and iron removal in co-precipitation process	80
Table 4.1 Investigated factors and factor levels for optimization ferrous oxidation ...	92
Table 4.2 Experimental design by CCD-RSM for factors optimization.....	93
Table 4.3 Experiment results	95
Table 4.4 ANOVA results of the input factors for the ferrous removal efficiency	97
Table 4.5 Prediction Vs Experiment of ferrous oxidation removal (%).....	99
Table 4.6 Variation of three factor levels of each impact parameter.....	105

Table 4.7 Experimental conditions for optimization influent factor.....	105
Table 4.8 Experimental results of ferrous iron and arsenic removal conditions	107
Table 4.9 ANOVA results of the input factors for the arsenic removal efficiency ...	109
Table 4.10 Prediction Vs Experiment of arsenic removal (%)	111
Table 4.11 Summary of factor levels studied and optimum conditions	118
Table 4.12 Turbidity of treated groundwater with various scouring sponge loading	121



LIST OF FIGURES

	Page
Figure 1.1 Distribution of low (<10µg/L As), medium (10-50 µg/L As) and high (>50 µg/L As) arsenic wells from four communes in the Kean Svay District, Kandal Province, Cambodia.....	18
Figure 2.1 The water supply source for drinking water in the dry season, Cambodia	25
Figure 2.2 The percentage of consumption tube well in the dry season, Cambodia ...	25
Figure 2.3 The concentration of iron in groundwater in Kandal Map (CDIC, 2012)..	30
Figure 2.4 Stability and predomination of As species in the water as a function of pH (Rajaković and Mitrović, 1992).....	35
Figure 2.5 Iron forms in water as functions of EH vs. pH (Crittenden et al., 2012) ...	39
Figure 2.6 Equilibrium condition of component A in air-water (Edzwald and Association, 2011)	47
Figure 2.7 Mass transfer for (a) stripping and (b) absorption by using two-film theory (Crittenden et al., 2012)	49
Figure 2.8 Schematic description of the dynamic technique desorption–absorption of oxygen for inert condition measurements (Garcia-Ochoa and Gomez, 2009).	52
Figure 2.9 General model of a process or system (Montgomery, 2017)	58
Figure 2.10 Contour plot of a response surface (Montgomery, 2017).....	59
Figure 2.11 Central composite designs for (a) k=2 and (b) k=3 (Montgomery, 2017)	60
Figure 2.12 A Box-Behnken design for three factors (Montgomery, 2017)	60
Figure 3.1 The framework of study overview of the research study	62
Figure 3.2 Experimental set-up of bubble column reactor (BCR).....	63
Figure 3.3 Schematic diagram of membrane experimental set-up	64
Figure 3.4 The overall flowchart of experimental procedures.....	67
Figure 3.5 Process of oxidation and K _{La} coefficient obtaining (Bun, 2015).....	77
Figure 4.1 Effect of various ranges gas velocity (V _g) on overall mass transfer coefficient (K _{La}) of each solid media types	84
Figure 4.2 Impact of solid media loading on K _{La} coefficient with gas velocity 0.70 × 10 ⁻² m.s ⁻¹	85

Figure 4.3 Effect of different solid media types on mean bubble diameter by varying V_g	87
Figure 4.4 Effect of solid media types on bubble rising velocity by varying V_g	88
Figure 4.5 Picture of each solid media performance with $V_g 0.3 \times 10^{-2} \text{ m.s}^{-1}$	88
Figure 4.6 Interfacial area of each solid media by variation V_g	89
Figure 4.7 Contact angle of solid media.....	91
Figure 4.8 Microbubbles holding inside scouring sponge.....	91
Figure 4.9 Experimental and predicted (full) ferrous removal (%).....	96
Figure 4.10 Experimental and predicted (short) ferrous removal (%).....	98
Figure 4.11 Main effects plot for Ferrous iron removal.....	100
Figure 4.12 Contour plot for Ferrous iron removal.....	100
Figure 4.13 Boxplot of initial pH effect on ferrous iron removal.....	101
Figure 4.14 Boxplot the comparison between initial pH and final pH of ferrous oxidation performance.....	102
Figure 4.15 Boxplot of a relative effect of ferrous initial concentration on ferrous iron removal efficiency.....	103
Figure 4.16 Scatter plot the relative effect of initial pH and initial ferrous concentration on ferrous iron removal efficiency.....	104
Figure 4.17 Experimental and predicted (full) ferrous removal (%).....	109
Figure 4.18 Experimental and predicted (short) ferrous removal (%).....	110
Figure 4.19 Main effect plot of arsenic removal.....	112
Figure 4.20 Contour plot for Arsenic removal.....	112
Figure 4.21 Boxplot of initial pH effect on arsenic removal efficiency.....	113
Figure 4.22 Boxplot of ferrous initial concentration effect on arsenic removal efficiency.....	115
Figure 4.23 Scatter plot of relative effect of initial pH and ferrous initial concentration on arsenic removal efficiency.....	116
Figure 4.24 Optimization plot of each variable to maximize ferrous iron and arsenic removal.....	118
Figure 4.25 Faction removal of insoluble ferric iron with overflow rate in BCR.....	120
Figure 4.26 Effect of solid media adding on turbidity removal.....	122

Figure 4.27 Scouring sponge before process in treatment (a), scouring sponge after process in treatment (b)..... 122

Figure 4.28 Water flux in comparison of tap water, raw groundwater, before settling process and after settling process..... 124

Figure 4.29 Images of filtered membrane sheet in different condition operation 124

Figure 4.30 Performance of adding solid media to increase oxygen mass transfer in BCR..... 126

Figure 4.31 Performance of combination process of aeration process, sedimentation process and membrane filtration process 128



CHAPTER 1

INTRODUCTION

1.1 Background

In the globe, groundwater is considered a significant freshwater source because of the largest storage layer. The total volume of surface water has 3% of all water on the earth, yet there is only 1% that can be counted as available usage besides groundwater (Zainab et al., 2020). A tiny fraction of this surface water can be found in streams, lakes, rivers, or reservoirs. Surface water is regularly restored through the precipitation process and lost again by the evaporation process and infiltration into groundwater. With the continuous growth of population, industrialization, and urbanization activities; the good quality water demand has raised. In addition, the available surface water source has been issued via the human activities and natural disaster, especially discharging wastewater or/and solid waste from factories, households, commercial areas and farms into water sources. Therefore, the effect of water quality is suffering. Also, one of the largest challenges of this century is to be able to afford safe drinking water and water supplement for life to the 7.8 billion people in the world (Shaji et al., 2021).

Groundwater is the most vital source and the main natural resources which provides almost half of the global people's needs. The volume of extracted groundwater is around 982 km³ annually to support many sectors (Margat and Van der Gun, 2013). About 38% of universal irrigation water consumption, 36% domestic and 27% industrial are supplied by groundwater (Dangar, Asoka, and Mishra, 2021). Groundwater is being used mainly in many parts of the world due to the updating and cheaper pumping and drilling technologies, the number of underground extractions is growing enormously (Shaji et al., 2021). Groundwater is not only a source of water to fulfill human needs but also providing many various services and multiple functions (van der Gun, 2021). However, the increasing of dealing with groundwater quality problems has been attended in the 21st century. The various types of rock layer, the interaction between rock and water duration, and the contribution of different natural and nonnatural sources can significantly affect the groundwater chemical

composition. Groundwater pollution is being recorded from the chemical contamination by aquifers throughout the world. According to the World Health Organization (WHO), potable water standard and groundwater contamination during this last decade exceeds the constituent limits and becomes non-potable (Shaji et al., 2021).

In Cambodia, groundwater is becoming an essential source of drinking water and irrigation supplement (Sthiannopkao et al., 2010). There is half of Cambodia population who relies on the groundwater resources while surface water cannot afford in the dry season. In some areas of the country where are not near the water surface or water source, groundwater has been importantly supplied for their domestic, irrigation systems and industrial sectors. Nonetheless, the groundwater contaminated with pollutants is frequently defined with the distinct well depth. Arsenic is a well-known of groundwater pollutant in Cambodia (Sampson et al., 2008). Indeed, arsenic contaminant is occurring in rocks and soil, water, air, and plants and animals and the most accepted explanation is that the arsenic is “bound” to iron containing minerals buried in the fine-grained sediments becomes anoxic (contains no dissolved oxygen) then the iron minerals dissolve and release arsenic. Arsenic contamination in groundwater originates from several natural and anthropogenic sources which are deemed responsible. However, in the arsenic impacted area, high concentration of arsenic is found in deeper tube wells as opposed to shallower dug wells (Ratha et al.). Figure 1.1 is indicated the distribution of arsenic level with the well depth in Kandal province, Cambodia (Sampson et al., 2008). Normally, the tube-well are mostly impacted by high contaminated arsenic concentration since the water are pumped directly form the buried aquifers to the surface. In constrast, shallow wells are not less contaminated with arsenic due to its depth, not enough to reach the arsenic contaminated aquifers or because of a large reservoir of oxygenated water in which dissolved arsenic is precipitated from the water before consumption (Ratha et al.).

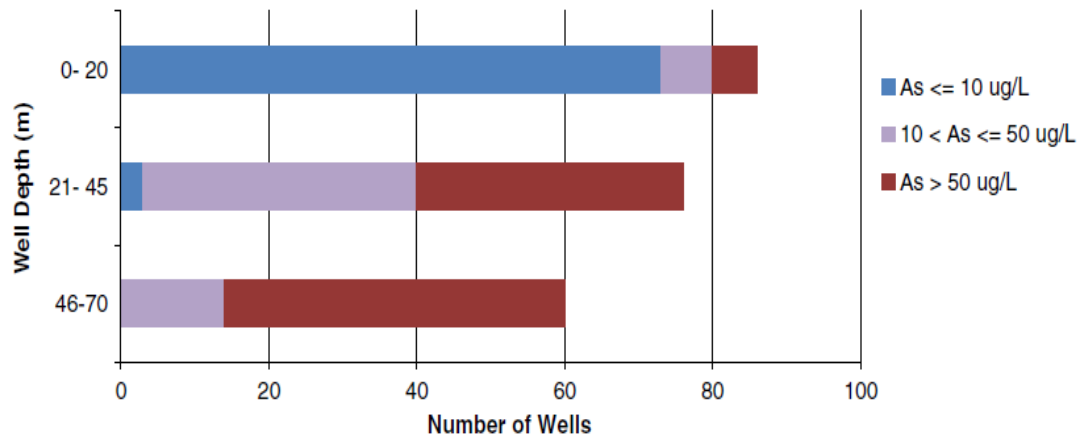


Figure 1.1 Distribution of low (<10 μ g/L As), medium (10-50 μ g/L As) and high (>50 μ g/L As) arsenic wells from four communes in the Kean Svay District, Kandal Province, Cambodia.

Two types of extraction water can be seen in Cambodia such as tube wells with 15-100m depth and dug well with 3-15m depth. The number of groundwater, being risen to 270 000 tube wells in recently, and consumed for livelihoods, domestic, industrial, irrigation and plant. With these amounts of needed groundwater, the risk of water quality is being taken as serious issues. Furthermore, the study is processing to prevent the human health problems, and ensure safety consumption (ODC, 2016).

In the recent years, arsenic contamination has been a major source of groundwater pollution as the reason of health effects (Shaji et al., 2021). Not only arsenic contamination is being concerned but also several dissolved minerals are being problemed in groundwater including iron, manganese, fluoride, and salinity. Among these pollutants, arsenic and ferrous iron are considered as the top of critical toxicity chemical in tube well in Cambodia (Guppy and Shantz, 2011). Since groundwater is also one of main water resource; therefore, groundwater contamination has taken an attention around the world as serious issue, especially, in Southeast Asia countries. There are around 94 to 220 million population who are consuming arsenic contaminated in groundwater for drinking water and water supplement, and 94% of them are from Asia (Timalsina et al., 2021). The observation of occurring arsenic contaminated in tube well/hand pump drinking water has been demonstrated in Cambodia, Thailand, Vietnam, Myanmar, India, Loa, Nepal, Pakistan, and Bangladesh (Cho et al., 2011). Actually, there are more 100 000 residents who are

accessing high dangers of chronic arsenic in Kandal province, Cambodia (Guppy and Shantz, 2011).

In general, arsenic exists in four distinct oxidation states (+V, +III, 0, and -III), yet it commonly presents in groundwater pH from 6.5-8.5 as the inorganic forms of arsenite (As(III)) and arsenate (As(V)). Moreover, the inorganic form of arsenic is more toxic than the organic form. Arsenic occurs in oxidizing conditions as well as reducing conditions (Timalsina et al., 2021). Drinking contaminated water with arsenic for a long time can cause chronic diseases, and the symptom of exposure depends on the minimum or maximum of consumed arsenic concentration in our body. The different stages of arsenicosis are recognized through keratosis, skin pigmentation, skin cancer, lung effect, bladder cancer, and the problem of cardiovascular and nervous system. In the developed countries, the World Health Organisation (WHO) has recommended arsenic concentration standard in drinking water is less than 10 µg/L while in developing nations WHO allows reaching the standard up to 50 µg/L in arsenic-affected areas (Berg et al., 2007). Besides arsenic, iron is also identified as one more interesting pollutant in tube well because of its solubility and undesirable appearance in the natural water system.

Iron is known as one of the important minerals in our body with a limited concentration by WHO. World Health Organization has approved a standard of iron concentration in drinking water and water supplies with a value of 0.3mg/L to avoid the negative impact on human health as hemochromatosis diseases (Tang et al., 2021) (S. Chaturvedi and P. N. Dave, 2012). The presence of iron in groundwater is considered an unpleasant component (Karakochuk et al., 2015). Iron, a problematic component in water sources, gives water a metallic flavor, odor, stains the product of food industry product, blocks the pipes, and allows water to turn a reddish color (Du et al., 2020). In groundwater, iron usually appears as ferrous iron (Fe^{2+}) in soluble form and ferric iron (Fe^{3+}) in complexed form or bacterial form. Furthermore, some bacteria use dissolved iron and easily growth in the water supply system including clogging the pipe, water pump, and water tank and reducing water flow rate which enhances pressure drop in the system. This problem is caused by gene enhancement of iron absorption; hemosiderosis is characterized by a high amount of hemosiderin

protein which stores in the liver and other tissues. However, intaking iron could provide a positive influence to human health, if only 1 to 2 mg of iron in water is consumed as the daily nutrition (S. Chaturvedi and P. N. Dave, 2012). Thus, controlling the moderate concentration of iron is significant for drinking water and water supplies.

Various technologies have been developed to solve arsenic and iron problems in groundwater such as chemical oxidation, aeration process, adsorption process, reverse osmosis, co-precipitation, and membrane-based filtration (Haldar, Duarah, and Purkait, 2020). Among these available technologies, co-precipitation of As with Fe oxides has been increasing the interest because the precipitate form of Fe can adsorb the As by their specific surface areas, and sufficient adsorption sites. If there is insufficient Fe in the water for As coprecipitation, an adsorbent could be incorporated into the coprecipitation process so that Fe adsorption and/or surface precipitation is induced, which will promote As removal (Nur et al., 2019). However, the performance of co-precipitation process is more effective for arsenate (As^{5+}) removal than arsenite (As^{3+}) (Xiu et al., 2015). Therefore, aeration and oxidation process are required to transform iron and arsenic to insoluble form. The supplement of oxygen in water is vital for oxidizing a high concentration of soluble iron in water whereas arsenic will take several days to oxidize. In the previous research showed that iron is able to catalyze As(III) oxidation on the surface of ferrihydrite under aerobic condition (Ding et al., 2018). Thus, it means that the presence of iron in groundwater plays a major role to enhance arsenic removal efficiency. However, this influence could be impacted by various parameters including the initial concentration of ferrous iron and arsenic in groundwater, pH, the concentration of oxygen transfer in liquid, as well as the kind of reactor. The bubble column reactor (BCR) is the most famous reactor used for transferring oxygen gaseous to the liquid phase in the laboratory and industrial application of aeration process (Abufalgha et al., 2020). This reactor type is simple and convenient in the operation of arsenic and iron removal, as well as cleaning process. Even though BCR has shown good performance as a gas-liquid contactor, improving its oxygen transfer efficiency is still necessary. Furthermore, to get completely drinking water standard, membrane technology is commonly required for water treatment and widely performed in several countries. Membrane filtration

has four various types (microfiltration (MF), ultrafiltration, nanofiltration (Rahmanian et al.), and reverse osmosis (RO)), which can be classified by the difference filter pore size (Magara, Kunikane, and Itoh, 1998). Hence, this research aims to remove arsenic and ferrous iron from polluted groundwater to receive the drinking water quality by combination process of co-precipitation with membrane filtration process. The effect of initial arsenic and ferrous iron concentration and other related parameters will be studied to increase the oxidation rate of arsenic and ferrous. Moreover, the addition of solid plastic media into the BCR will be performed for increasing the mass transfer of oxygen gaseous to the liquid phase. Lastly, membrane filtration process is operated to obtain drinking water quality following the WHO standard.



1.2 Objectives

The main objective of this research is to treat contaminated groundwater with arsenic and ferrous iron pollutants to be drinking water with the quality following the regulation/recommendation from WHO by co-precipitation process and membrane separation process. To achieve this purpose, several sub-objectives are defined as below:

- To investigate the relative effect of different solid media types on oxygen mass transfer and bubble hydrodynamic characteristic, and its physical mechanism
- To investigate the effect of the initial concentration of ferrous iron, ferric iron addition, pH, and gas flow rate (Q_g) on ferrous iron-oxidizing
- To study the impact of the initial concentration of ferrous iron, ferric iron, and pH on arsenic treatment in the bubble column reactor (BCR)
- To perform the separation process by combination of sedimentation and membrane filtration to remove suspended solid particles from the co-precipitation process

1.3 Scope of study

Many scopes are specified to reach the objectives of this research:

- (1) The groundwater in this study will be synthesized by using ferrous iron and arsenite for representing the toxic contaminants commonly found in actual groundwater.
- (2) The enhancement of oxygen mass transfer rate will be studied by adding solid media in the bubble column reactor.
- (3) The influential parameters on the removal of arsenic and iron will be examined such as initial concentration of Fe^{2+} , Fe^{3+} , pH and Q_g .
- (4) The study will be conducted at room temperature in a batch-scale bubble column reactor.
- (5) The hollow-fiber membrane will be used to remove the suspended solid in groundwater to achieve the drinking water quality following the regulation/recommendation from WHO.

(6) The experiment will be processed in the laboratory of the Department of Environmental Engineering, Faculty of Engineering at Chulalongkorn University.

1.4 Hypotheses

- The foam sponge media added as a filter can increase the oxygen mass transfer rate in a liquid phase and can be used to remove the suspended solid particles from precipitation.
- The oxidation rate of ferrous iron in groundwater can be rapidly oxidized by improving the oxygen transfer rate in the gas-liquid contactor.
- The arsenic removal loading can be increased by increasing the initial concentration of ferrous iron in groundwater.

1.5 Results Expectation

The expected outcomes of this work are:

- Enhancement of oxygen mass transfer rate in bubble column reactor through applying solid media
- Optimal conditions for arsenic and ferrous iron removal from groundwater
- Obtaining drinkable groundwater after treatment by combined process of co-precipitation with membrane separation process

CHAPTER 2

THEORY AND LITERATURE REVIEW

2.1 Groundwater in Cambodia

During the dry season, groundwater is a critical supply of drinking water for Cambodia's 13 million-plus inhabitants. Groundwater is used for both community and town water supplies, especially for irrigation. Groundwater usage is still more common in rural regions and certain small towns. More than 81 percent of the population lives in rural areas, and about 60% of this group uses tube wells. In contrast, only 15% of the population in Phnom Penh city is supplied by a water pipe system.

There are 12,000 tube wells which recently were operated in seven provinces for utilization of irrigation in the lowland or cropping patterns (Vang et al., 2009). The total exploitation of groundwater in Cambodia is no available data, but around 270,000 tube wells are working for drinking water. Figure 2.1 is demonstrated the drinking water source in the dry season. Only 23% of surface water is supported for Cambodian households drink while groundwater source is used 53% in the dry season. Besides, the piped system and rainwater are supplied 14% and 1% for Cambodian households drink, respectively (Sophally, 2011).

Dry season Drinking Water Source Breakdown

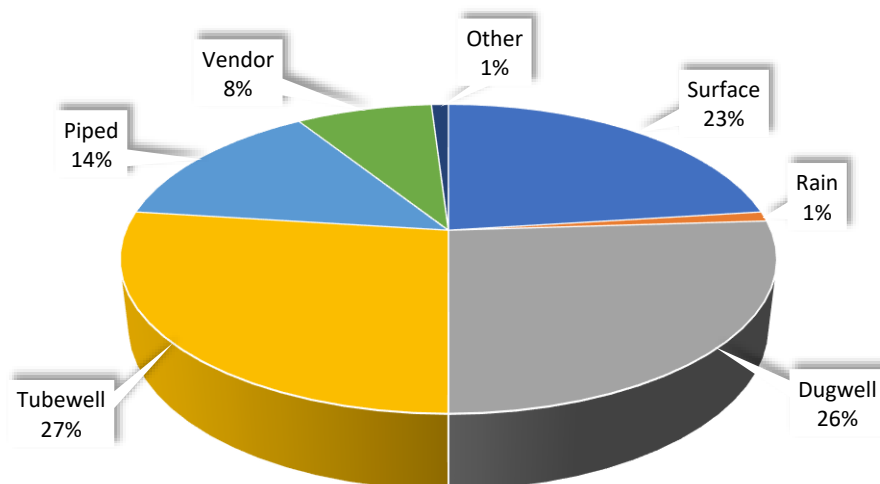


Figure 2.1 The water supply source for drinking water in the dry season, Cambodia

2.1.1 Groundwater consumption

Figure 2.2 shows the percentage of tube wells which have been used in the dry season. Two provinces, namely Prey Veng and Svay Rieng, the most consumed groundwater in the range of 50% to 100% (Sophally, 2011). However, tube well almost supplies in every province during the dry season.



Figure 2.2 The percentage of consumption tube well in the dry season, Cambodia

In Cambodia, tube well is largely used for domestic water supply, but recently is becoming more popular for small-scale irrigation. Small-scale pump irrigation from groundwater can help farmers to control the water supply and reliable manner. For the dry season, farmers prefer to install shallow dug and tube wells to produce dry season crops. Kampong Chhnang, Siem Reap, Battambang in the Tole Sap region; Prey Veng, Kampong Cham, Kandal, and Takeo provinces are well-known groundwater use for irrigation purpose. The growth of tube wells extraction is from 1600 in 1996 to 25,000 by 2005 in Prey Veng, and 90% of them are farmers. In addition, groundwater is also accessed for late wet season crops (rice crops). For irrigation, Mechanized and

treadle pumps are used, rather than hand pumps. On the other hand, shallow tube wells or hand-dug wells have been supported for around 53% of household's domestic water supply in the dry season. With a maximum water level depth of around 6m, tube wells are mostly taken out with simple suction hand pumps; however, mechanized pumps capable of pumping are required when the water table is lower than 6m. In Prey Veng and Svay Rieng, there are 91% of almost 145,000 tube wells are drained for domestic by hand pump. Indeed, groundwater is also supplied to urban by extracting deeper tube well with higher results. Currently, many industries, surrounding areas in Phnom Penh, drill wells for their water supply (IWMI, 2013).

2.1.2 Groundwater quality

In rural sites, groundwater normally was determined where irrigation and domestic used for the water resource. Even though groundwater is a necessary water resource in the dry season, low groundwater quality is troubling to the rural inhabitants' health (Tweed et al., 2020). Tube wells in Cambodia have been detected contaminants in groundwater such as arsenic, fluoride, nitrate, manganese, E.coli, total coliforms, male-specific coliphage, chloride, conductivity, iron, hardness, total dissolved, turbidity, pH (Bennett et al., 2010). Among these pollutants, arsenic is considered the most harmful element and is commonly found in groundwater in Cambodia. The analysis of groundwater quality indicates a negative impact on human health. Table 2.1 demonstrates the groundwater quality in Cambodia (RDI, 2008). The deep aquifer contains more toxic chemical than shallow aquifer; however, arsenic and iron contamination were considerable for these two well types.

Table 2.1 Groundwater Quality in Cambodia

Parameter	Units	Sample	Mean	Max	Min	CDWQS*	Exceeding (%)
Health-impacting							
Arsenic	µg/L	8488	28.28	1000	0	50	12.49
Fluoride	mg/L	8484	0.68	110	0	1.5	4.21
Nitrate	mg/L NO ₃	8486	7.96	1361	0	50	3.09

Manganese	mg/L	8486	0.37	28	0	0.4	19.48
Aesthetic-impacting							
Iron	mg/L	8485	3.43	100	0	0.3	76.51
Manganese	mg/L	8486	0.37	28	0	0.1	40.45
Turbidity	NTU	8488	26.18	2960	0	5	46.55
Chloride	mg/L	8487	107.63	2303	0	250	20.42
pH		8482	6.72	9.95	0	6.5-8.5	29.5
Hardness	mg/L CaCO ₃	8488	202.92	3186	0	300	21.05
Salinity	ppt	8473	0.32	19	0	N/A	N/A

*CDWQS: Cambodia Drinking Water Quality Standard

Source: RDI-Cambodia (2016)

Table 2.2 Summary groundwater quality in Kandal province, Cambodia from different sources

Parameter	Buschmann et al. (2008)	Luu et al. (2009)	et al. (CDIC, 2012)	YANN et al.(2020)	WHO (2008)
Arsenic (µg/L)	155	-	1000	50	10
Mn (mg/L)	0.6	-	28	0.1	0.4
Fe (mg/L)	2.2	0.07	100	0.3	0.3
pH	6.92	7.2	7-8	6.5-8.5	-
Total hardness (mg CaCO ₃ /L)	-	319.4	1440	300	-
DOC (mg/L)	3.1	4.998	-	-	-
TDS (mg/L)	-	325	-	-	1800
SO ₄ ²⁻ (m/L)	-	175.9	-	-	-
References	(Buschmann et al., 2008)	(Luu, Sthiannopkao, and Kim, 2009)	(CDIC, 2012)	(YANN, MIYANAG A, and TAN, 2020)	(WHO, 2008)

Table 2.3 The drinking water standard from WHO, Cambodia, and Maximum real concentration in groundwater

Parameters	WHO drinking water standard for develop countries	Cambodia drinking water standard	Maximum concentration in groundwater
Arsenic (µg/L)	10	50	1000
Mn (mg/L)	0.4	0.1	28
Fe (mg/L)	0.3	0.3	100
References	(WHO, 2008)	(YANN et al., 2020)	(CDIC, 2012)

2.2 Iron in groundwater

Iron is one of the most abundant elements on the global, a major public health problem, and an environmental pollutant. The dissolved iron in groundwater can be a huge environmental issue due to changing water characteristics. The presence of iron causes water to reddish color, unpleasant metallic taste, burden laundry machine, and high turbidity (El Azher et al., 2008); (Sharma et al., 2005). The ferrous (Fe^{2+}) and ferric (Fe^{3+}) iron are the oxidation states of iron in natural water.

However, iron has several forms in groundwater depending on the characteristics of its chemical, minerals, and solubility. For mineral forms, the classification of iron is divided into four different types expressly, silicates, oxides, sulfides, and carbonates. Furthermore, the difference of each category is broken down as silicates into pyroxene, biotite, amphiboles, and olivine; oxides to magnetite, hematite, and limonite; carbonate into pyrite, siderite, and sulphides. Generally, iron forms are commonly found in two forms in groundwater namely, soluble forms (Fe^{2+}) and insoluble forms (Fe^{3+}). Wherefore, the pH value in groundwater plays a vital role in iron forms. At pH lower than 6 iron commonly exists as ferrous hydroxide ($\text{Fe}(\text{OH})_2$) whereas ferric hydroxide ($\text{Fe}(\text{OH})_3$) occurs as at a pH higher than 6. A variety of anthropogenic processes, such as the construction of hazardous waste generated from

the mining, iron, and steel industry, resulting in the production of high levels of iron in water sources. But on the other hand, the contamination of iron in surface water has been caused via natural activities including rain passing soil, minerals, and rocks. Hence, many distinct processes of natural and anthropogenic activities lead to contaminate iron in groundwater and surface sources. The major occurrence of iron in groundwater is principally detected because of drainage of rainwater migrated through iron in rocks and minerals being in soil. Recently, the concern of disclosure on human health by consumption of iron contaminated water is deliberated since a safe iron concentration in drinking water-limited via WHO standard with 0.3 mg/L, which is appropriated to aesthetic effects, as Cambodia Water Drinking Standard (MoIMAE, 2004). Several symptoms such as feeling exhausted, knee pain, conjunctivitis, and retinitis pigmentosa are noticed by the impact of high iron concentration. Furthermore, some bacteria use iron as a substrate for their living and growth, which can clog in the pipelines and broken instruments (Haldar et al., 2020). Groundwaters are moderately acidic and dissolved oxygen; as a result, ferrous iron is soluble in groundwater because it contacts with rocks or other minerals. Indeed, iron existence in drinking water might happen when water (with a high concentration of salinity) passes through the pipelines, then the metal pipes appear to be corrosive. Therefore, abundant iron in the world is a major issue for a scientist to figure out with new technologies to prevent water pollution (El Azher et al., 2008).

In Cambodia, Iron concentration is commonly found in rang 0.07 to 100 mg/L (Table 2.2) in Kandal province. Moreover, there also have research is conducted to work on iron concentration in groundwater assessment maps in Cambodia. In the map, iron concentration is exceeded 10 mg/L in Kandal province which is demonstrated in Figure 2.3 (CDIC, 2012).

appears as soluble form as ferrous iron. The pH values increase due to ferrous precipitate to insoluble iron after releases carbon dioxide (CO₂) into the atmosphere.

The particle size of precipitated iron which has a pore size higher than 0.45 μm, is identified as an insoluble iron form. Iron has a major role in natural contaminant mobility, breakdown, and sorption because the iron in the environment plays an electron donor during the oxidation state. Moreover, its different forms respond as sorbent substrate or a precipitant. Surface adsorbed metals and radionuclides, as well as co-precipitated metals and radionuclides, can be absorbed into the (Fe) oxide structure. In the range of contaminants, non-oxide Fe such as sulphides, phosphates, and carbonates play as co-precipitants and sorbents too (Cundy, Hopkinson, and Whitby, 2008).

The various states of iron are classified depending on the mineral state, nature of the chemical, and its solubility. For the mineral form of iron, there are four different types including silicates, oxides, sulphides, and carbonates. For chemical nature form is mostly found as inorganic iron in groundwater with less dissolved oxygen concentration, which means iron has oxidized to insoluble form and produces turbidity in water. With this issue, the filtration process should be considered the best technology to treat it. However, the organic iron form represents the complicated form in groundwater and surface water. Furthermore, the solubility of iron raises in water because of the complex form combined with its organic compounds. Generally, the complex form of iron is not easy for the oxidation process, and hard to remove via filtration. Thus, the coagulation process is needed before filtration process (Khatri, Tyagi, and Rawtani, 2017).

2.2.2 The Solubility and Precipitation

The solubility of iron can be defined as the kind of its forms which can be soluble or insoluble form in water. The pH and redox potential condition are also the factors to classify iron form. The ferrous iron (Fe²⁺) is a reduced form of ferric iron which is known as a soluble form in groundwater. This form does not affect water's physical appearance (no change in watercolor), but ferrous iron remains low in concentration with the presence of oxygen in the water. Meanwhile, ferric iron (Fe³⁺) occurs after

ferrous oxidizing in groundwater, and dissolved oxygen becomes lower and lower. The trivalent iron is an insoluble form of iron in water, and it changes the physics of water such as more suspended solids or cloudy, and brownish-red color. The oxidation of ferrous to ferric gets faster with increasing pH and dissolved oxygen in water (Khatri et al., 2017).

2.3 Arsenic in groundwater

In Cambodia, the evaluation of arsenic standard was firstly defined in 1999 while the Ministry of Rural Development cooperation with the World Health Organization prepared a program of country drinking water quality assessment. Several thousand tube wells were surveyed and classified arsenic levels in groundwater. As a result, many regions were being impacted by high arsenic-contaminated in drinking water (Sampson et al., 2008).

Arsenic (As) is distributed throughout the environment, importantly in air, water, soil earth crust, via many anthropogenic activities including the breakdown of minerals, ores, rocks; fossil fuels combustion, a natural disaster of volcanic emission, and the wastewater from industrial discharges (Nielsen and Larsen, 2014). Plus, the usage of fertilizer in fertile fields has been found to raise the arsenic concentration in the groundwater (Halдар et al., 2020). In the air, arsenic concentration ranks $3\text{mg}/\text{m}^3$ while it is around $10\mu\text{g}/\text{L}$ and $100\text{ mg}/\text{kg}$ in freshwater and soil, respectively (Nidheesh and Singh, 2017). In Cambodia, the poor quality of groundwaters with high arsenic-contaminated are mostly located along the rivers (the Mekong and Tonle Sap), southeast provinces, and industrial zones. The untreated industrial wastes and discharging to the environment is one of the main reasons for groundwater contamination. Even though the consumption of groundwater is less in small states, it seems to handle for agricultural irrigation and industrial supply in further. Around seven provinces area have 38% of tube wells that are polluted by arsenic above standard (50ppb).

Arsenic is increasingly recognized as a serious, worldwide public health concern. Arsenic has been known as the most toxic element in the periodic table and is normally defined in groundwater as a pollutant because of its carcinogen. Arsenic is

the main danger pollutant in groundwater. There are partially ten provinces that have been analyzed arsenic appearing in groundwater, and Kandal province is extremely impacted. According to estimates based on population and tube well quality data for Cambodia's Kandal Province, more than 100,000 inhabitants are at the top toxic of chronic arsenic hazard. In natural water, arsenic concentration is identified in various ranges from 0.5 $\mu\text{g/L}$ to upper than 5000 $\mu\text{g/L}$. The consumption of arsenic-contaminated in drinking water for the long term will affect to human health and result in arsenicosis, namely as skin cancers, skin disorders, diseases of the blood vessels of the legs and feet, internal cancer (kidney, lung, and bladder), high blood pressure, reproductive disorders, and diabetes. The standard arsenic concentration in Cambodia is only 50 $\mu\text{g/L}$, but some regions have levels as high as 3500 $\mu\text{g/L}$. In Cambodia, more work need to be done to accurately determine the scope of the As threat and its possible health repercussion. Arsenicosis is one of the most concerning because many people are expected to exposure health issues attributed to As. Consumption drinking water contaminated with arsenic can cause a chronic disease, minimal risk levels (MRLs) of arsenic is 0.0003 mg/kg/day , the threshold limit value(TLV) is 0.01 mg/m^3 average over an 8-hour work shift (C.-H. S. J. Chou, Holler, and De Rosa, 1998). Arsenicosis symptoms are usually thought to appear after 8–10 years of drinking water with high amounts of arsenic, but recent cases found in Cambodia have been reported after just 3 years of arsenic exposure (Sampson et al., 2008).

2.3.1 Chemical Property

Arsenic is a metalloid ground and has an atomic mass of 74.92 amu, an atomic number 33, and a density of 5.72 g/cm . There are different allotropes of arsenic form such as gray, black, and yellow; and the most popular form for industrial purposes is the grey form. In an environment, both forms of arsenic are commonly present, namely organic, and inorganic forms. Arsenic is a kind of insoluble element in the water and occurs in four oxidation states arsenide (As(+III)), metallic arsenic (As(0)), arsenite (As(III)), and arsenate (As(V)). Among these, arsenite and arsenate, inorganic form of arsenic, a common species in water sources (Nidheesh and Singh, 2017). Generally, the organic form of arsenic is less dangerous than inorganic form arsenic

such as arsenite (As(III)) and arsenate (As(V)). The trivalent inorganic species is more mobile in groundwater, more toxic than the pentavalent species from 25 to 60 times due to its carcinogenic and non-biodegradable nature (Shankar and Shanker, 2014). The stability of arsenite is mostly found in an anaerobic environment, in contrast; arsenate is steady in aerobic conditions. However, arsenite and arsenate have been analyzed in groundwater with both conditions of anaerobic and aerobic conditions. Table 2.4 is demonstrated the identity and physicochemical properties of arsenic and arsenic species identified in water (Nielsen and Larsen, 2014).

Table 2.4 Identity and physicochemical properties of selected arsenic species identifies in water (Nielsen and Larsen, 2014)

Species	CA S-no	Molecular formula	Molecular weight	Physical state	Melting point (°C)	Boiling point (°C)	Density (g/cm ³)	Water solubility
Arsenic	744	As	74.92	Silver	817	614	5.73	insoluble
	0-38-2			-gray or tin-white solid				
Inorganic arsenic, trivalent								
Arsenic trioxide	132	As ₂ O ₃	197.84	White	313	460	3.8	37 g/l at 20°C
	7-53-3			solid				
Sodium arsenite	778	NaAsO ₂	130.92	White	-	-	1.87	Freely soluble
	4-46-5			to gray-white solid				
Inorganic arsenic, pentavalent								
Arsenic acid (arsenate)	777	AsO(OH) ₃	141.94	White	35	Loses H ₂ O at 160	~ 2.2	302 g/L at 12.5°C
	8-39-4			solid				
Arsenic	130	As ₂ O ₅	229.84	White	~300	-	4.32	2300

pentoxid	3-			solid	(decom			g/L at
e	28-				poses)			20°C
	2							
	777							
Sodium	8-	Na ₂ HA		Color				1:3
arsenate	43-	sO ₂	185.91	-less	57	-	1.87	parts
	0			solid				

Normally, arsenic mainly presents as oxyanion in two states of oxidation (As(III) & As(V)) with natural pH in groundwater range of 6-9. The pH value is an influent factor dominant of arsenic form and its stability in groundwater. Generally, groundwater pH is in the range of 6.0 – 8.5. Figure 2.3 is illustrated the predominant As species depending on pH value (Rajaković and Mitrović, 1992). The oxidation-reduction condition with pH value in groundwater is determined by the arsenic species and valence (Halдар et al., 2020). In the anaerobic condition, arsenite forms are H_3AsO_3 , $H_2AsO_3^-$ and $HAsO_3^{2-}$, but in groundwater at neutral pH, As (III) appears as unchanged form H_3AsO_3 which has less ability in oxidation (Zhang et al., 2017). Nevertheless, As(V) is existed as $H_2AsO_4^-$ when the pH is in the range of 2-6.9, and form as $HAsO_4^{2-}$ with pH 6.9-11.8; which has a potential for oxidation (Tran, 2017a). In addition, the treatment method of As(III) is fancier than As(V) removal in groundwater. Therefore, the primary As (III) oxidizing is being interested to transform to As(V) species state.

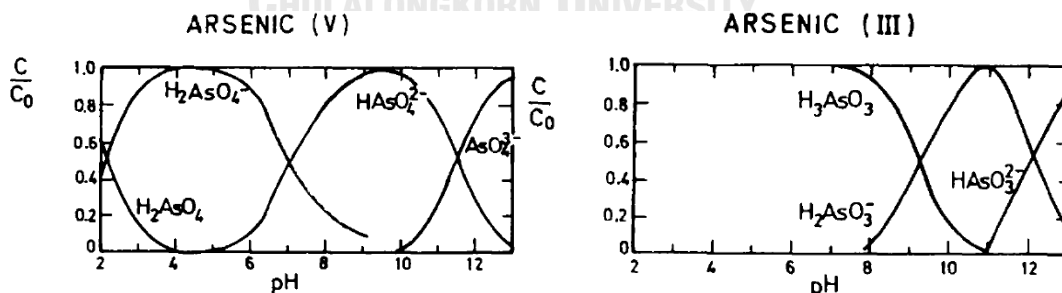


Figure 2.4 Stability and predomination of As species in the water as a function of pH (Rajaković and Mitrović, 1992)

2.3.2 Chemistry of precipitation of ferric iron and arsenate

In most natural waters, ferric iron (Fe(III)) and arsenate (As(V)) coexist. In addition, Fe(III) compounds are commonly employed to remediate As(V) in water. In most natural waters, ferric iron (Fe(III)) and arsenate (As(V)) coexist. In addition, Fe(III) compounds are commonly employed to remediate As(V) in water. Changes in pH affect the development of Fe(III)-As(V) complexes. At acidic circumstances (pH 2), the soluble Fe(III)-As(V) complex formed with a Fe:As mole ratio of 1:1. Changes in pH affect the development of Fe(III)-As(V) complexes. At acidic circumstances (pH 2), the soluble Fe(III)-As(V) complex formed with a Fe:As mole ratio of 1:1. When the pH was raised to 2-5, Fe(III) and As(V) produced a precipitate instead of a soluble complex, resulting in Fe(III) solubility being decreased at pH 2-5. At pH > 5, the soluble Fe(III)-As(V) complex reappeared with a Fe:As mole ratio of 1:2. These soluble Fe(III)-As(V) complexes were found to be monodentate according to DFT calculations. The chloride was discovered to be coordinated with the Fe(III)-As(V) complexes, resulting in better thermodynamic stability. With an initial concentration of 0.1 M Fe(III), the presence of these soluble complexes improved the solubility of Fe(III) at neutral pH (total soluble Fe(III) increased to 0.73 mM (55 mg/L)) (Q. Shi et al., 2020).

Numerous investigations have supported the hypothesis that ferric oxides regulate As mobility, which has been linked to the development of surface complexes on iron (hydro)oxides or co-precipitates. The solubility of pure ferric oxides ranges from $10^{10.9}$ to $10^{-3.1}$ μM (less than $1\mu\text{g/L}$) Fe at neutral pH, while increase to 0.1-73 mg/L in the presence of As(V). Moreover, increasing the As/Fe ratio tends to enhance the Fe solubility of Fe-As precipitate. The definition of “soluble” is the species after filtration using a $0.02\mu\text{m}$ pore size filter. The soluble Fe decreases at $\text{pH} > 1.5$ because of the formation of the iron oxides, but in the presence of As(V), the soluble Fe significantly decreased at pH 2-5 and increased at $\text{pH} > 5$. Moreover, a different kinetic behavior might result from the rapid formation of solid ferric arsenate ($\text{FeAsO}_4 \cdot 2\text{H}_2\text{O}$) at acidic conditions ($\text{pH} < 5$) and the slow formation of hematite (Q. Shi et al., 2020).

2.4 Iron treatment method

Due to taste and annoyance issues, the World Health Organization (WHO) recommends that the iron concentration in drinking water be less than 0.3 mg/l. The consuming drinking water iron contaminated is considered to a health risk. In Cambodia groundwater always detects the presence of iron. Therefore, there are a lot of projects have been studied to deal with this issue.

For iron treatment from groundwater, many techniques have been used, including ion exchange, oxidation with precipitation and filtration process, adsorption process (lime softening), and membrane processes. With these methods, aeration or chemical oxidation is the most practiced pre-treatment method, and it is more effective following the filtration process. The aeration process is commonly used even in rich countries and poor countries because it costs less, convenient, and no chemical use (Sharma et al., 2005).

2.4.1 Oxidation Process

The oxidation process is the most effective method to remove ferrous iron in groundwater, but a filtration process is required as well to complete iron treatment systems. In groundwater, the soluble form of iron is commonly seen under anaerobic conditions. Thus, the aeration process is needed for physicochemical removal processes because dissolved ferrous iron (Fe^{2+}) can be oxidized to ferric iron (Fe^{3+}) by the presence of oxygen in water or chemical oxidants (S. Chaturvedi and P. N. Dave, 2012). Table 2.5 presents the ferrous ion oxidation in stoichiometric expressions with a requirement of oxygen, alkalinity, and sludge production. The oxidant chosen for iron treatment is determined by the expense of the oxidant as well as the quantity of water to be treated.

Table 2.5 Chemical oxidants for iron oxidation

Oxidant	Reaction	Oxidant Needed	Alkalinity Consumed	Sludge Produced
		mg/mg- Fe^{2+}	mg/mg- Fe^{2+}	kg/kg- Fe^{2+}

Oxygen	$4\text{Fe}(\text{HCO}_3)_2 + \text{O}_2 + 2\text{H}_2\text{O} \rightarrow$	0.14	1.80	1.90
	$4\text{Fe}(\text{OH})_3 + 8\text{CO}_2$			
Chlorine	$2\text{Fe}(\text{HCO}_3)_2 + \text{Ca}(\text{HCO}_3)_2 + \text{Cl}_2 \rightarrow$	0.64	2.70	1.90
	$2\text{Fe}(\text{OH})_3 + \text{CaCl}_2 + 6\text{CO}_2$			
Chlorine dioxide	$\text{Fe}(\text{HCO}_3)_2 + \text{NaHCO}_3 + \text{ClO}_2 \rightarrow$	1.21	2.70	1.90
	$\text{Fe}(\text{OH})_3 + \text{NaClO}_2 + 3\text{CO}_2$			
Potassium permanganate	$3\text{Fe}(\text{HCO}_3)_2 + \text{KMnO}_4 + 2\text{H}_2\text{O} \rightarrow$	0.94	1.50	2.43
	$3\text{Fe}(\text{OH})_3 + \text{MnO}_2 + \text{KHCO}_3 + 5\text{CO}_2$			

The aeration process is a technique of using oxygen as an oxidant in the oxidation process to remove iron from the system. This method has been operated in many studies to treat metal. The basic mechanism of iron removal is its precipitation after ferrous iron-oxidizing to ferric iron in the water. Generally, aeration is induced when the concentration of iron in groundwater is higher than 5 mg/L. This process is beneficial due to no chemical use (Khatri et al., 2017). Oxygen is the popular one due to its natural occurrence in the environment, costs less, and convenience. The stoichiometry of physicochemical of ferrous iron-oxidizing by using oxygen in water is indicated as following Eq. 2.1:



The reaction above is a kind of exothermic reaction as energy is released from the reaction of Fe^{2+} with O_2 . The existed energy is considered useful for bacteria to break down and take in the carbon from CO_2 , so they can synthesize nutrients for their living. However, to assimilate 1 mole of carbon, 600 moles of ferrous iron is required; therefore, enormous amounts of ferrous irons must be oxidized to produce enough energy for iron-oxidizing bacteria growth (Sharma et al., 2005).

According to Eq. 2.1, it demonstrates that four mol of iron is oxidized by one mol of oxygen which similarly means the oxidizing of ferrous iron 7mg coupling with 1mg of oxygen. Indeed, only 1 mol of iron is converted to 2 mol of acidity and 1 mol of

Fe^{3+} . The reaction rate of ferrous oxidation can be calculated as equation below (El Azher et al., 2008):

$$r_{(Fe^{2+})} = K[Fe^{2+}][OH^{-}]^2[O_2] \quad \text{Eq. 2.2}$$

The oxidation of ferrous iron also depends on several parameters in water characteristics such as pH value, dissolved oxygen (DO), bicarbonate, temperature, etc. The iron solubility is low and turns to precipitate under reduction conditions ($EH < 0$) and higher pH in a wide range. However, under oxidizing conditions, iron tends to $Fe(OH)_3$ precipitated with $pH > 5.0$ and $EH > 0$ (Crittenden et al., 2012).

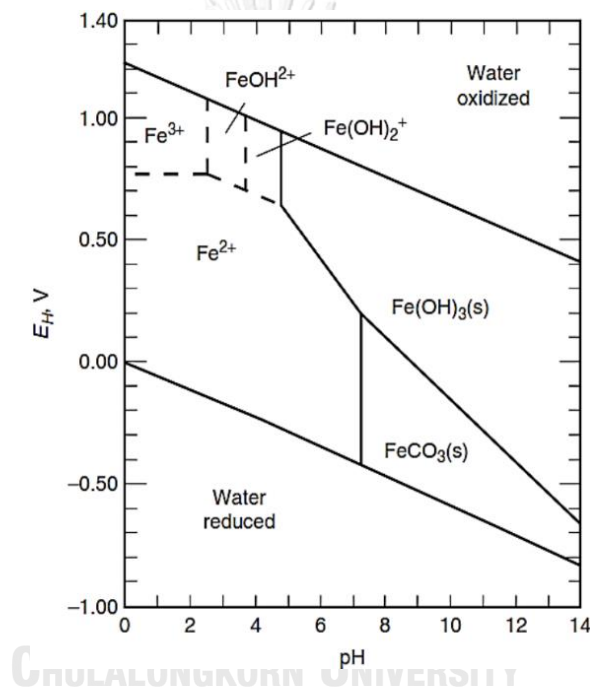


Figure 2.5 Iron forms in water as functions of EH vs. pH (Crittenden et al., 2012)

The EH-pH diagram of iron species in water is indicated in Figure 2.4 which describes as total iron activity $5.6 \mu\text{g/L}$, SO_4 96 mg/L , species of CO_2 at $1000 \text{ mg-HCO}_3\text{-/L}$, the temperature at 25°C , and 1 atm pressure. In EH range from 0.20 to 0.10 V with pH from 5 to 9 , ferrous iron relatively soluble under groundwater condition with free space.

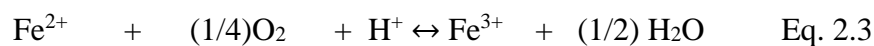
The precipitation process is also needed after the ferrous iron oxidation process. The precipitation of iron is found in water containing a high concentration of carbonate ($Ca(OH)_2$), and iron hydroxide and iron carbonate are appeared (El Azher et al.,

2008). A basic filtration procedure is used to isolate the precipitated iron from the water. This method is a traditional technique that commonly applies to treat iron in groundwater (Khatri et al., 2017).

2.4.2 Electrocoagulation (EC) method

Electrocoagulation (EC) is a technique for destabilizing dissolved or suspended contaminants in water by introducing an electric current through the polluted solution. Chemicals are not used in the procedure, and there is less sludge generated, which is the benefit of this process. For the removal of iron from aqueous environments, EC has been commonly used (Khatri et al., 2017).

This method involves potential generates the coagulant species in situ as the sacrificial metal anode dissolves (aluminum or ferric), and at the cathode, hydrogen is simultaneously derived. The coagulant species accumulates the precipitation of suspended solids and dissolved contaminants adsorption. The iron removal mechanism involved the oxidation of Fe to Fe (III), followed by adsorption and precipitation of Fe (III) by aluminum hydroxide complexes (Khatri et al., 2017). In the electrocoagulation process during electrolysis tiny bubbles of hydrogen and oxygen are generated, which pollutant particles can stick with air bubbles and float. However, at favorable operating conditions, iron and aluminum have been confirmed to be very efficient and competitive in pollutant removal. Normally, iron occurs as the ferrous state in solution, and with the presence of oxygen ferrous cannot stay in solution. Ferrous iron is oxidized in the air with a pH value is less than 6.5 according to the following reaction (Eq. 2.3):



The pH and redox potential are the most important factors in determining the form of iron in the water. Dissolved iron (Fe or Fe(III)) hydrolyzes to form precipitates as increasing pH. Between pH 7 and 14, the ferrous ion hydrolyzes to create a variety of mononuclear species, FeOH^+ to $\text{Fe}(\text{OH})_4^-$. The precipitation relies on the size and shape formed of particles after coagulation followed by the adsorption on the active surfaces of the coagulants formed at the time of the electrocoagulation process. The removal of iron is obtained because of iron hydroxide adsorption in the form of brown

flocks at higher pH as enough coagulants in medium (S. Chaturvedi and P. N. Dave, 2012).

2.4.3 Ion Exchange Process

Ion exchange is the mechanism of exchanging cationic or anionic ions between two electrolyte solutions. The method is useful for separating, purifying, and decontaminating solutions containing ions (Khatri et al., 2017). Because of the possibility of accelerated clogging, ion exchange can only be used for the removal of limited amounts of iron and manganese. Ion exchange uses synthetic resins where a pre-saturant ion on the solid phase (the “adsorbent”, normally sodium) is exchanged for undesirable ions in the water. One of the main drawbacks to using this method to regulate iron and manganese is that if the solution oxidizes during the process, the resultant precipitate will cover and foul the media. Then, chemical cleaning is needed via applying sodium bisulfate or acid (S. Chaturvedi and P. N. Dave, 2012).

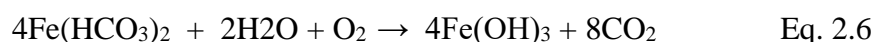
In groundwater, Iron can react with CO₂ and ferrous bicarbonate is formed. This form of iron is easily treated by normal softening resin since it is a positive-charged ion. The reaction that usually occurs with ion exchange resin (R) is summarized by the following Eq 2.4:



The resin produces two sodium molecules for every molecule of ferrous iron that the resin picks up. This reaction can be reversed by using a high concentration of salt (8–26%), as seen in the equation below (Eq. 2.5):



The following reaction (Eq. 2.6) represents the precipitation process after iron-oxidizing to make red water iron:



The fouling appears on the surface of the resin when ferrous iron is oxidized. Indeed, the capacity of the resin is decreased due to this fouling, also iron can excess to bleed via the system. When there is a lot of iron fouling on the appliance, it can be cleaned manually using a stronger cleaner. The resin which has a smaller particle size “fine

mesh resin” tends to have a better capacity to pick up and release clear water iron (S. Chaturvedi and P. N. Dave, 2012).

2.4.4 Membrane Filtration Process

Membrane technology-based strategies have been interested all over the world for the pollutant’s treatment from water. Microfiltration (MF), ultrafiltration (Painmanakul et al., 2004) and reverse osmosis (RO) are various types of membranes that commonly use. These methods have been mostly used to remove different metals from wastewater. As the pore size of ultrafiltration and microfiltration membranes is larger than metal ions pore size, so the ions must be pre-treated with surfactants and hydrophilic polymers to maximize their size. In water supply, iron has been treated by practicing various methods depending on membrane technology.

Some researchers have used UF to remove iron from water. The initial iron concentration in feed water was 1 mg/L, and the efficiency of iron removal was obtained around 98% at pH 7.1. The mechanism of iron treatment is associated with the formation of sparingly soluble iron hydroxide particles due to iron ions oxidation with the dissolved oxygen present in the water. Iron removal performance was higher in the dead-end UF process (90–98%) than in the crossflow UF process (65–85%).

MF systems have also been studied with the combination of oxidation processes to remove iron from groundwater. The method had a high iron removal efficiency (> 95%) at pH 8, with an initial iron concentration of 10 mg/L in the feed water. Enhanced mixing decreased the cake resistance because of iron oxides; therefore, assisted in raising the efficiency of the MF system.

The membrane technology may be a viable alternative to traditional methods for removing iron from the aqueous system. However, the disadvantages of this method are membrane fouling and cake formation which can reduce the treatment efficiency of the membrane process after few cycles of performance. Membrane technology still needs high expenses, energy usage, and affordability. With this development, membrane technology can become a useful method for remediation of iron from water (Khatri et al., 2017).

2.5 Arsenic treatment method

Arsenic is increasingly recognized as a serious, worldwide public health concern. Arsenic has been known as the most toxic element in the periodic table and is normally found in groundwater as a pollutant because of its carcinogen. Therefore, WHO has set a standard of arsenic concentration in drinking water 10 ppb for rich countries, and some countries arsenic can load to 50ppb. The traditional methods used for the arsenic treatment from water medium have their advantages and drawbacks as described in detail in each section (Nidheesh and Singh, 2017).

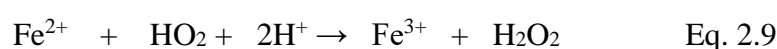
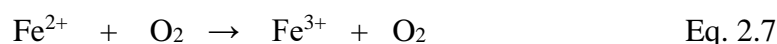
2.5.1 Oxidation Process

Arsenic is predominantly as Arsenite (As(III)), which is more toxic and mobile than arsenate (As(V)), therefore, oxidizing it from arsenite to arsenate is highly desirable for reducing its mobility as well as for arsenic removal before using coagulation, sorption, and membrane filtration technologies.

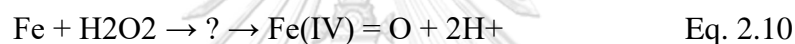
The objective of the oxidation process is to transform the soluble form of arsenite (As^{3+}) to arsenate (As^{5+}), which is then precipitated As^{5+} . Since As^{3+} is the predominant type at near pH 7, it is critical for anoxic groundwater. Arsenate (As^{5+}) adsorbs more readily into solid surfaces than As^{3+} ; therefore, oxidation followed by adsorption is the most effective method for removing total arsenic (Luong et al., 2018). There are many oxidants to use for arsenic oxidation. With relation to both As^{3+} and oxidants, the kinetics of the reaction with O_3 , H_2O_2 , Cl_2 , NH_2Cl , and ferrate are the first-order reactions, so the concentrations of As^{3+} and the oxidant are the important parameters for effective removal of As from aqueous solution.

For the oxidation of As^{3+} to As^{5+} , the oxidants of permanganate, ozone, and chlorine reaction are faster than chloramine and hydrogen peroxide. In polluted groundwater, air and pure oxygen can oxidize 54–57 percent of As^{3+} to As^{5+} for many days, while ozone can complete the oxidation of As^{3+} in short time. Another oxidant is manganese dioxide polished powder, which has the distinction of being both an oxidizer and an adsorbent. The use of manganese dioxide polished sand in conjunction with Fe-containing compounds is more influential since the processed materials are easier to manage (Shankar and Shanker, 2014).

In the case of iron co-presence with arsenic, few studies examined the iron-catalyzed oxidation and removal of arsenic in neutral groundwater. The rapid oxidation of ferrous iron at pH 7.0 and 7.5 also can lead to partial co-oxidation of arsenite even in the absence of hydrogen peroxide through a cascade of Fe³⁺/Fe redox chemical reactions (Eq. 2.7 – 2.9)



High-valent-oxoiron (Fe(IV) species) were responded for arsenite oxidation at neutral pH (Equation 2.10 and 2.11). Therefore, As(IV) reacts with dissolved oxygen to As(V) and O₂, as expressed in Equation 2.12.



Another relative effect of iron co-presence on arsenic goes through the adsorption of arsenic on ferric hydroxide. It can be concluded that the co-presence of iron affects arsenic removal through two paths. Firstly, the co-oxidation/precipitation of arsenite with ferrous iron through high valent iron to form arsenate. Secondly, there might have possible adsorption of both arsenite and arsenate onto ferric hydroxide (Pierce and Moore, 1982).

2.5.2 Precipitation Process

The precipitation process is a method followed by the flocculation process, and suspended particles are precipitated at the bottom through gravity form. A possible approach for removing As from groundwater is to include a coagulant followed by the creation of flocculation. Positively charged cationic coagulants reduce the negative charge of colloids, resulting in the formation of larger particles due to particle aggregation. The flocs are formed during the flocculation process as a result of polymeric bridging between the flocculent particles, which then agglomerate to form bigger mass particles. Arsenic is removed from an aqueous solution when soluble

arsenic is precipitated/coprecipitated on the floc's surface. Among the numerous chemical coagulants, Fe and Al based coagulants are commonly used for As elimination. Kaolinite and FeCl_3 is widely used as coagulant-flocculent, which can treat more than 90% and 77% of As^{5+} and As^{3+} , respectively, using 9.2 ppm of Fe^{3+} . Fe-based coagulants are more efficient in water treatment than Al-based coagulants among chemical coagulants. The As needs to be adsorbed on the amorphous metal hydroxides produced by the coagulant for efficient treatment. However, the crucial restriction of the coagulation-flocculation process is producing a large volume of sludge with a high concentration of arsenic. The treatment of polluted sludge is critical for preventing secondary contamination in the atmosphere, which limits the applicability of this process in environments (Shankar and Shanker, 2014).

2.5.3 Membrane process

When cellulose–acetate RO membranes were first tested for arsenic removal with high pressure (typically 2760 kPa), and more than 90% arsenate was rejected. Arsenic treatment was also tended to be successful using NF membranes, which are more permeable and can work at pressures lower than 690 kPa. The drawback of RO and NF membrane is that the permeability of raw water flows through the membrane with a small amount from 10-15%. The RO membranes perform at pressures in the range from 280 – 2760 KPa, arsenate, and arsenite rejection were 96-99% in natural water. The efficiency of the NF membrane comparable to the RO membrane, although the conducting pressure was much low 280-283 KPa for NF and 1380-2760 for RO (Nguyen et al., 2009).

2.6 Aeration Process

Aeration is a process that generates air as the gaseous phase into the water in order to increase the amount of dissolved oxygen content in the liquid phase. There are different ways conducted with aeration processes such as diffusers, stacked trays, or surface turbine and wheels. Moreover, some main points should be considered such as the theory of gas transfer to liquid, bubble aeration, and the theory of oxygen transfer rate.

2.6.1 Dissolved Oxygen in Water

Dissolved oxygen (DO) is the quantity of gaseous oxygen dissolved in any liquid or water, and it is determined in milligrams per liter (mg/L) or parts per million (ppm). The level of DO is very important for aquatic life in the freshwater of oceans that used to support biological activity. Table 2.6 indicated the level of DO in water at temperature $T=20^{\circ}\text{C}$.

Three main factors that affected the solubility of DO include temperature, pressure (Henry's law), and mineral content in water.

Table 2.6 Water quality and DO content in ppm at 20°C (Bun, 2015)

Water quality	DO level (ppm) at 20°C
Good	8.0 – 9.0
Slightly polluted	6.7 – 8.8
Moderate polluted	4.5 – 6.7
Heavily polluted	Below 4.5
Gravely polluted	Below 4.0

Saturated dissolved oxygen in the water as a function of temperature and barometric pressure is defined in Appendix 2. The advantages of DO level are (i) to limit a biological reaction (aerobic bacteria/ anaerobic bacteria) to monitor the process to ensure that there is enough dissolved oxygen for aerobic bacteria metabolism in wastewater treatment, septic condition, and to control DO level in activated sludge of aeration tank, (iii) to indicate the pollution of water stream and (iv) to determine the level of BOD in water. A standard method for measure the value of dissolved oxygen are included the membrane electrode method by using DO meter (commonly used for the present work), aside modification (chemical method), and copper sulfate-sulfamic acid flocculation modification.

2.6.2 Gas-liquid Transfer

The knowledge about the theory's gas-liquid transfer, equilibrium partition between water and air is the crucial task in both aeration and air stripping processes, to improve the level of design and operation as well. Moreover, the rate of mass transfer across the water-air interface also important and should be considered (Edzwald and Association, 2011). The definition of equilibrium is the last state of the system to move towards. The system displacement from equilibrium determined the amount of fluid needed for aeration as a driving force to govern mass transfer.

❖ Equilibrium

Henry's law can be defined to describe the equilibrium partition between air and water in both cases aeration and air stripping process in the water treatment system. It will be considered in a close system as present in Figure 2.5 as follow.

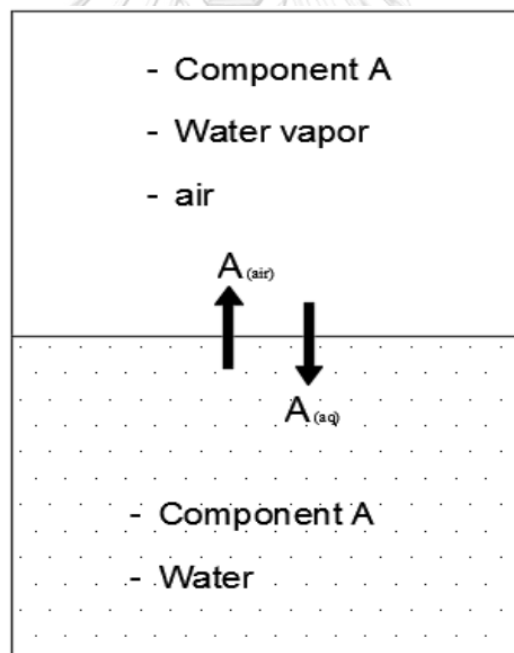


Figure 2.6 Equilibrium condition of component A in air-water (Edzwald and Association, 2011)

The equilibrium can be defined as an expression in Eq. 2.13, while component A is in the equilibrium stage of both liquid and gas phases for a constant temperature. This equation can be reduced the form to Eq. 2.14 after applying 1 atm of pressure, where K_{eq} is equilibrium constant, the air is component A activity in the gas phase, the air is

component A activity in the aqueous phase. H is Henry's law constant of component A [atm-L/mol], P_A is a pressure A in the gas phase [atm], γ_A is an activity coefficient of component A in the aqueous phase, A is a molar concentration in aqueous-phase of component A [mol/L] (Edzwald and Association, 2011).

$$K_{eq} = \frac{a_{air}}{a_{aq}} \quad \text{Eq. 2.13}$$

$$H = K_{eq} = \frac{P_A}{\gamma_{AA}} \quad \text{Eq. 2.14}$$

❖ Henry's Constant

If the vapor pressure and aqueous solubility of component A are known, Henry's constant can be estimated. There are two different situations to estimate Henry's constant of component A (Edzwald and Association, 2011). Component A is perfectly miscible and immiscible in an aqueous phase. In the case of the perfect miscible in the aqueous phase, the exerted pressure and the vapor pressure will be the same at the desired temperature and the mole fraction of component A is 1 (X H₂O). The following expression is written as Eq 2.15. Where $P_{v,A}$ is the vapor pressure of component A at the desired temperature [atm]. In contrast, it is immiscible in the aqueous phase.

$$H = P_{v,A} \quad \text{Eq. 2.15}$$

❖ Effects of temperature and solution property

Several factors affect the equilibrium partitioning of air and water such as pressure, temperature, pH, surfactant, and ionic strength. The effects of pressure on H are usually negligible due to the operation of aeration of air stripping in the atmospheric pressure. Increasing temperature tends to increase the H value because of the decreasing of aqueous solubility after the vapor pressure increase. The quantity pH does not affect Henry's constant but the distribution of species if ionized and unionized forms. Surfactant is another factor that affects the volatility of the compounds, while the lowest of surfactant's concentration, not affect the aeration or air stripping. VOCs or gases in the water supply usually have high volatility that will result in an increase in the solubility of volatile components and increase a component

An activity coefficient. Ionic strength also increases when the activity coefficient increases (Edzwald and Association, 2011).

❖ Mass transfer

In water treatment process mostly conducted the transfer concept to change a material phase from a liquid into gaseous or some case change from the liquid state to solid-state. Aeration, air stripping, adsorption, ion exchange, and reverse osmosis are considered as an application of mass transfer. The displacement from the equilibrium is the force for mass transfer of one phase to another phase.

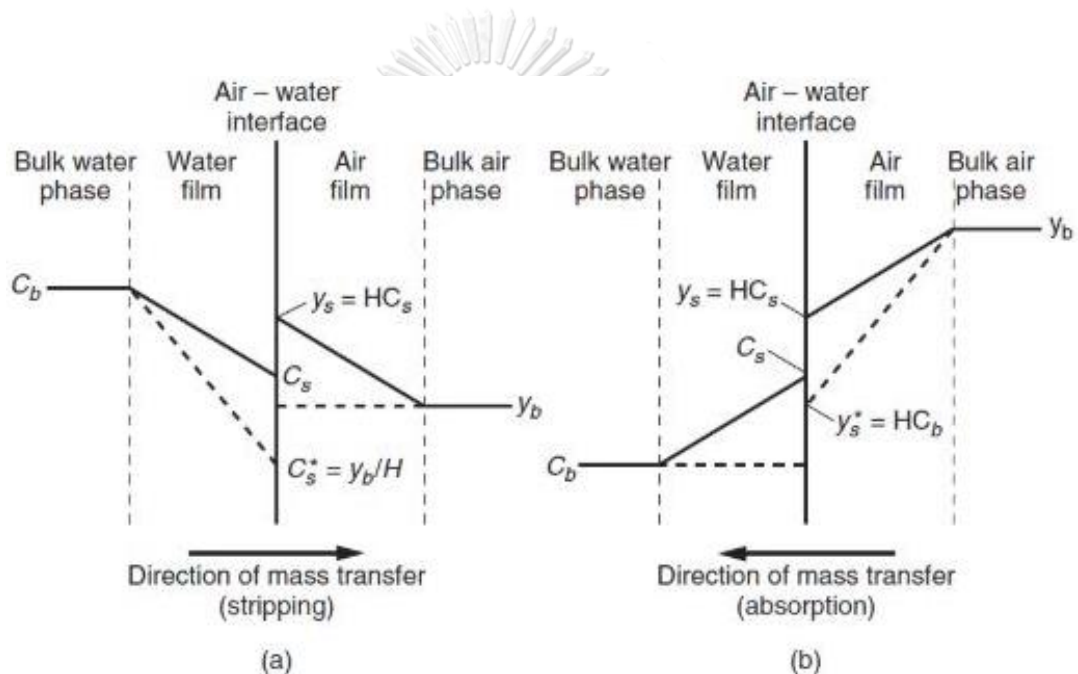


Figure 2.7 Mass transfer for (a) stripping and (b) absorption by using two-film theory (Crittenden et al., 2012)

Two different mass transfer situations of air and water at a steady-state are presented in Figure 2.6. A two-film model is normally applied to represent the rate of mass transfer for air stripping and adsorption. It is a simple theory on gas-liquid mass transfer which is a product of the driving force through each film.

2.6.3 Oxygen Transfer Rate

Oxygen transfer rate, OTR is one of the crucial variables of the gas-liquid contactor. It indicates the quantitative that corresponds to a volumetric mass transfer coefficient, K_La , the concentration gradient, and total liquid volume carried in the system. It has

been paid attention to and studied by many researchers over the last decade (Garcia-Ochoa and Gomez, 2009). Exactly measurement of the OTR parameter plays an important role to achieve the most favorable design, operation, and scaling process for the interesting reactor. OTR value of an interesting gas-liquid contactor can estimate by using Eq. 2.16. Where the coefficient K_{La} can be separated into two-term, mass transfer coefficient (K_L) and specific interfacial area (a). However, two parameters are difficult to measure separately, therefore K_{La} is usually defined as a combination term and called a volumetric mass transfer coefficient.

$$\text{OTR} = K_{La}(C^* - C_L)V \quad \text{Eq. 2.16}$$

$$\text{OTR} = K_L a C^* V \quad \text{Eq. 2.17}$$

Only a small amount of gaseous is normally dissolved in a liquid solution with the limiting of the maximum concentration gradient. For example, oxygen dissolves in the water. The oxygen transfer rate can be rewritten as Eq. 2.17. Where C_L presents the concentration level of gaseous in the bulk liquid at the initial step that can eliminate. The K_{La} is not easy to evaluate due to various phenomena simultaneously occurred. Many researchers are studied and provided empirical equations to estimate the K_{La} value of the pneumatic reactor. Furthermore, the various experiment works commonly used to determine the essential K_{La} that described as following.

❖ Experimental determination of OTR

Both empirical and experimental could estimate the quantitative of OTR. However, it probably disagrees between the actual experiment result and the proposed empirical equation. The incompatibility may cause strongly by the size and/or type of reactor, the different operational conditions, the physicochemical properties, and the performance of the measurement method. Several experimental methods are considered and described (Garcia-Ochoa and Gomez, 2009).

In case absence of biomass or non-respiring cell, the K_{La} value can be simplified from Eq. 2.16 to Eq. 2.18 as follows:

$$\frac{dC}{dt} = K_L a (C^* - C_L) \quad \text{Eq. 2.18}$$

This equation can also be used for the different techniques (both chemical and physical methods) from measuring the concentration value of dissolved oxygen inside the interesting reactor.

Chemical method: is the first method that is widely accepted but not recommended in the case of sparged bioreactors. This method sometimes obtained a higher OTR value than that in the real case, due to enhancement of the absorption rate by a fast chemical reaction inside the solution.

Sodium sulfite oxidation method: this method uses sodium sulfite to eliminate the dissolved oxygen in the liquid phase to produce sulfate, in the presence of cation of cobalt or copper as a catalyst. The reaction that involved in this method are:

- Absorption: $O_2 + 2Na_2SO_3 = 2Na_2SO_4$
- Detection of sulfite: $2Na_2SO_3 + 2I + 2H_2O = 2Na_2SO_4 + 4HI$
- Back titration (unreacted I₂): $4Na_2S_2O_3 + 2I_2 = 2Na_2S_4O_6 + 4NaI$

From experiment, concentration of sulfite is measured along the time, then rate of sulfite depletion is calculated and K_{La} can be determined from Eq. 2.19 as well.

$$-\frac{dC_{Na_2SO_4}}{dt} = 2K_L a C^* \quad \text{Eq. 2.19}$$

However, the sodium sulfite oxidation method has a limitation, and the value obtained mostly greater than that from the other techniques.

- Absorption of CO₂ method: this method uses carbon dioxide taking place in an alkaline solution, and the mass transfer coefficient can be obtained from the equation following Eq. 2.20 below.

$$-\frac{1}{2} \frac{dC_{CO_2}}{dt} = 2K_L a C^* \sqrt{K C_{CO_2}} \quad \text{Eq. 2.20}$$

This method has limitation as the reaction rate involved in the system should be the first-order reaction, even sometimes it is the second-order reaction, yet the reaction acts like one of pseudo-first-order due to the partial pressure of CO₂ is low.

- Dynamic method: is one of those that based on assessing the value of dissolved oxygen in the system. The equation that is used in this method

was obtained by integration of equation 2.11 between two different of time as equation 2.21 as well.

$$\ln \frac{C^* - C_2}{C^* - C_1} = -K_L a \cdot (t_2 - t_1) \quad \text{Eq. 2.21}$$

Two ways can be determined the volumetric mass transfer coefficient, $K_L a$ inside the medium system, included absorption technique and desorption technique.

In the case of using the dynamic method, the absorption phenomena have occurred during the elimination of dissolved oxygen in the system by using the reducing agent such as nitrogen bubble or sodium sulfite.

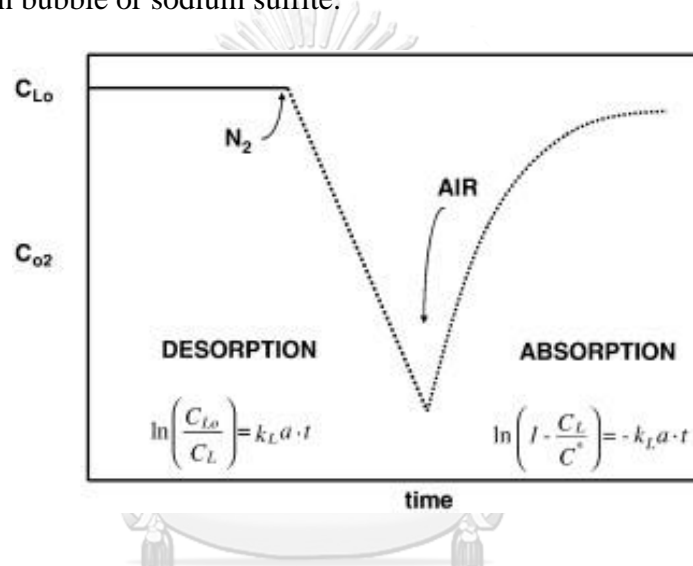


Figure 2.8 Schematic description of the dynamic technique desorption–absorption of oxygen for inert condition measurements (Garcia-Ochoa and Gomez, 2009).

Then, the air was supplied into the liquid phase and simultaneous monitor an increase of dissolved oxygen concentration in the system along the time. On the other hand, the desorption technique is conducted by supplying the air to the solution until reaches the saturated level of oxygen, then turn off the air and introduce nitrogen gas to reduce the level of dissolved oxygen concentration. The decreasing of DO in the system is measured as a function of time. Figure 2.7 is described the phenomena of both techniques and formulas use to indicate the quantitative volumetric mass transfer coefficient, $K_L a$ respectively.

2.7 Membrane technology

Membrane treatment is one of the latest advanced technologies for water treatment and widely performed in several countries (Magara et al., 1998). Four various types of membrane filtration have been known as microfiltration (MF), ultrafiltration, nanofiltration (Rahmanian et al.), and reverse osmosis (RO). MF membrane's function is to treat suspended solids with high pore size or small and light particles of colloid and some bacteria. For UF membranes, the medium up to high molecular weight components is separated while NF membranes are used to remove the low molecular weight components. However, RO membrane is the most membrane filtration type that needs a high pressure in operation due to the effective removal of all inorganic pollutants. The use of different operation pressure, membrane pore sizes and their application are illustrated in Table 2.7 The performance pressure raises when the pore size declines as a result of reducing the amount of space available for water to pass through (Maddah et al., 2017). There are several different membrane device configurations available, including polymeric and inorganic membranes. Spiral, tubular, and hollow fiber membranes are polymeric membrane types whereas ceramic and stainless steel membranes are inorganic membrane types (Sen, Manna, and Pal, 2010). The polymeric membrane is usually used for low-pressure membrane filtration operations.

Table 2.7 The characteristic of application of membrane processes (Pangarkar, Sane, and Guddad, 2011)

Membrane Type	Pore Size (μm)	Operating Pressure (bar)	Pollutant removal
Microfiltration (MF)	0.1-10	1-5	Turbidity (>99%); bacteria (>99.99%)
Ultrafiltration	0.01-0.1	1-10	Turbidity (>99%); bacteria (>99.99%); TOC (20%)

Nanofiltration (Rahmanian et al.)	< 0.001	20-40	Turbidity (>99%); color (98%); TOC (>95%); hardness (>90%); sulfate (>97%); virus (>95%)
Reverse Osmosis (RO)	<0.001	30-100	Salinity(>99%); color &DOC (>97%); nitrate (85-95%); pesticide (0-100%); As, Cd, Cr, Pb, F removal (40-98%)

2.7.1 Membrane permeability

The permeability of the membrane is a possibility of water passing through the membrane pore size. The pure water permeability is the normalized productivity of membranes, which is calculated as the pressure-normalized flux of deionized water through the membrane and is commonly used to describe low-pressure membranes (Guerra, Pellegrino, and Drewes, 2012). The occurrence of membrane fouling is a major to cause of less membrane permeability in the system. Membrane fouling happens when the transmembrane pressure increases, or water flux decrease during the system performance at a steady pressure. The membrane structure affects the permeability of the membrane including porosity, tortuosity, thickness, etc. The resistance flow is less if the porosity membrane is higher. Eq. 2.21 below is the hydrodynamic resistance of the cake layer $R_c [m^{-1}]$ is defined as:

$$R_c = \hat{R}_c \cdot m_d \quad \text{Eq. 2.21}$$

where $\hat{R}_c [m/kg]$ is the specific cake resistance of the cake layer on the membrane surface and $m_d [kg/m^2]$ is the mass of the deposited layer per unit surface area of the membrane. The corresponding permeate flux (J , m^3/m^2s) is expressed using Darcy's law and a resistance-in-series model (RIS) as below (Eq. 2.22):

$$J = \frac{\Delta P}{\mu(R_m + R_c)} \quad \text{Eq. 2.22}$$

where $\Delta P (Pa)$ is transmembrane pressure, $\mu (Pa.s)$ is the solution viscosity and $R_m (1/m)$ is the hydrodynamic resistance of a clean membrane.

2.7.2 Membrane fouling

Membrane fouling is one of the obstacles in the membrane filtration process. Fouling might affect to operation's economy because of more energy consumption, additional labor for maintenance, cleaning chemical costs, and a shorter membrane life (X. Shi et al., 2014). Four main categories cause membrane fouling including suspended particles, organic matter, scaling, and biofouling (Baker, 2012). Membrane fouling is resulted from the adhesion and deposition of particles and colloids onto the membrane surface and into the membrane pores, and it is the most significant obstacle in the application of low-pressure membrane processes. The fouling phenomenon necessitates a more effective strategy for eliminating, preventing, and cleaning fouling formation.

The developing techniques are to control and minimize the impact and scale of membrane fouling and more competitive with other technologies. In general, macromolecules, colloids, or particulate matter can form or clog on the membrane surface. The membrane filtration process can properly operate when membrane fouling is well managed. To reduce membrane fouling, membrane cleaning; module, and pretreatment are considered as favorable methods (Ma, Shu, and Lu, 2020). Pretreatment of the feed solution (prescreening chlorination or acidification), enhancement of membrane properties (change in hydrophobicity and material), modification of working conditions (increase fluid velocity, higher transmembrane pressure (TMP)), and cleaning are some of the fouling control techniques.

2.7.3 Membrane cleaning process

The membrane cleaning process is a method to reduce membrane fouling. A fouled membrane can be cleaned in a variety of ways. Normally, membrane cleaning is separated into two different categories (physical and chemical cleaning method) depending on the chemical agent that uses in the procedure. Physical cleaning is applied to force foulants to release the membrane material by changing hydrodynamics, applying turbulence, or varying temperature to the system. The chemical cleaning process is to use chemicals to adjust in solution and evolve the EDL of electrostatic repulsion between membrane surface material and foulants or to

dissolve foulants. Physical and chemical processes are often combined in practice to improve cleaning efficacy (X. Shi et al., 2014). The different types of foulants and the effective treatment concepts are introduced in Table 2.8.

Table 2.8 Effects of operating strategies on membrane fouling.

Type of fouling	Effects of operating strategies			
	Feed pre-treatment		Cleaning	
	Chlorination	Acidification	Physical	Chemical
Inorganics	-	++	-	++
Particulate	-	-	++	++
Microbe	++	+*	+	++
Organics	+	-	-	++

Note: - no/negative effects, + some positive effects, ++ positive effects, * with feed chlorination

Physical cleaning usually associates the use of one or more cleaning forces including electrical, hydraulic, or mechanical. Relaxation, forward flush, backwash flush, and air flush are some of the methods used to manually clean fouled membranes for MF and UF during service (Lenntech and htm, 2009).

Membrane relaxation: is to disperse foulants at the surface of membrane filter by non-continuous operation system and the concentration gradient (Le-Clech, Chen, and Fane, 2006). Membrane relaxation is the easiest method to remove reversible fouling and allowing filtration to be maintained a long time before the next cleaning process (Le-Clech et al., 2006). However, the efficiency of removing foulants will be raised when the air scouring, and relaxation process are worked together. The drawback of this method is reducing the total flux and requiring a larger membrane surface. Anyway, the increasing of membrane fouling might happen while the period of relaxation is too short (Chua, Arnot, and Howell, 2002).

Air flush: is the method to use air or air/water to flush the membrane or the concept of forwarding flush. It is because air bubble impacts the turbulence and increases cleaning efficiency. As a cleaning method, air can be used in a surface flushing and backwashing medium. UF is not well operated with air backwashing in reason of the

different size range from 100 nm to 1 mm that is about two orders of magnitude higher than the average pore size in ultrafiltration membrane. Hence, the flushing stream is applied for UF first because the particulates can be left from the surface membrane before the backwashing process. This would be a more effective method. In comparison, the air bubbles injection increases turbulence and improves the treatment efficiency under the same conditions as hydraulic flushing (Verberk, Van Dijk, and Supply, 2003).

Backwashing: is the process of practicing reversible flow pushed from the permeable part of the membrane to the feed side. The reversed flow dislodges the deposits from membrane pores and loosens fouling cakes on the external side. Backwashing normally necessitates a working flux at least two times higher than normal filtration. However, energy consumption is more required for the backwashing process, but the effectiveness is also better than forwarding flushing (Chen, Kim, and Ting, 2003). For the backwash flushing process, the permeate pressure is higher than operating pressure which is typically about 2.5 times.

2.8 Design of Experiment (DOE)

In the experimental studies such as physical and chemical studies of elements, designing and developing technologies processes, optimization of composition properties or procedures in the system, selection of parameters by their significant effects on the measured value responses, etc. It should have a new scientific discipline deals with the analysis and designing because a large number of experiments will be required in the research, development, and optimization of the system. For example, a system is affected by five factors and each factor is varied 3 different values; thus, the total experiment is 53 equals to 125 different combinations of factors-trials. Therefore, it is essential to apply the innovative method into experimental research in order to reduce the number of experiments, especially the expense of materials as well as time-consumed (Lazic, 2006). Design of Experiment (DOE) is a statistical and mathematical method for analyzing the relationship of inputs and outputs in the experiment and providing the maximum conditions with a minimum expenditure of time and materials. Hereby, the advantages of using DOE are:

- To minimize the number of trial experiments
- To vary all parameters in simultaneousness of an experimental activities
- To choose a suitable strategy for an experiment after each sequence of trials

2.8.1 Concept of DOE

Generally, the experiments are conducted to study the performance of a system or process which can be represented by the model of DOE as illustrated in Figure 2.9. The inputs can be transformed into the output (or response) by a process which is a combination of methods, operations, machines, and other materials. In that process, some factors and material properties are controllable, whereas other factors are uncontrollable. Therefore, DOE could determine the factors that are the most influential on the response, select the conditions where the inputs make the variability in response small and almost near to the maximum value and where the effects of the uncontrollable factors are minimized (Montgomery, 2017). The DOE method of response surface methodology is described as follows.

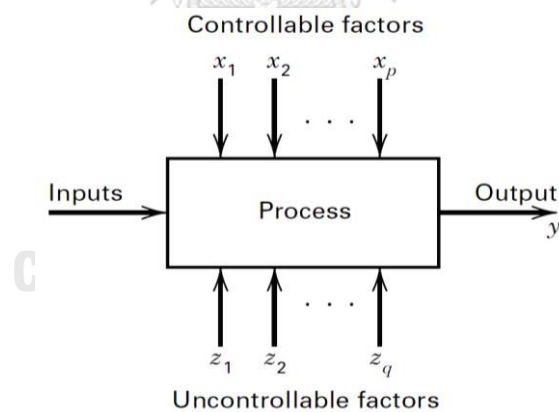


Figure 2.9 General model of a process or system (Montgomery, 2017)

2.8.2 Response surface methodology

Response surface methodology (RSM) is a combination of mathematical and statistical techniques for modeling and analysis of the experiment and optimizing the experimental results which are influenced by various factors. For example, in a process that is influenced by the levels of concentration (x_1) and time (x_2). Thus, the

maximum yield (y) of the process is a function of the levels of concentration and time which can be expressed as Equation 2.23 where ϵ is the error observed in the response y . If the expected response is noted as $E(y) = f(x_1, x_2) = \eta$, then the response surface is written as Equation 2.24 and the contour plot for better visualize is represented in Figure 2.10, each contour corresponds to a particular height of the response surface (Montgomery, 2017).

$$y = f(x_1, x_2) + \epsilon \quad \text{Eq. 2.23}$$

$$\eta = f(x_1, x_2) \quad \text{Eq. 2.24}$$

Mostly, the relationship between response and the independent variables is unknown. Thus, the first-order model of RSM is expressed as Equation 2.35 represented the relationship between y and the set of independent variables in linear function. If it is curvature or the degree of polynomial is high, then the second order model in Equation 2.26 is applied.

$$y = \beta_0 + \beta_1 x_1 + \beta_2 x_2 + \dots + \beta_k x_k + \epsilon \quad \text{Eq. 2.25}$$

$$y = \beta_0 + \sum_{i=1}^k \beta_i x_i + \sum_{i=1}^k \beta_{ii} x_i^2 + \sum \sum_{i < j} \beta_{ij} x_i x_j + \epsilon \quad \text{Eq. 2.26}$$

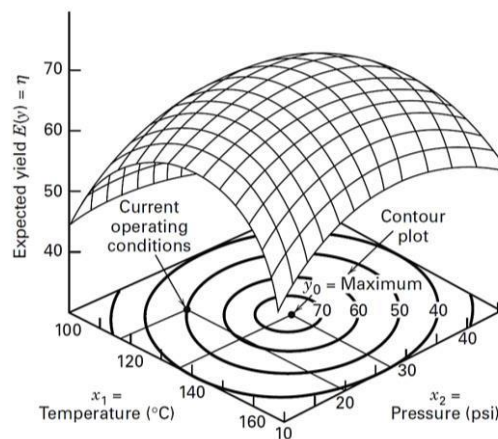


Figure 2.10 Contour plot of a response surface (Montgomery, 2017)

There are two types of response surface methodology such as central composite design (CCD) and Box-Benhen design (BBD), which are briefly described as following:

(A) Central composite design

Central composite design (CCD) is applied for fitting the second-order model of RSM, which consists of 2^k factorial with n_F factorial runs, $2k$ axial, and n_C center runs as illustrated in Figure 2.11 for $k = 2$ and $k = 3$. In this design, two parameters need to be specified such as the distance of the axial runs from the center (α) and the number of center points (n_C).

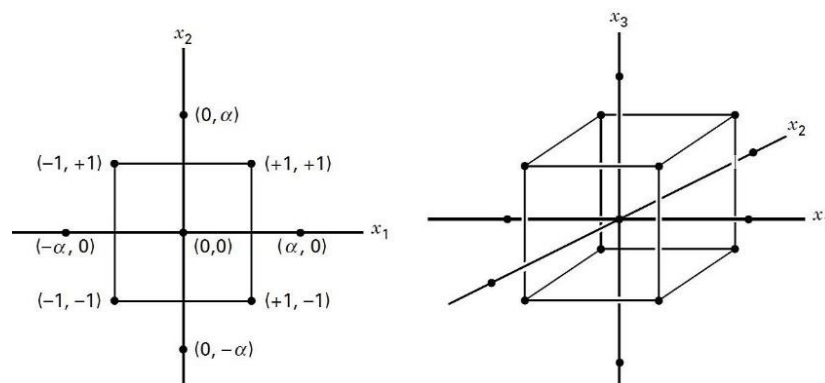


Figure 2.11 Central composite designs for (a) $k=2$ and (b) $k=3$ (Montgomery, 2017)

(B) Box-Behnken design

Box-Behnken design (BBD) is a combination of 2^k factorials with an incomplete block design for fitting the response surface model which has three levels of design. The BBD is a spherical design with all points on a radius sphere, but no points at the vertices of the cubic zone defined by the upper and lower bounds for each variable. The geometrical of BBD is showed in Figure 2.12.

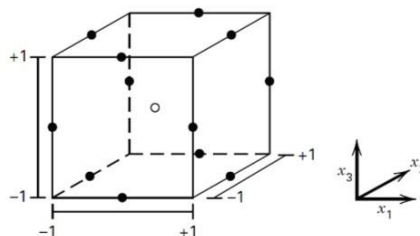


Figure 2.12 A Box-Behnken design for three factors (Montgomery, 2017)

CHAPTER 3

METHODOLOGY

3.1 Study Overview

In this chapter, an overview of the methodology in this research is described. The main objective of the study is to remove ferrous iron and arsenic from contaminated groundwater via co-precipitation coupling with membrane separation process. To achieve this objective, the overall mass transfer coefficient is analyzed to understand the operation of BCR and diffuser and the effect of solid media addition. Various crucial variables related to ferrous iron oxidation and arsenic removal are going to be evaluated including gas flow rate (Q_g), pH, adding ferric concentration, and initial ferrous concentration. Finally, membrane filtration is introduced to treat suspended solids or particle impurities in solution. The methodology overview is portrayed in Figure 3.1.

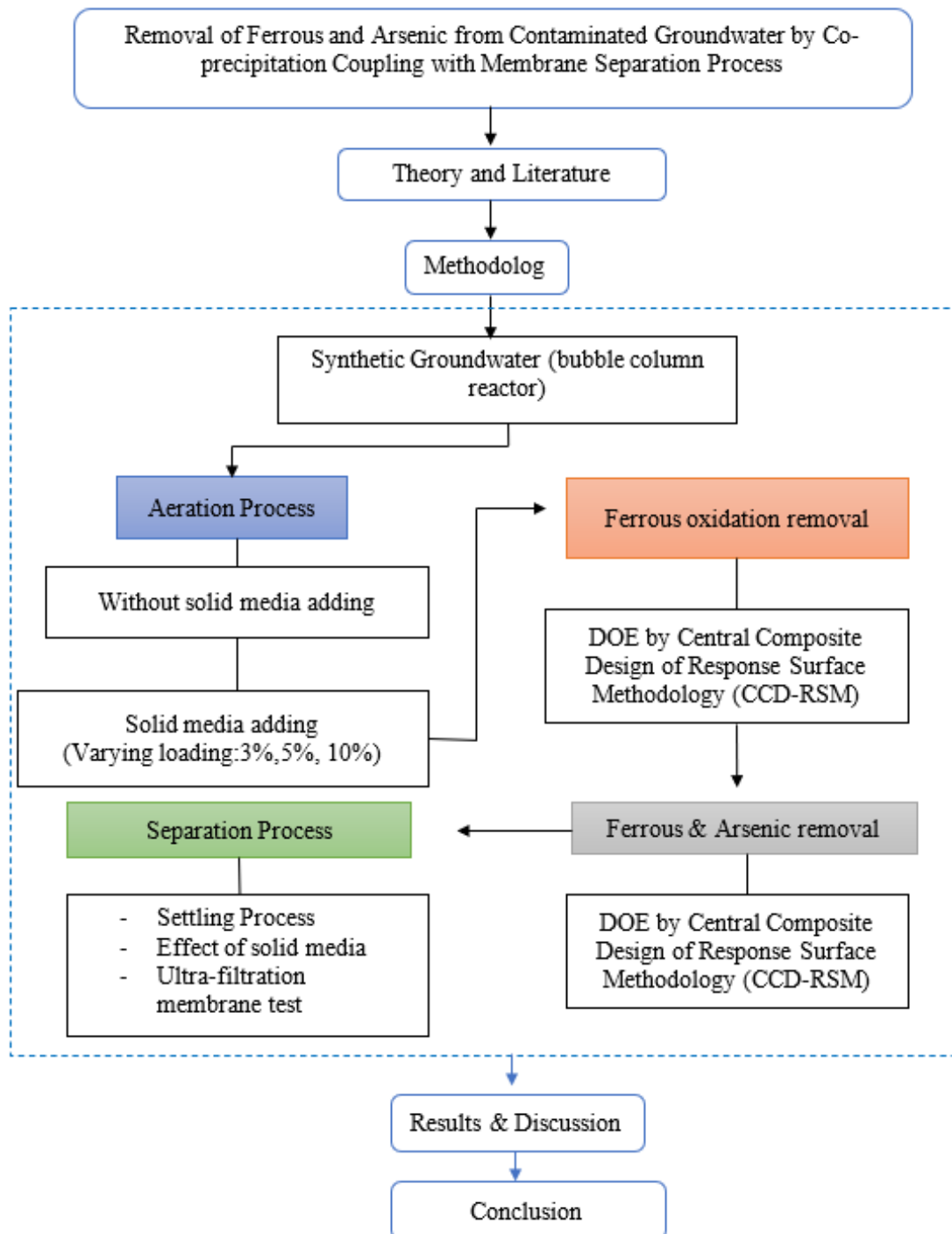


Figure 3.1 The framework of study overview of the research study

3.2 Experimental set-up

3.2.1 Bubble column reactor (BCR)

In this study, the experiment will be operated in a bubble column reactor (BCR) as shown in Figure 3.2. The large scale of regular BCR has a cylindrical column of 20cm outside diameter, 19cm inside diameter with a height of 78cm. The volume of a water sample is 18 liters with the freeboard 13cm of the reactor. This column reactor was produced from an acrylic material. The rigid stone diffuser with a sphere shape of 6.1 cm in diameter was installed at the bottom of the tank to provide air to contact a water sample.



Figure 3.2 Experimental set-up of bubble column reactor (BCR)

The rigid stone diffuser functions for the air injection place, and the air pump was used for air generation. Next, a gas flow meter was placed to regulate the flow rate while air valve controlled the amount of air supplement system. Furthermore, the

pressure gauge is built to maintain the operation of the air pump in a system, also to assess the power utilization for air generates. Lastly, the water drainage pipe was located at bottom of the column reactor to drain the water.

3.2.2 Membrane Filtration

The membrane filter is installed for the experiment as shown in Figure 3.3. The membrane experimental setup is followed from pre-oxidation in the bubble column reactor. The crossflow membrane module with a hollow fiber is selected for this study as it is commonly used in drinking water filtration and easy operating. The pump is connected to the reactor tank circulating feed water through the module where up and downstream pressure gauges and bypass control valves are used to measure and control transmembrane pressure. Rotameters and control valves are used to determine and control flow through the system. Every new set of the membrane is initially performed for 30 min with a pressure of 15 kgf/cm² using deionized water before actual separation study employing the membrane (Sen et al., 2010).

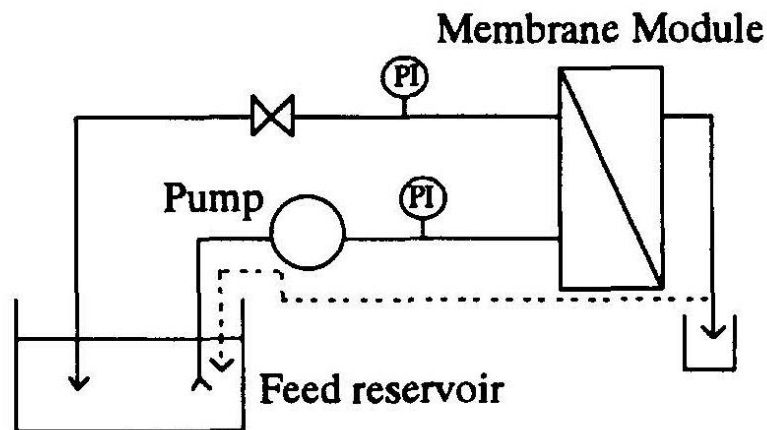


Figure 3.3 Schematic diagram of membrane experimental set-up

3.3 Chemical reagents and equipment

3.3.1 Equipment

To complete the installation of the reactor for experiment performance, several accessories are needed as mentioned below:

- Check valve is used to the maintenance flow direction.
- Gate valve is beneficial for adjusting the water flow.
- PVC (1/2") Plastic Clear Transparent pipe is conducted to transfer water flow.
- PVC (1/2") pipeline is helping to attach a complete system.
- Steel beams are accessed to bear the weight of the reactor with a liquid sample.

There are many devices are used to study in aeration process in bubble column reactor as following:

- Air pump: Atman aquarium air pump Atman HP-12000 model is used to pump air into the system for the aeration process. Since the diffuser is chosen in this study, the pressure of pump operation would not be much concern.
- Airflow meter (Rotameter): a model of DWYER® 0 to 23 LPM is used to vary and manage the airflow rate of the experiment.
- DO meter: dissolved oxygen of water sample is identified by dissolved oxygen meter model DO-5512SD, and the accuracy of dissolved oxygen is ± 0.4 mg/L at $23 \pm 5^\circ\text{C}$.
- pH meter: a significant instrument to measure pH value in a water sample, also to monitor the reaction kinetics.
- Pressure gauge (Manometer): apparatus for measuring air pressure supplement into the system to vary the limit of dissolved oxygen saturation. Moreover, the energy consumption can be explained.
- UV Spectrophotometer

3.3.2 Chemical reagents

Several chemical reagents are used in this research experiment, listed as the following.

- Sodium Sulphite (Na_2SO_3)
- Sulphuric acid (H_2SO_4)
- Cobalt (III) Chloride (CoCl_3)
- Potassium permanganate (KMnO_4)
- Ferrous hydroxide ($\text{Fe}(\text{OH})_2$)

- Hydroxylamine solution ($\text{NH}_2\text{OH}\cdot\text{HCl}$)
- Sodium acetate solution ($\text{NaC}_2\text{H}_3\text{O}_2\cdot 3\text{H}_2\text{O}$)
- Ferric Hydroxide ($\text{Fe}(\text{OH})_3$)
- Hydrochloric acid (HCl)
- Sodium hydroxide (NaOH)
- Ammonium acetate buffer solution ($\text{NH}_4\text{C}_2\text{H}_3\text{O}_2$)
- 1, 10-Phenanthroline monohydrate ($\text{C}_{12}\text{H}_8\text{N}_2\cdot\text{H}_2\text{O}$)

3.4 Experimental procedures

To obtain the objectives of this research, five important parts will be studied. Groundwater will be synthesized with two major pollutants in groundwater such as arsenite species and ferrous iron species. Firstly, the oxygen mass transfer is tested in BCR without adding media and developed with adding solid media. Then, the effect of gas flow rate, initial ferrous iron concentration, ferric iron concentration and pH on the oxidation rate of ferrous iron is observed in a batch reactor. Indeed, arsenic removal is critically studied due to the impact of initial ferrous iron concentration, adding ferric iron concentration, and pH in groundwater synthesis; with this part, pH is adjusted to the optimum condition of arsenic treatment. After that, the precipitation of arsenic and iron is interested to study. Last but not least, the filtration and treatment of groundwater impurities to be a drinking water is studied by using membrane technology. All experiment is conducted in room temperature. Figure 3.4 shows the flowchart of an experimental procedure in this research.

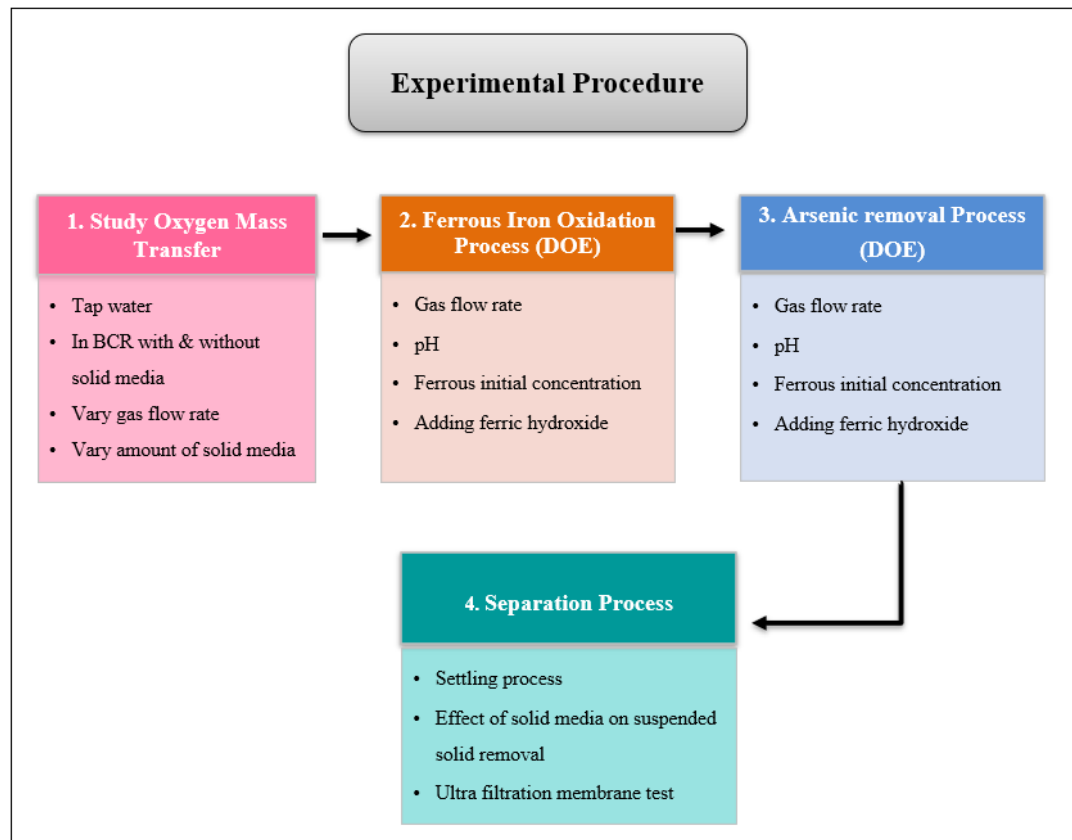


Figure 3.4 The overall flowchart of experimental procedures

3.4.1 Groundwater synthesis

The groundwater solution in this study is synthesized by arsenite and ferrous iron in de-aerated tap water to process in the batch reactor.

Arsenic (As^{3+}): In this case study, the total concentration of arsenic is obtained from dissolved As_2O_3 which bases on the concentration of arsenite. The stock solution is approximately prepared at the concentration of 1000 mg/l of As_2O_3 in distilled water and stored at 4°C in the refrigerator for using throughout the work. In this study, Arsenite represents the total concentration of arsenic in groundwater.

Iron (Fe^{2+}): The concentration of ferrous in groundwater is groomed by dissolving ferrous iron sulfite ($\text{FeSO}_4 \cdot 7\text{H}_2\text{O}$) in de-aerated tap water which has a DO concentration less than 10 percent of saturated DO level (El Azher et al., 2008). The maximum concentration of ferrous iron is based on actual concentration in

groundwater which is around 50 mg/L. Thus, the groundwater is synthesized with 100 µg/L of initial concentration of arsenite equivalent to $[\text{As(III)}]_0:[\text{Fe}]_0 \approx 1:000-1:500$.

pH: To control the pH in synthetic groundwater, hydrochloric acid (HCl) and sodium hydroxide (NaOH) is added to adjust in the prepared solution. The concentration of NaOH and HCl is diluted by distilled water to get 1 M concentration of each solution before adjusting into the groundwater sample.

3.4.2 Effect of solid media addition on mass transfer rate in BCR

(A) Without solid media addition

In the aeration part, the alternative concentration of dissolved oxygen (DO) in groundwater is the main point of research. The measurement of DO level is conducted when DO in tap water is reduced to lower than 10 percent of saturation point. The sodium sulfite (Na_2SO_3) and cobalt chloride (CoCl_2) is used to decrease DO level in the tap water sample and as a catalyst, respectively (He, Petiraksakul, and Meesapya, 2003). Eq. 3.1 shows the reaction of oxygen reduction in the system.



According to this stoichiometry, 1 mole of oxygen can produce 2 moles of sodium sulfite; therefore, the sodium sulfite is needed 8 kg to decline 1 kg of DO. Moreover, the catalyst should be added around 0.5 mg/L in solution. The air pump, used for air supplement in this system; connected with diffuser, rotameter, and manometer to check air flow rate, and determine the pressure of air pump. However, the air pump is turned on after the DO level is reduced to the desired level (less than 10 percent of saturated point in water). The performance of the aeration process is continued until the DO concentration of the water sample increases to more than 80% of saturated point as mentioned in Appendix 2 at room temperature (Stenstrom, Leu, and Jiang, 2006). Moreover, the gas flow rate is varied from 3, 6, 8, 10, 12, 14, 16 LPM to investigate its effect in the system.

(B) With solid media addition

There are many methods to improve the characteristics of gas-liquid hydrodynamic and oxygen mass transfer operation in the system, for instance, the development of

reactor structures design or applying the internal configuration. According to a previous study, an interesting effect of adding solid plastic media in the gas-liquid phase of the aeration process has demonstrated the enhancement of oxygen mass transfer and hydrodynamic mechanism in bubble column reactor (BCR) due to the increasing of surface contact area between gas and liquid. Sastaravet et al.(2020) has studied various the shape of solid media types (ring, sphere, cylinder, and square) to observe oxygen mass transfer and bubble hydrodynamic characteristics. Moreover, the influent concentration of solid media (square shape) was ranged from 2% to 10%, and V_g from 0.6 to 1cm/s (Sastaravet et al., 2020). Among these different solid plastic media, ring media was known as the most influential for rally K_{La} value in BCR.





In this case study, the solid ring plastic and the different kind of sponge media are chosen to study the improvement of mass transfer coefficient (K_{La}) in BCR. The sponge applications to control membrane fouling due to declining turbidity in water during the ferric iron precipitation, also to increase oxygen mass transfer rate in aeration process (Psoch and Schiewer, 2006). Moreover, the various types of sponge media, and varying solid media concentration are considered to provide the different effect of oxygen mass transfer rate. However, solid ring media is selected to compare the efficiency with cube sponge media in this study in order to confirm the previous research. For solid ring media, polypropylene (PP) is interested as the most proper material due to its density of 946 kg/m^3 which is slightly different from water's density (997 kg/m^3) (Wongwailikhit et al., 2018), polyurethanes is material for sponge media. The addition of solid media is not only lowering the bubble velocity but also breaks down the bubble size in the reactor.

The condition of solid media study is mentioned in Table 3.1. In this part, sodium sulfite (Na_2SO_3) and cobalt chloride (CoCl_2) is also used to reduce DO level in tap water. The solid media properties such as size, density, and shape; are described Table 3.2.

Table 3.1 Term condition of solid media study

Type of solid media	Qg (LPM) at 10% of solid media	Solid media (v%/v) at 12 LPM
1. Plastic ring	3, 6, 8, 10, 12, 14, 16	3%, 5%, 10%,
2. Scouring sponge	3, 6, 8, 10, 12, 14, 16	3%, 5%, 10%,
3. Scouring pad	3, 6, 8, 10, 12, 14, 16	3%, 5%, 10%,
4. Black carbon sponge	3, 6, 8, 10, 12, 14, 16	3%, 5%, 10%,

Table 3.2 The details of physical properties and characteristics of solid media (Sastaravet et al., 2020)

Parameters	Ring Media	Plastic Sourcing sponge	Sourcing pad	Black carbon sponge
Diameter (mm)	5.00	10.00	10.00	10.00
Surface area (mm ²)	156.69	150	150	150
Volume (mm ³)	49.48	125	125	125
Density (g/mm ³)	9.50 × 10 ⁻⁴	0.48 to 9.6 × 10 ⁻⁴	11.5 × 10 ⁻⁴	2.267 × 10 ⁻⁴
Picture				

3.4.3 Optimization of Ferrous oxidation process

The objective of this part is to investigate the affected parameters of the ferrous oxidation process including initial soluble ferrous iron concentration $[\text{Fe}^{2+}]_0$, the autocatalytic insoluble ferric iron $[\text{Fe}^{3+}]_0$, pH value, and gas flow rate (Qg). Ferrous iron presents as soluble in groundwater; therefore, the oxidation process is a famous and convenient method to transfer soluble form to insoluble iron. After that, ferric iron or an insoluble form of iron starts to precipitate, so an iron can be removed out by the separation process.

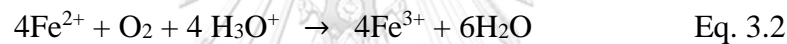
Eighteen liters of ferrous synthetic solution sample is prepared for an experiment in BCR by dissolving Iron sulfite ($\text{FeSO}_4 \cdot 7\text{H}_2\text{O}$) in de-aerated tap water that have to DO less than 10% of saturated level (El Azher et al., 2008), and supplying nitrogen gas (N_2) for mixing before starting experiment. All experiments are designed for Design of Experiment (DOE) by Minitab computer program, and carried out at room temperature and pressure around 1atm. After sampling immediately, the sample is mixed with HCl 2% in order to prevent further ferrous oxidation; then, it is added 1,10-phenanthroline to react with ferrous iron and resulted in a color. Last, the ferrous iron concentration is measured by a UV spectrophotometer. Meanwhile, the DO level and concentration of iron is analyzed as a function of time during the experiment by DO meter and Phenanthroline method, respectively. Table 3.2 indicates the different conditions of influent parameters on the ferrous iron oxidation process.

Table 3.3 The influent parameters on ferrous oxidation

Parameter	Value
<ul style="list-style-type: none"> Fixed variable 	
Reactor class	Regular BCR with 18 L
Gas-phase (absorbate)	Oxygen
Liquid phase (absorbent)	Synthesis groundwater
Temperature / Pressure	$27 \pm 2^\circ\text{C} / 1 \text{ atm}$
<ul style="list-style-type: none"> Independent variable 	

Gas flow rate	8-16 LPM
Initial concentration of ferrous iron	5-50 mg/L
Initial pH	5-8 (± 0.2)
Adding autocatalytic ferric hydroxide	0-25 mg/L
Operating time	5-25min
<ul style="list-style-type: none"> Dependent variable 	
Removal efficiency	Ferrous concentration

The dissolved oxygen (DO), pH value, ferrous and ferric iron concentration are monitored over time by DO meter, pH meter, and UV spectrometer (following Phenanthroline method); respectively. Stoichiometry of ferrous iron oxidized into ferric iron by mean oxygen following two steps and expressed as Eq. 3.2 and 3.3.



The concentration of ferrous iron can be determined following Eq. 3.4 below.

$$-\frac{d[\text{Fe}^{2+}]}{dt} = k[\text{Fe}^{2+}][\text{Fe}^{2+}]^2[\text{O}_2] \quad \text{Eq. 3.4}$$

3.4.4 Optimization of arsenic and iron removal in co-precipitation process

Arsenic is predominantly as arsenite (As(III)), which is more toxic and mobile than arsenate (As(V)), therefore, oxidizing it from arsenite to arsenate is highly desirable for reducing its mobility as well as for arsenic removal before using coagulation, sorption, and membrane filtration technologies. In this section, the arsenic removal condition is optimized with different initial concentrations of Fe^{2+} & adding Fe^{3+} , pH, Qg and time. The experiment is conducted by using 18 liter of synthetic groundwater in a bubble column reactor. As mentioned above, the groundwater sample is synthesized with various ferrous initial concentrations but the arsenic initial concentration in groundwater is constantly 100 $\mu\text{g/L}$. Therefore, the arsenic stock solution is diluted by deoxygenated tap water to obtain the synthetic groundwater with the desirable concentration.

For DO measurement, the DO meter probe is submerged in a bubble column reactor to analyze dissolved oxygen during the experiments. After sampling, 2% of HCl is mixed to prevent further ferrous oxidation before analysis. Next, the solution is filtered by using filter with size 0.45 μm to avoid the noise of suspended solids in solution. The experiment is processed at room temperature. The total concentration of arsenic and iron are determined as the main parameter for removal efficiency in this section. Samples are acidified by few drops of 50% HNO_3 for a 20 mL water sample and stored for analysis. The detailed condition of experimental parameters is described in Table 3.4.

Table 3.4 Condition of each parameter for arsenic removal experiment

Parameter	Value
<ul style="list-style-type: none"> Fixed variable 	
Reactor class	Regular BCR with 18 L
Gas-phase (absorbate)	Oxygen
Liquid phase (absorbent)	Synthesis groundwater
Temperature / Pressure	$27 \pm 2^\circ\text{C} / 1 \text{ atm}$
<ul style="list-style-type: none"> Independent variable 	
Flow rate (Qg)	8-16LPM
Initial concentration of ferrous iron	5-50 mg/L
pH	5-8 (± 0.2)
Adding autocatalytic ferric hydroxide	0-25 mg/L
Operating time	5-40min
<ul style="list-style-type: none"> Dependent variable 	
Removal efficiency	Fe^{2+} & total arsenic

3.4.5 Separation process

(A) Settling Process

Ferric particles form as a result of ferrous iron oxidation, and arsenic was also predicted to be eliminated by co-oxidation/precipitation with ferrous iron oxidation, as well as adsorption onto ferric hydroxide. The separation of these ferric particles was removed after reaction operations.

The process of gravity sedimentation was examined first, followed by the method of membrane filtration. The sedimentation process is considered to study before membrane filtration process in order to reduce blocking by suspended solid particles from ferrous oxidation process. Normally, sedimentation process is suggested to follow by filtration process to get a completely removal of insoluble iron (S. Chaturvedi and P. N. J. D. Dave, 2012). This section experimented the fraction removal of insoluble ferric particles in the BCR as the batch settling column test. After completed the optimization process from previous section by DOE, batch settling column reactor was conducted. The settling process is performed by gravity force to settle all particles. Water samples withdrawn at various water depth in the bubble column for a periodic time of 30 min until 300 min. Batch settling studied in small rectangular reactor with 12x9x60 cm and sample height is 60 cm. Five sampling ports named Port I, Port II, Port III, Port IV and Port V place at 15, 25, 35, 45 and 55 cm from the top of water surface, respectively. After that, membrane filtration process is applied to treat all impurities and pass WHO's water drinking and supply standard.

(B) Membrane filtration

The filtration is carried out in a batch module through micro membrane filtration. Microfiltration (MF) is selected in this case study because the size of ferric particles with arsenic after oxidation process is ranged from 1.5 to 50 μ m, so MF is effective to remove suspended solid at a high concentration. The porosity of the MF membrane is lower than 1 μ m, it should be a suitable separation process to treat the suspended solids particle from co-precipitation (Ellis, Bouchard, and Lantagne, 2000). However, if effluent water quality is not reached WHO drinking standard NF or RO would be recommended.

A volume of 18 liter of groundwater sample is fed into the membrane module. The hollow fiber with the cross MF is selected for the filtration process with a size of 0.1 μm to remove remained suspended solids and some bacteria. However, pressure is the main key to membrane filter performance to avoid pressure drop by membrane fouling. Therefore, the supplying pressures are varied to find the optimum condition. The permeate flux is monitored through the filtration time.

Table 3.5 Condition of membrane filtration for suspended solids removal

Parameter	Value
<ul style="list-style-type: none"> Fixed variable 	
Reactor class	Regular BCR with 18 L
Membrane filtration	Microfiltration (Hollowfiber)
Liquid phase	Suspended solution
Temperature / Pressure	$27 \pm 2^\circ\text{C} / 1 \text{ atm}$
<ul style="list-style-type: none"> Independent variable 	
Pressure	1-3 bar
<ul style="list-style-type: none"> Dependent variable 	
Removal efficiency	Total suspended solids (TSS), Iron and arsenic

3.5 Analytical Parameters and Method

3.5.1 Dissolved oxygen concentration

The oxygen concentration illustrates the influence of air injection in synthetic groundwater by an air pump. The concentration of dissolved oxygen in water is one of the factors which impacts the ferrous and arsenite oxidation process. Therefore, the studying of dissolved oxygen concentration in the water sample has been selected in this research. The dissolved oxygen meter (DO meter) is chosen for determining dissolved oxygen concentration in groundwater due to easy operation and popular equipment. DO-5512SD is used with an SD card data logger.

3.5.2 Overall volumetric mass transfer coefficient (K_{La})

The volumetric oxygen transfer coefficient (K_{La}) is one of the parameters to determine the various phases of reactor operation by using the dynamic method. K_{La} is defined to understand the absorption rate of oxygen in a system. The measurement of DO concentration is analyzed along the time of aeration process in deoxygenation tap water (Sastaravet et al., 2020), by using DO meter. This experiment is operated until saturated DO in liquid. To calculate K_{La} , the log deficit method is practiced as Eq. 3.5 and integral form is Eq. 3.6 (Bun et al., 2019):

$$\frac{dc}{dt} = K_L a (C^* - C_t) \quad \text{Eq. 3.5}$$

$$\ln(C^* - C_t) = -K_L a \cdot t + \ln C^* \quad \text{Eq. 3.6}$$

Where C_t is the dissolved oxygen concentration in the water sample over time, and C^* is DO concentration at the saturated level. The slope of the equation provides a value of $(-K_{La})$. The values of K_{La} can be read from the slopes of $\ln(C^*-C_t)$ as a function of time and assumed it is liquid ideal-mixing. C^* could be estimated from the table of temperature and pressure standard (Appendix II) (Sastaravet et al., 2020).

The liquid side mass transfer coefficient (K_L) is the division of the volumetric mass transfer coefficient (K_{La}) with the bubble interfacial area (a). The liquid side mass transfer coefficient can be calculated by Eq. 3.7:

$$K_L = \frac{K_{La}}{a}, \quad \text{Eq. 3.7}$$

The K_{La} coefficient is one of the parameters to evaluate the system operation of the aeration process. Generally, the mass transfer K_{La} coefficient can be read from the slope of graph $\ln(C^*-C)$ with aeration time which is demonstrated in Figure 3.5 (Bun, 2015).

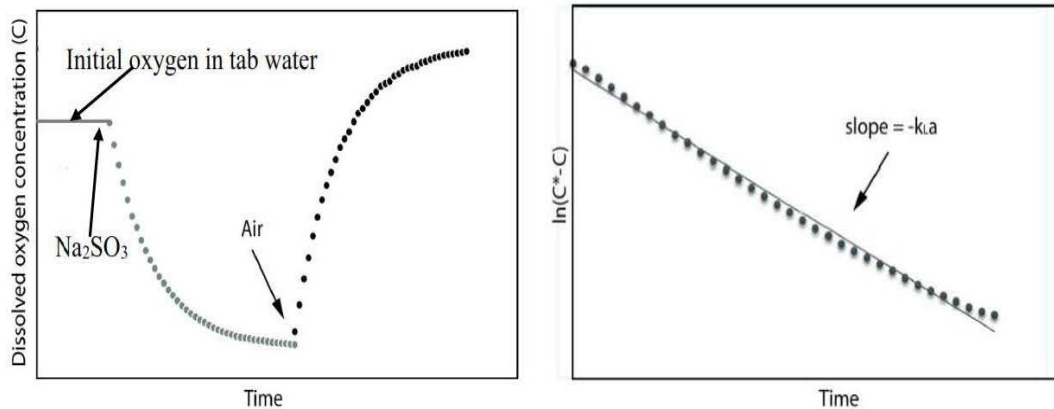


Figure 3.5 Process of oxidation and $K_L a$ coefficient obtaining (Bun, 2015)

3.5.3 Ferrous ion concentration

There are many analysis methods to determine the concentration of ferrous iron in a groundwater sample. However, the phenanthroline method is an affordable, convenient, and effective technique besides using instruments including Inductive Coupled Plasma (ICP), Atomic Absorption Spectrophotometry (AAS), Iron test kit, etc. The spectrophotometric is the support apparatus for the Phenanthroline method to analyze iron concentration by using 1, 10 phenanthrolines.

A brief description was mentioned here. To determine ferrous iron, the sample is acidified by 1 mL HCl for 50 mL sample at the time of collection immediately. After that, adding 20 mL phenanthroline solution (prepared by dissolving 100 mg of 1,10-phenanthroline monohydrate in 100 mL DI water by stirring and adding 2 drops of HCl) and 10 mL $\text{NH}_4\text{C}_2\text{H}_3\text{O}_2$ solution (prepared by dissolving 250 g $\text{NH}_4\text{C}_2\text{H}_3\text{O}_2$ in 150 mL DI water before adding 700 mL glacial acetic acid) with vigorous stirring. Then, the solution is diluted to 100 mL and keeping in the dark space for 5 to 10 minutes. Last, it is measured the color intensity by using UV-Vis Spectrophotometer at 510 nm wavelength. Ferrous iron concentration can be calculated from Eq. 3.15.

$$\text{mg-Fe/L} = \frac{\mu\text{g-Fe (in 100 mL final volume)}}{\text{mL sample}} \quad \text{Eq. 3.15}$$

For total iron, add 2 mL HCl and 1 mL hydroxylamine solution (prepared by dissolving 10 g $\text{NH}_2\text{OH}\cdot\text{HCl}$ in 100 mL DI water) into a 50 mL water sample. Then, add a few glass beads and heat to boiling until the volume is reduced to 15 to 20 mL

to ensure dissolution of all the iron. If the sample is ashed, take up residue in 2 mL HCl and 5 mL water. Then, cool the samples to room temperature and transfer to a 50 mL or 100 mL volumetric flask or Nessler tube. Add 10 mL $\text{NH}_4\text{C}_2\text{H}_3\text{O}_2$ solution and 4 mL phenanthroline solution and dilute to mark with water. Last, mix thoroughly and allow a minimum of 10 minutes for maximum color development before measuring the color intensity by UV-Vis Spectrophotometer. Its concentration can be calculated by Eq. 3.15.

3.5.4 Arsenic concentration

In this study, the concentration of arsenic was measured by Inductively Coupled Plasma (ICP). However, the various experiment was aimed to measure arsenite only. Therefore, arsenite and arsenate were speciated before sending for analysis. Arsenic speciation cartridge was used to speciate arsenic. This disposable cartridge placed an adsorbent, which removes arsenate (As(V)) but does not adsorb arsenite (As(III)). Speciation of arsenic is accurate under the conditions: sample pH values between 4 and 9, arsenate concentration less than 500 $\mu\text{g/L}$ per cartridge or use two cartridges in series for a concentration between 500 and 5000 $\mu\text{g/L}$, sample volume between 20 and 60 mL, and filtration rate approximate 60 ± 30 mL/min.

For total arsenic measurement, it was directly prepared by acidifying with 50% HNO_3 about few drops for a 20 mL water sample. The arsenic concentration of filtrated sample through arsenic speciation cartridge represents arsenite concentration while the non-filtrated sample is total arsenic. It should be noted that the ferric particles present simultaneously in a water sample, samples have to be firstly filtrated through 0.45 μm to remove particulate particles before arsenic speciation and analysis. Therefore, the measured arsenic concentration should be the soluble arsenic concentration.

3.5.5 Removal efficiency

To understand the removal efficiency of ferrous iron and arsenic in groundwater, the influent and effluent concentration of pollutants is necessary to analyze. This parameter is indicated the effective or ineffective performance of the groundwater treatment systems including condition parameters, reactor scale, etc. The removal

efficiency can be defined by the proportion between the initial and final concentration of arsenic or ferrous iron concentration in the synthetic water sample as showed below Eq. 3.16.

$$\%R = \frac{C_i - C_f}{C_i} \times 100 \quad \text{Eq. 3.16}$$

Where: %R: the removal efficiency parameter (%), C_i : the initial concentration of pollutant (mg/L), C_f : the final concentration of pollutant (mg/L).

3.5.6 Membrane permeability

The performance of permeation was at constant temperature 25°C, and permeability of membrane can be directly calculated by Eq. 3.17 shown below:

$$J = \frac{\Delta V}{PA\Delta t} \quad \text{Eq. 3.17}$$

J: water flux, P: membrane pressure, ΔV : different volume, A: membrnae area, Δt : changing time

3.6 Design of Experiment (DOE)

This study is to achieve high ferrous iron and arsenic removal efficiency from oxidation process and co-precipitation process, respectively. The Design of Experiment (DOE) is a very useful tool to evaluate and optimize the influent factors such as initial ferrous iron concentration, adding ferric iron concentration, pH value, gas flow rate (Q_g) on ferrous oxidation process; also effective parameters on arsenic removal in co-precipitation including initial ferrous iron concentration, adding ferric iron concentration and pH value. This predicted model could identify the condition of the experiment and determine the relationship between factors affecting oxidation process and co-precipitation process, and the response of this process.

Minitab 17 statistical software is selected to design the experimental conditions using DOE methodology. In this software, the DOE has four different types of designs such as Factorial design, Response Surface Methodology, Mixture, and Taguchi design. In this study, the central composite design of response surface methodology (CCD-RSM) is selected for experimental design and optimization with the variation of four factors for ferrous iron oxidation experiment, and 3 factors for arsenic removal in co-

precipitation process ranging from low to high levels as shown in Table 3.5 and Table 3.6. After completing the experiment, results are input back into the software then the analytical and graphic tools were provided.

Table 3.6 Factors designed and its levels for optimizing ferrous oxidation process

Factors	Symbol	Unit	Levels	
			Min	Max
Initial [Fe²⁺]	A	mg/L	5	50
Adding [Fe³⁺]	B	mg/L	5	50
pH value	C	-	5	9
Q_g	D	LPM	3	16

Table 3.7 Factors designed and its levels for optimizing arsenic and iron removal in co-precipitation process

Factors	Symbol	Unit	Levels	
			Min	Max
Initial [Fe²⁺]	A ₁	mg/L	5	50
Adding [Fe³⁺]	B ₁	mg/L	5	50
pH value	C ₁	-	5	9

The Analysis of Variance (ANOVA) is also employed to validate the predicted model and evaluate the statistical effect of each factor. The result analysis is carried out using F-test and p-value with 95% confidence level of statistical analysis. The second-order polynomial equation (Equation 3.1) describes the connection between the independent variables and the responses.

$$y = \beta_0 + \sum_{i=1}^K \beta_i x_i + \sum_{i=1}^K \beta_{ii} x_i^2 + \sum_{i=1}^K \sum_{i < j} \beta_{ij} x_i x_j + \epsilon \quad \text{Eq. 3.1}$$

where y : the predicted response by the model, β_0 : a constant, β_i : the linear coefficient, β_{ii} : the second-order coefficient, β_{ij} : the interaction coefficient, x_i and x_j : the independent factor, k : number of factors, ϵ : noise or error



CHAPTER 4

RESULTS AND DISCUSSIONS

This chapter the experimental and analytical results are described. To completely understand, the results are separated and group into four main parts as follows:

1. Study the effect of solid media addition on mass transfer and bubble dynamics in BCR
 - Mass transfer performance : Volumetric mass transfer coefficient (K_{La})
 - Bubble hydrodynamics : bubble size distribution (D_B), bubble rising velocity (U_B) and interfacial area (a)
 - Solid media characteristic: density and contact angle
2. Optimization of ferrous oxidation process
 - Experiment design by using DOE in Minitab computer program
 - Using Central Composite Design of Response Surface Methodology (CCD-RSM) as an optimization process.
 - Empirical model for ferrous oxidation
 - Process optimization
3. Optimization of ferrous and arsenic removal in co-precipitation process
 - Experiment design by using DOE in Minitab computer program
 - Using Central Composite Design of Response Surface Methodology (CCD-RSM) as an optimization process.
 - Empirical model for ferrous oxidation
 - Process optimization
4. Separation process
 - Settling process: gravity velocity
 - Effect of solid media on suspended solid removal
 - Ultra-filtration membrane: performance test by comparison between before settling process, after settling process, and raw groundwater

4.1 Effect of adding solid media on mass transfer rate

The expected results of this study were divided into three main points: the impact of adding solid media types on mass transfer (K_{La}), hydrodynamic characteristic and understanding the wettability of solid medias.

4.1.1 Mass transfer coefficient (K_{La})

(A) Effect of gas velocity

The overall mass transfer coefficient (K_{La}) is the most critical parameter for determining the system's effective oxygen transfer performance. The betterment of the K_{La} coefficient is related to the superficial gas velocity parameter, as previously established (Zheng et al., 2018). Figure 4.1 indicates the results of the mass transfer coefficient in which solid media loading 5% was used to observe the influence of varying gas velocity (V_g). The K_{La} coefficient value significantly rose for all solid media types, corresponding to an increase in gas velocity both with and without solid media addition, which is precisely like Sastaravet et al. (Sastaravet et al., 2020). The mass transfer coefficient was dramatically improved from 9% - 80% by adding 5% solid media, which is higher than not adding solid media. The scouring sponge and plastic ring provided the highest K_{La} coefficient around 0.005 - 0.021 s^{-1} compared to other media types. However, the scouring pad and activated carbon foam obtained K_{La} coefficient around 0.004 - 0.018 s^{-1} compared to the non-addition media of 0.003 - 0.017 s^{-1} . This low performance is probably because of their density, as scouring pad density is ($1.15 \times 10^{-3} \text{ g/mm}^3$) higher than water density ($0.997 \times 10^{-3} \text{ g/mm}^3$) but activated carbon foam is much lower ($0.2267 \times 10^{-3} \text{ g/mm}^3$). A lower density of solid media results in a greater terminal velocity, which leads to a higher U_B value and, as a result, a lower K_{La} value. (Sastaravet et al., 2020). In contrast, higher density has a lower terminal velocity and accumulates at the bottom of the reactor; therefore, bubble coalescence will be promoted, for instant, scouring pad density. However, scouring sponge (its density is increased when it fully absorbs water) and plastic ring density is almost like water density, resulting in higher K_{La} because its density is not too low and high. These results proved that different densities of solid media can positively or negatively affect the K_{La} coefficient. Thus,

solid media density that is very higher than water density is not recommended. Moreover, the K_{La} coefficient is ultimately increased as gas velocity increases with solid media (Kim and Kim, 1990). This effect is due to the number of bubbles growing via increasing V_g ; thus, gas-liquid interfacial area (a) is also considered to rise (Ferreira et al., 2010). Therefore, solid media addition and higher gas velocity are mainly influenced by raising the K_{La} coefficient in BCR.

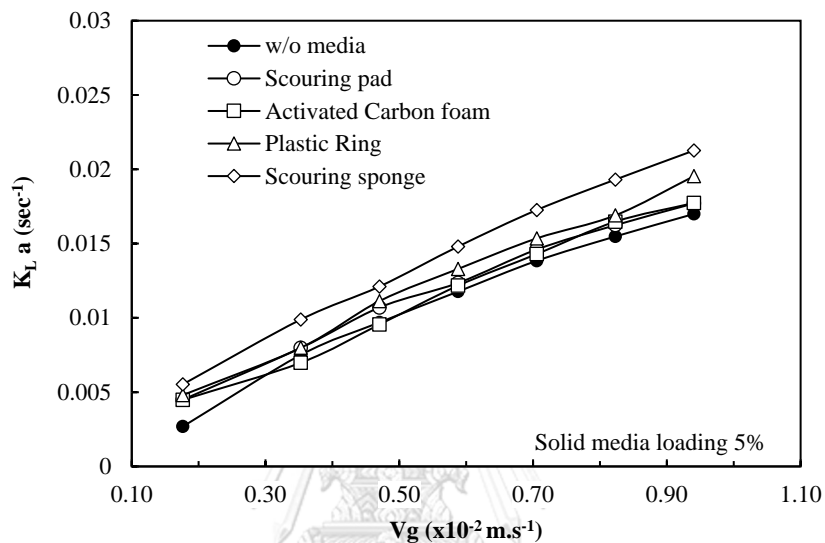


Figure 4.1 Effect of various ranges gas velocity (V_g) on overall mass transfer coefficient (K_{La}) of each solid media types

(B) Effect of solid media loading

A superficial gas velocity of $0.7 \times 10^{-2} \text{ m.s}^{-1}$ was chosen for discussion in this part because of the limitation in a bubble column reactor with a high solid media concentration. Figure 4.2 exhibits the effect of adding various solid media types and their concentration on mass transfer coefficient (K_{La}) in a bubble column reactor. The consequences of adding different solid media types and loading acquire a dissimilar K_{La} coefficient value. Two patterns of effects on K_{La} were categorized from the operation of solid media in BCR to discuss without adding solid media, i.e., scouring sponge and pad, and plastic ring and activated carbon foam. Firstly, the K_{La} coefficient rose rapidly from $0.011 - 0.015 \text{ s}^{-1}$ at 3% loading of scouring sponge and scouring pad. However, after increasing scouring sponge and scouring pad loading from 5% to 10%, the K_{La} coefficient remained constant at 0.015 s^{-1} for scouring

sponge and decreased to 0.013 s^{-1} for scouring pad. Hence, the optimum scouring sponge and scouring pad loading was 3% for obtaining an excellent K_{La} coefficient at $V_g 0.7 \times 10^{-2} \text{ m.s}^{-1}$. This response could be explained by the fact that both solid media offer the bubble coalescence phenomena at higher loading. Secondly, adding 3% of plastic ring did not affect the K_{La} coefficient at $V_g 0.7 \times 10^{-2} \text{ m/s}$ due to low loading plastic ring media not being able to break up bubble size and lower gas velocity. In addition, activated carbon foam provided a slightly decreased K_{La} coefficient value of $0.011 - 0.010 \text{ s}^{-1}$ compared to without solid media. As a result, a very small loading of solid media results in a more significant number of bubble collisions to heighten the coalescence phenomenon (Zheng et al., 2018), in which K_{La} was decreased. In contrast, 5% - 10% solid loading plastic ring and activated carbon foam raised the K_{La} coefficient value. The increase in K_{La} coefficient at higher solid media concentration may be due to the bubble break-up rate and bubble rising velocity mechanism; therefore, increasing gas-liquid interfacial area and K_{La} , as mentioned by Sastaravet et al. (Sastaravet et al., 2020). Briefly, adding solid media can positively and negatively impact K_{La} depending on solid media type and its loading.

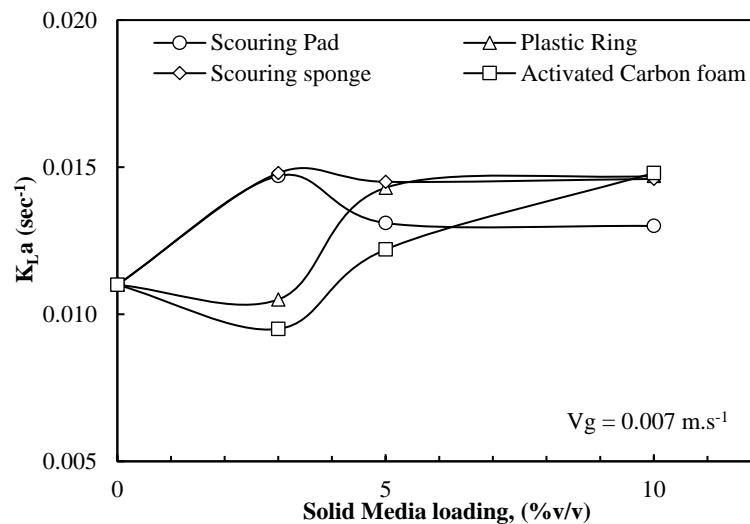


Figure 4.2 Impact of solid media loading on K_{La} coefficient with gas velocity $0.70 \times 10^{-2} \text{ m.s}^{-1}$

4.1.2 Bubble dynamics

The 3% solid media loading was selected for further study since the optimal mass transfer coefficient was obtained. The results obtained with four different solid media types and different superficial gas velocity ranges (0.35 to $0.94 \times 10^{-2} \text{ m.s}^{-1}$) are discussed in this section

(A) Bubble diameter (D_B)

Figure 4.3 demonstrates the mean bubble diameter by adding 3% solid media with various superficial gas velocities (V_g) in BCR. The bubble size distribution is increased as the accrued gas velocity increases from $0.3 - 0.94 \times 10^{-2} \text{ m.s}^{-1}$ in the case of no solid media. It is due to the bubble coalescence boost at greater airflow. As mentioned in DeSwart et al. (Zheng et al., 2018) and Wongwailikhit et al. (Wongwailikhit et al., 2018), three significant bubble behaviours occur with the addition of solid-phase, including promoting bubble break-up, bubble coalescence rate, and decelerating rising velocity. Larger bubbles were discovered at lower gas flow ($0.94 \times 10^{-2} \text{ m.s}^{-1}$), and 3% added solid media loading. This means that the ineffective addition of solid media to break bubble size at low V_g but developed coalescence rate. At a gas velocity of $0.94 \times 10^{-2} \text{ m.s}^{-1}$, the plastic ring, and scouring pad media impacted to break down the bubble size from 4.51 mm to 4.24 mm and 4.47 mm , respectively. This is due to the increasing bubble breaking rate and turbulence of the liquid mixing at a higher gas flow rate in BCR, decreasing the mean bubble size. Plastic ring media was discovered to have the effect on bubble break-up rate due to its harder edges and the ability to keep bubbles inside at higher gas flows (Kim and Kim, 1990) (Sastaravet et al., 2020). However, the scouring sponge, scouring pad, and activated carbon foam were unable to break bubble diameter because of their soft surface. Thus, only plastic ring is influent to bubble break up rate at $V_g 0.9 \times 10^{-2} \text{ m.s}^{-1}$.

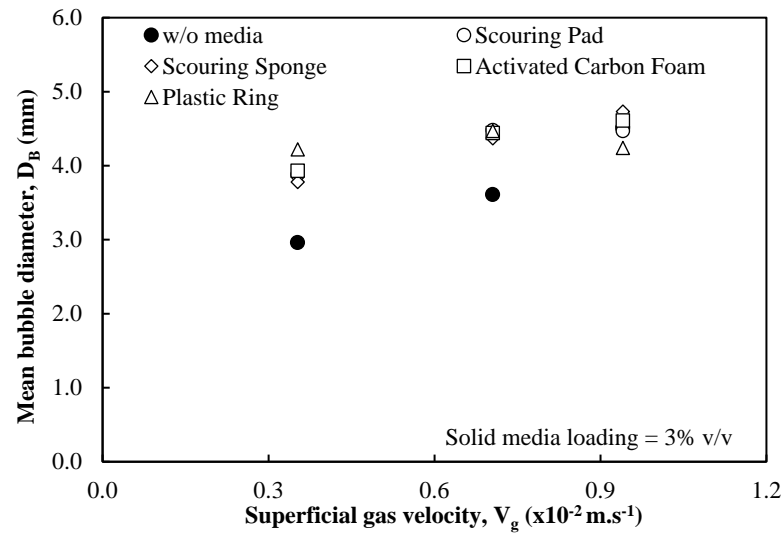


Figure 4.3 Effect of different solid media types on mean bubble diameter by varying V_g

(B) Bubble rising velocity (U_B)

Bubble rising velocity (U_B) is a significant parameter to clearly understand the effect of each solid media on hydrodynamic characteristics for a three-phase bubble column reactor. The impact of various solid media types by variation in gas velocity on U_B is described in Figure 4.4. While bubble rising velocity was enhanced with increasing V_g for without solid media adding, and decreased U_B with present solid media. It may be because solid media enhances flow resistance, resulting in lower liquid velocity, which can also be the moving bed to catch or block the bubbles from free rising. At lower V_g , activated carbon foam showed a slight change in U_B compared to without solid media. This could be because activated carbon foam is very light (low density) and cannot move properly at low gas velocity in bubble column reactor. Thus, this media stays at the surface water and poor ability to block bubble from free rising (shown in Figure 4.5). The scouring sponge provided the maximum lower U_B of 0.17 - 0.11 m/s at a gas velocity of $0.3 - 0.6 \times 10^{-2} \text{ m.s}^{-1}$, respectively. However, at higher gas velocity ($0.94 \times 10^{-2} \text{ m.s}^{-1}$), the scouring sponge increased bubble rising velocity to 0.22 m/s. This might be because of two main reasons, firstly the presence of less scouring sponge may not have lowered the liquid velocity as when sponge get soaked and saturated, its density is almost equal to water density, and secondly, the drag force

might decrease at highest V_g . It also responds to the results in Fig. 2 that obtained an optimum K_{La} coefficient at $V_g 0.7 \times 10^{-2} \text{ m.s}^{-1}$ by scouring sponge loading (3%).

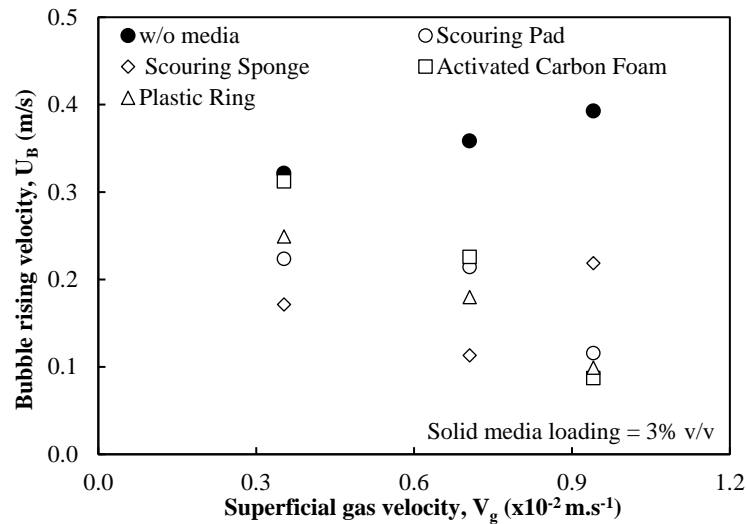


Figure 4.4 Effect of solid media types on bubble rising velocity by varying V_g

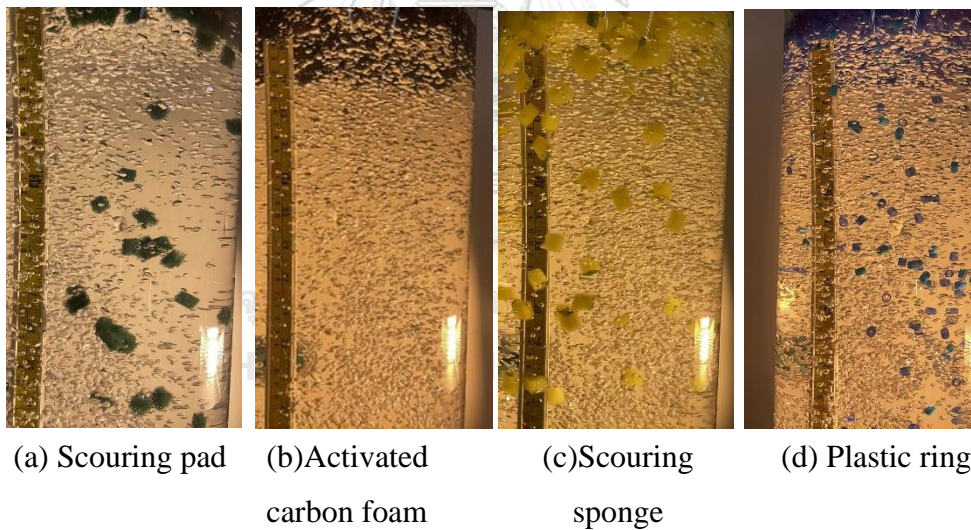


Figure 4.5 Picture of each solid media performance with $V_g 0.3 \times 10^{-2} \text{ m.s}^{-1}$

(C) Interfacial area (a)

This part aims to determine bubble interfacial area in bubble column based on the results from a previous part which studied at 3% of solid media and varying V_g ($0.35 - 0.94 \times 10^{-2} \text{ m.s}^{-1}$). Figure 4.6 indicates the results of the bubble interfacial area (a) in the bubble column reactor for different operation conditions. It can be seen that the

plastic ring and activated carbon foam added into the BCR resulted in the highest interfacial area while that of scouring sponge was decreased at the highest V_g . It can be explained that the optimum condition of scouring sponge (3% loading) is at $V_g 0.70 \times 10^{-2} \text{ m.s}^{-1}$ because increasing V_g may cause to decrease drag force in a system with presence of scouring sponge. However, adding a scouring pad, activated carbon foam, and plastic ring to the BCR tended to increase the interfacial area as superficial gas velocity increased. This may be because adding solid media with the low terminal rising velocity has the bubble break-up mechanism and bubble captured, causing to the smaller air bubble (Sastaravet et al., 2020). Another remark is that adding 3% of plastic ring and activated carbon foam did not improve interfacial area at a very low $V_g (0.35 \times 10^{-2} \text{ m.s}^{-1})$. Thus, 3% of scouring sponge is recommended to be used at $0.70 \times 10^{-2} \text{ m.s}^{-1}$ to get the optimum condition, while other media (scouring pad, plastic ring, and activated carbon foam) could be used at high V_g .

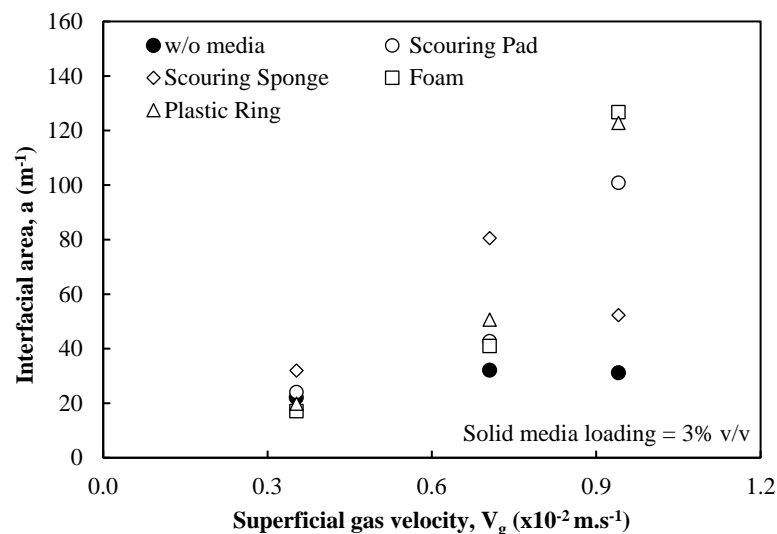


Figure 4.6 Interfacial area of each solid media by variation V_g

4.1.3 Physical mechanism of solid media

Figure 4.7 illustrates the contact angle of the scouring sponge, scouring pad, and activated carbon foam. The contact angle of the scouring pad is only $71.18^\circ \pm 3$, while the scouring sponge and activated carbon foam are $109.17^\circ \pm 5$ and $138.06^\circ \pm 6$, respectively. However, due to its surface is rough which it could cause some error in experiment. In addition, the plastic ring is a kind of PVC, hydrophobic with a contact

angle of 103° (Ferreira et al., 2010). This result means the scouring pad is the most wettable, followed by the plastic ring, scouring sponge, and activated carbon foam. Since the scouring pad exhibits as hydrophilic which absorbed and accumulated water (Kratochvil, Manna, and Lynn, 2017) at the bottom of the reactor, where bubble coalescence appeared by adding too much solid media concentration. It answered the previous section (Fig. 4.2) that the higher loading of the scouring pad resulted in decreasing K_{LA} coefficient. Therefore, the scouring pad was not suggested for use at high loading in the gas-liquid-solid reactor because of its low properties. Activated carbon foam is superhydrophobic and is made with large cell walls and holes through which liquid and air can easily travel. Its properties affect its performance similarly to plastic ring media. A scouring sponge was found to have a hydrophobic property, yet the water can be absorbed onto a sponge surface by the balance between adhesive and cohesive forces (Oberli et al., 2014). The scouring sponge was ducked through external force (Brite, 2021) from the air pump to cause the turbulence flow or mixing in BCR. It might be due to external pressure that the sponge could absorb some water into its micropores. Thus, there will be an interaction between microbubbles inside the sponge body with water and form two emulsion types: air-in-water and water-in-air. Indeed, the micropores of sponge could have three distinct interfacial areas: solid-liquid, solid-gas, and liquid-gas. Hence, the scouring sponge may contain microbubbles and attach some bubbles to its surface layer, affecting its gas holdup (Figure 4.8). Banisi (1995) mentioned that hydrophobic particles cling to bubbles, which change their motion sufficiently to provide an extra influence on gas holdup, unlike hydrophilic particles (Banisi et al., 1995). However, the scouring sponge will float on the water surface by applying an external force to release the remaining water, as predicted by the Cassie-Baxter model (Wang et al., 2014). Due to this ability, scouring sponge is more effective than other media to enhance oxygen mass transfer in BCR.

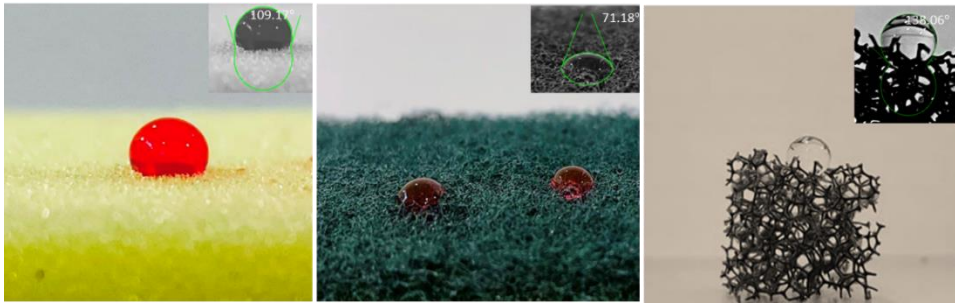


Figure 4.7 Contact angle of solid media

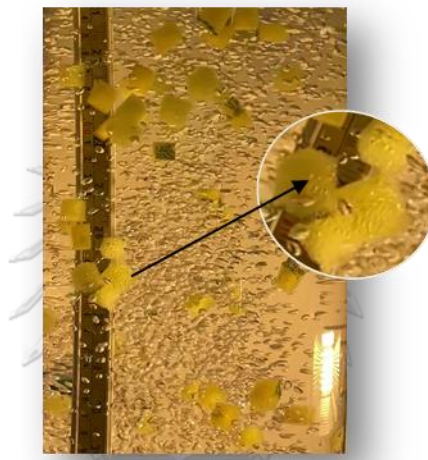


Figure 4.8 Microbubbles holding inside scouring sponge

4.1.4 Summary

This section aims to determine the relative impact of solid media types (scouring sponge, scouring pad, activated carbon foam and plastic ring) and operating conditions on oxygen mass transfer coefficient (K_{La}) and hydrodynamic bubble parameters a bubble column reactor. The performance was studied in rank gas velocity $0.35-0.94 \times 10^{-2} \text{ m.s}^{-1}$, and solid media concentration 3 - 10%. The oxygen mass transfer coefficient was studied to understand the overall effect of solid media loading and gas velocity. Then, bubble size (D_B), bubble rising (U_B), and specific interfacial area (a) were investigated in different superficial gas velocities to understand the internal mechanism of bubble hydrodynamics at the optimum loading of scouring sponge and scouring pad. The following is a summary of the experimental findings:

- Adding solid media could enhance the oxygen mass transfer coefficient in BCR around 9% – 80% compared to without solid media due to its effect on bubble break-up and bubble increasing velocity.
- The scouring sponge could provide the highest enhancement of K_{La} due to the effect of reducing bubble rising velocity, resulting in increased bubble retention time, not bubble break-up rate.
- The optimum condition of applying the scouring sponge is 3% loading with $V_g 0.7 \times 10^{-2}$; however, if gas velocity is increased, the amount of scouring sponge should be increased.

Overall, the study concludes that a scouring sponge is recommended as the most effective solid media for improving oxygen mass transfer by enhancing bubble retention time in BCR.

4.2 Optimization of process condition for ferrous oxidation

The factorial analysis was determined to define the significance of each variable and the effect on the responding variable, ferrous iron removal. The impact of process conditions was observed by varying time (t), initial pH (pH), airflow rate (Qg), initial concentration of ferrous iron ($[Fe^{2+}]_0$), and additional ferric hydroxide ($[Fe(OH)^3]_0$).

4.2.1 Experimental design by CCD-RSM

The examined variables and their levels were prepared for Central Composite Design of Response Surface Methodology (CCD-RSM) as an optimization process. Minitab's design of experiment (DOE) was used to create the experimental conditions. Table 4.1 shows the three levels of the experimental condition for five components.

Table 4.1 Investigated factors and factor levels for optimization ferrous oxidation

Factors	Unit	Factor levels		
		-1	0	+1
Air flow rate (Qg)	L/min	8	12	16
Initial pH	-	5	6.5	8
Initial concentration of ferrous iron	mg/L	5	27.5	50

([Fe ²⁺])					
Additional ferric hydroxide ([Fe(OH)₃])	mg/L	0	12.5	25	
Time operation	min	5	15	25	

Table 4.2 Experimental design by CCD-RSM for factors optimization

Run	Qg [L/min] ±5	pH [-]±5	[Fe ²⁺] ₀ [mg/L] ±5	[Fe ³⁺] ₀ [mg/L] ±5	Time [minute]
1	8	5.0	50.0	0.0	5
2	8	8.0	50.0	0.0	25
3	12	6.5	27.5	12.5	15
4	12	6.5	27.5	25.0	15
5	12	6.5	5.0	12.5	15
6	12	6.5	27.5	0.0	15
7	8	5.0	50.0	25.0	25
8	12	5.0	27.5	12.5	15
9	16	5.0	50.0	25.0	5
10	12	6.5	50.0	12.5	15
11	8	6.5	27.5	12.5	15
12	16	5.0	5.0	0.0	5
13	16	6.5	27.5	12.5	15
14	12	6.5	27.5	12.5	15
15	12	8.0	27.5	12.5	15
16	16	8.0	50.0	25.0	25
17	16	8.0	5.0	25.0	5
18	16	5.0	50.0	0.0	25
19	8	5.0	5.0	25.0	5
20	8	8.0	50.0	25.0	5
21	16	5.0	5.0	25.0	25
22	12	6.5	27.5	12.5	25
23	8	5.0	5.0	0.0	25
24	12	6.5	27.5	12.5	15
25	12	6.5	27.5	12.5	15
26	12	6.5	27.5	12.5	15
27	8	8.0	5.0	0.0	5
28	16	8.0	5.0	0.0	25
29	16	8.0	50.0	0.0	5
30	12	6.5	27.5	12.5	15
31	12	6.5	27.5	12.5	5
32	8	8.00	5.00	25.00	25

Starting pH was set between 5.0 and 8.0, with initial ferrous concentrations ranging from 5 to 50 mg/L. The optimal airflow rate for mass transfer increasing was determined to be between 8 and 16 L/min. The operation time was studied between 0 to 25 minutes. Ferric hydroxide ($\text{Fe}(\text{OH})_3$) was determined from 0 - 25 mg/L to understand the effect on ferrous oxidation removal. As a result, the 32-experiment run was implemented with a single replication, as indicated in Table 4.2.

4.2.2 Experimental result

The experiments were carried out by running experiment design as Table 4.3, with the measurement of actual pH, ferrous concentration, and total arsenic concentration being measured throughout designed operating time. The run number 32, 28, 27, and 17 provided the highest removal efficiency (99-100%), which the actual pH is around 8 same as designed condition with running initial ferrous iron 5mg/L. In contrast, the initial pH value 5 and ferrous iron 5 mg/L were also designed for experiment number 19 and 12, and the removal efficiency are 80% and 61%, respectively. Another finding is run number 7, 8, 9, and 18 which provided removal efficiency is only around 50% and design experiment was pH value 5 and higher initial ferrous loading 27.5-50 mg/L. It indicates that ferrous could not be effectively removed through oxidation at lower pH. However, excepting run number 21 & 23 experimented at lower ferrous iron (5 mg/L) and same pH 5, obtaining removal efficiency 77% and 74%, respectively. This might be because of the performance at maximum time 25 min, resulting in completely oxidizing of ferrous iron. Various experimental runs were also found as the condition resulted between 69% and 98% removal efficiency, including 3, 4, 5, 6, 10, 11, 13, 14, 22, 24, 25, 26, 30, and 31, which was examined under the initial pH 6.5. In case of ferrous iron was 27.5-50 mg/L in the synthetic water, the removal efficiency was given 68-94%, including run number 2, 15, 16 and 20.

Table 4.3 Experiment results

Run	Initial pH	Actual pH	% Removal Efficiency	Run	Initial pH	Actual pH	% Removal Efficiency
1	5.00	5.09	87	17	8.00	7.99	100
2	8.00	8.19	86	18	5.00	5.37	55
3	6.50	6.80	79	19	5.00	5.30	80
4	6.50	6.68	73	20	8.00	8.11	68
5	6.50	6.70	98	21	5.00	4.97	74
6	6.50	6.38	90	22	6.50	6.64	94
7	5.00	4.89	53	23	5.00	4.98	77
8	5.00	5.31	55	24	6.50	6.71	85
9	5.00	5.19	54	25	6.50	6.63	82
10	6.50	6.85	71	26	6.50	6.80	82
11	6.50	6.45	67	27	8.00	7.90	100
12	5.00	4.75	61	28	8.00	8.38	99
13	6.50	6.62	72	29	8.00	8.23	73
14	6.50	6.64	69	30	6.50	6.72	80
15	8.00	7.92	94	31	6.50	6.81	69
16	8.00	7.94	90	32	8.00	7.99	100

4.2.3 Empirical Model for ferrous oxidation

The empirical correlation for ferrous iron oxidation was created using a comprehensive quadratic model that included square, interaction, linear, and constant components, as well as the following major influencing factors: gas flow rate (Q_g), initial pH, initial ferrous iron concentration ($[Fe^{2+}]$), adding ferric hydroxide ($[Fe^{3+}]$), and operating time (Time). The experimental data from factor optimization was applied to define the empirical correlations. Therefore, the model prediction of ferrous iron oxidation removal efficiency (%) provided by RSM is expressed in Equation 4.1.

$$\begin{aligned} \% \text{Ferrous Removal} = & 4.3 + 5.88 Q_g + 19.5 \text{ pH} - 0.351 [Fe^{2+}] - 2.02 [Fe^{3+}] - 3.25 \text{ Time} \\ & - 0.540 Q_g * Q_g - 1.66 \text{ pH} * \text{pH} + 0.0114 [Fe^{2+}] * [Fe^{2+}] + 0.0198 [Fe^{3+}] * [Fe^{3+}] \\ & + 0.0314 \text{ Time} * \text{Time} + 0.646 Q_g * \text{pH} - 0.0006 Q_g * [Fe^{2+}] + 0.0956 Q_g * [Fe^{3+}] \end{aligned}$$

$$+ 0.0775 Qg*Time - 0.0710 pH*[Fe^{2+}] + 0.059 pH*[Fe^{3+}] + 0.233 pH*Time - 0.01170 [Fe^{2+}]*[Fe^{3+}] - 0.00223 [Fe^{2+}]*Time + 0.0101 [Fe^{3+}]*Time \text{ (Eq.4.1)}$$

Table 4.4 indicated the results of statistical analysis of variance (ANOVA) analysis for ferrous iron oxidation removal. A p-value was also defined to determine the probability of difference. Based on the F-test with 95% confidence level, the lower p-value is the more statistically significant factor whereas p-value of more than 0.05 indicates insignificance. The result showed two significant single terms were initial pH (p-value <0.01), and initial concentration of ferrous iron (p-value <0.05) while Two-way interaction was $Qg*[Fe^{3+}]$ (p-value <0.05). However, the large F-value of 12.91 and the low p-value (0.000) indicate that the model was statistically significant. This also means initial pH and initial ferrous iron concentration are the most impact factor on ferrous oxidation operation.

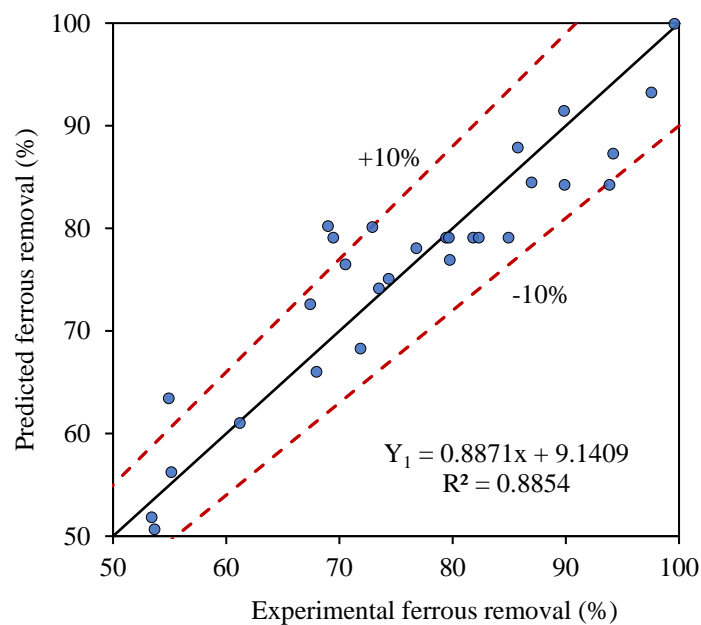


Figure 4.9 Experimental and predicted (full) ferrous removal (%)

Figure 4.9 indicates the plot of experimental and predicted result of ferrous iron removal efficiency. The R^2 of this compared results was obtained 0.8854. The second-order polynomial equation (Equation 4.1) is made up by full quadratic with 21 terms, including 5 square terms, 10 interaction terms, 5 linear terms, and another constant value. As seen in Table 4.4, this full quadratic model has an excessive number of

unimportant terms. Hence, changing the model by deleting unimportant components may result in a better expression.

Table 4.4 ANOVA results of the input factors for the ferrous removal efficiency

Source	DF	Adj SS	Adj MS	F-Value	P-Value
Model	20	5589.22	279.46	4.25	0.009
Linear	5	4035.58	807.12	12.26	0.000
Qg	1	82.99	82.99	1.26	0.285
pH	1	2529.50	2529.50	38.42	0.000
[Fe2+]	1	1269.74	1269.74	19.29	0.001
[Fe3+]	1	77.21	77.21	1.17	0.302
Time	1	76.14	76.14	1.16	0.305
Square	5	283.45	56.69	0.86	0.536
Qg*Qg	1	183.75	183.75	2.79	0.123
pH*pH	1	34.35	34.35	0.52	0.485
[Fe2+]*[Fe2+]	1	81.75	81.75	1.24	0.289
[Fe3+]*[Fe3+]	1	23.55	23.55	0.36	0.562
Time*Time	1	24.32	24.32	0.37	0.556
2-Way Interaction	10	1270.19	127.02	1.93	0.148
Qg*pH	1	240.64	240.64	3.66	0.082
Qg*[Fe2+]	1	0.05	0.05	0.00	0.978
Qg*[Fe3+]	1	365.86	365.86	5.56	0.038
Qg*Time	1	153.82	153.82	2.34	0.155
pH*[Fe2+]	1	91.92	91.92	1.40	0.262
pH*[Fe3+]	1	19.43	19.43	0.30	0.598
pH*Time	1	195.51	195.51	2.97	0.113
[Fe2+]*[Fe3+]	1	173.25	173.25	2.63	0.133
[Fe2+]*Time	1	4.03	4.03	0.06	0.809
[Fe3+]*Time	1	25.68	25.68	0.39	0.545
Error	11	724.16	65.83		
Lack-of-Fit	6	580.36	96.73	3.36	0.102
Pure Error	5	143.80	28.76		
Total	31	6313.38			
Model summary					
S	R-sq	R-sq(adj)	R-sq(pred)		
8.11374	88.53	67.67%	0.00%		

DF: Degree of freedom, Adj SS: adjust sum of squares, Adj MS: adjust mean of squares

The new model prediction was derived via keeping the important factors which are the main parameters for optimization. The new prediction model is rewritten as following:

$$\begin{aligned} \text{\%Ferrous Removal} = & 107.7 - 5.93 Qg + 0.15 \text{ pH} - 0.3733 [\text{Fe}^{2+}] - 1.313 [\text{Fe}^{3+}] \\ & + 0.206 \text{ Time} + 0.646 Qg \cdot \text{pH} + 0.0956 Qg \cdot [\text{Fe}^{3+}] \quad (\text{Eq.4.2}) \end{aligned}$$

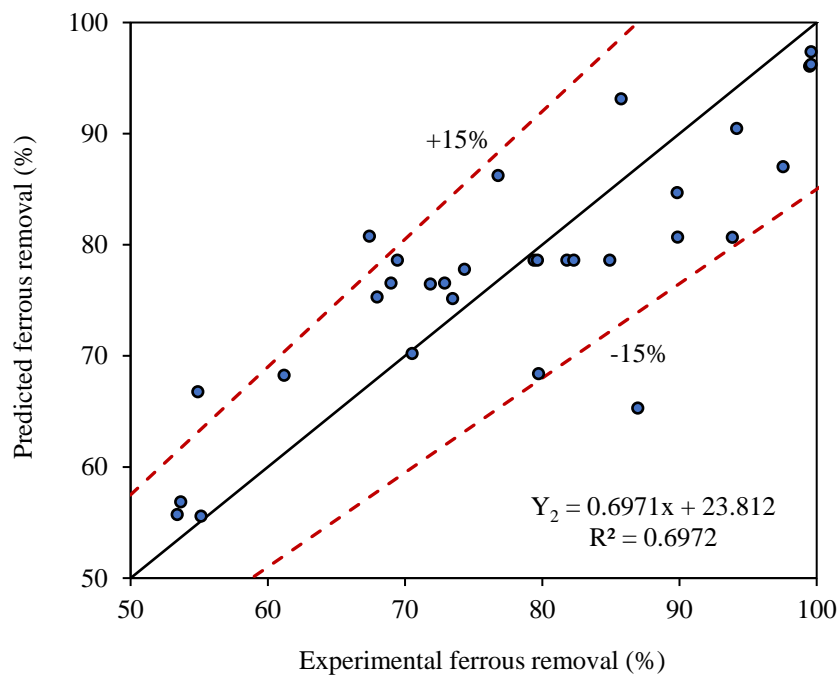


Figure 4.10 Experimental and predicted (short) ferrous removal (%)

All the predicted responses were fitted to the experimental data with 15% discrepancy. After adjustment, all unimportant were taken out and the DOE could provide a new equation as seen in Equation 4.2. This equation is shorter than previous (full quadratic). Moreover, the R^2 of this equation is 0.6972 as seen in Figure 4.10, represents the relationship between the experimental data and the predicted data from Equation 4.2. The comparison of the correlation coefficient was represented in Table 4.5.

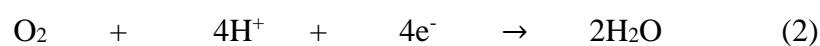
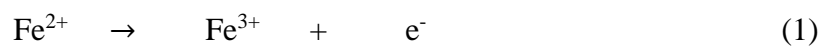
Table 4.5 Prediction Vs Experiment of ferrous oxidation removal (%)

Equation Model	Ferrous oxidation removal	R ²
Full Equation	$4.3 + 5.88 Qg + 19.5 pH - 0.351 [Fe^{2+}] - 2.02 [Fe^{3+}] - 3.25 Time - 0.540 Qg * Qg - 1.66 pH * pH + 0.0114 [Fe^{2+}] * [Fe^{2+}] + 0.0198 [Fe^{3+}] * [Fe^{3+}] + 0.0314 Time * Time + 0.646 Qg * pH - 0.0006 Qg * [Fe^{2+}] + 0.0956 Qg * [Fe^{3+}] + 0.0775 Qg * Time - 0.0710 pH * [Fe^{2+}] + 0.059 pH * [Fe^{3+}] + 0.233 pH * Time - 0.01170 [Fe^{2+}] * [Fe^{3+}] - 0.00223 [Fe^{2+}] * Time + 0.0101 [Fe^{3+}] * Time$	0.8854
Short Equation	$107.7 - 5.93 Qg + 0.15 pH - 0.3733 [Fe^{2+}] - 1.313 [Fe^{3+}] + 0.206 Time + 0.646 Qg * pH + 0.0956 Qg * [Fe^{3+}]$	0.6972

4.2.4 Factorial analysis

This section aimed to determine the optimal ferrous oxidation condition of the influential parameters. Figure 4.11 demonstrated the major effects plot of each factor on the response. It was provided by fitting means for each value of variances in the model. The initial pH value and initial ferrous iron concentration were exhibited to be the most important parameter impacting the ferrous iron removal efficiency. Moreover, Figure.8 shows contour plots to assess the interaction effects of independent factors on responses.

The combined effect of initial pH value and initial $[Fe^{2+}]$ on ferrous iron removal was revealed in 4.12. As can be seen, to obtain the removal efficient higher than 90%, the initial pH value should be around higher than 6.5 with initial $[Fe^{2+}]$ lower than 30 mg/L. Appelo, 1990 also mentioned that the exchange reaction rate of ferrous iron oxidation with oxygen is faster at $pH > 6.5$. The ferrous oxidation reaction with oxygen is defined as following: (Appelo et al., 1999).



The precipitates could absorb Fe^{2+} :



Where x and y: the stoichiometric coefficients for ferrous iron sorption

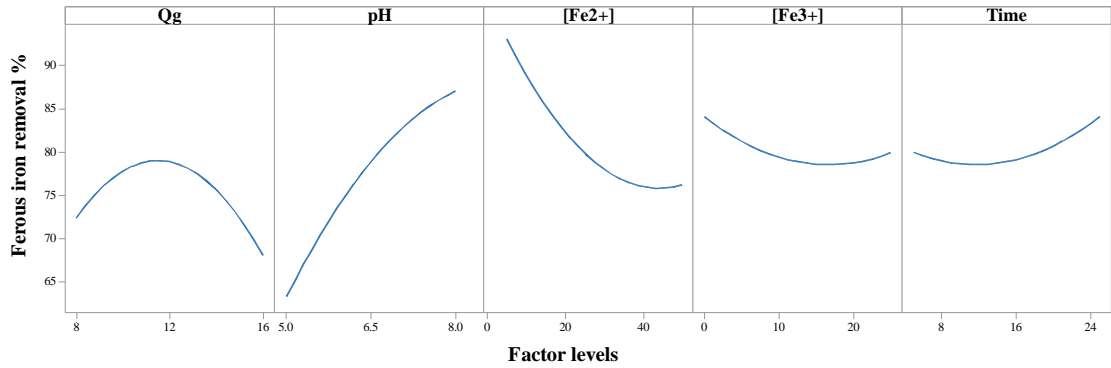


Figure 4.11 Main effects plot for Ferrous iron removal

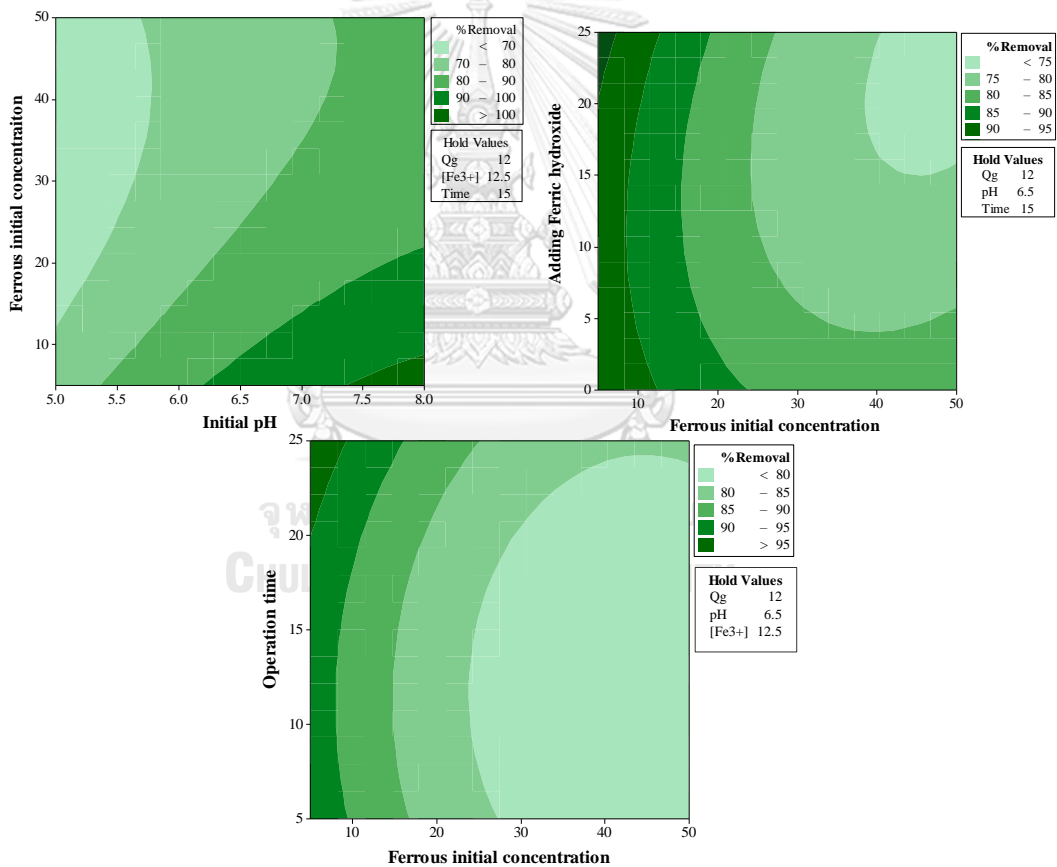


Figure 4.12 Contour plot for Ferrous iron removal

4.2.5 Process optimization

This section is about to discuss the most significant factor which affect on ferrous oxidation removal. The initial pH and ferrous initial concentration showed as the most effect parameters.

(A) Effect of initial pH

The initial pH value is the most impact factor on ferrous iron removal efficiency as it reveals in concave plot in Figure 4.11. Thus, this section is discussed the relative effect of initial pH between ferrous oxidation removal. Figure 4.13 demonstrated the boxplot of a relative effect of pH on ferrous oxidation removal efficiency. The effect of changing the initial pH from 6.5 to 7.5 resulted in a reduction in removal efficiency of between 53 and 99%. The result was found that the removal efficiency rapidly increased from 67 to 97% after enhancing initial pH ≥ 6.5 . In addition, it indicated that removal of ferrous could be given higher than 99% under the operation of initial pH 8. In contrast, the removal of ferrous iron could reached around 50 to 80% under pH 5. It clearly showed the treatment performance distribution at various initial pH conditions. The removal efficiency of ferrous iron is definitely different with changing of initial pH from 5 to 8.

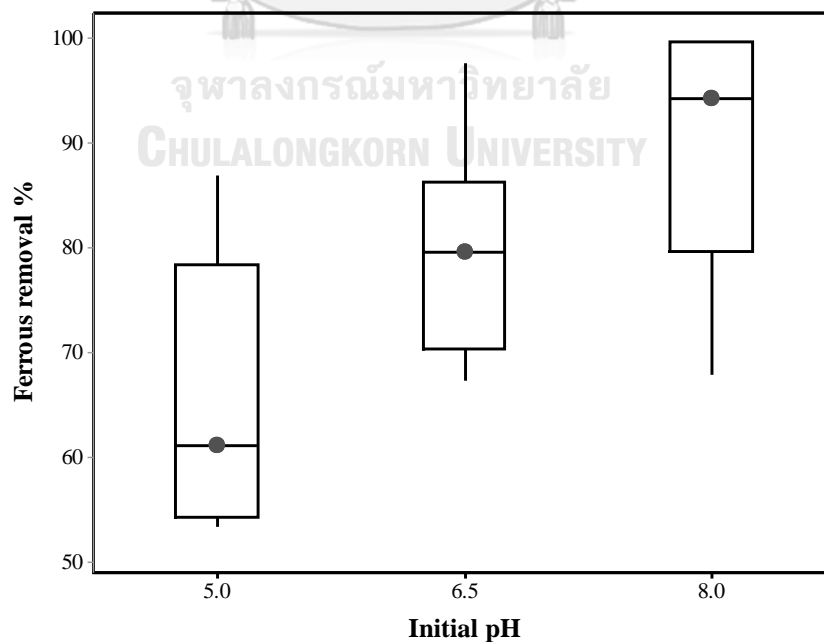


Figure 4.13 Boxplot of initial pH effect on ferrous iron removal

The relative variance of aquatic pH between the initial and final pH of each experiment condition was depicted in Figure 4.14. At initial pH 5, the final pH (after 12 or 25 minutes) illustrated between 3.77 and 6.05, for initial pH 6.5, distributed between 6.24 and 7.27, and initial pH 8, represented between 6.67 and 8.4. This changing of pH in ferrous oxidation might be because of the releasing acidity from reaction. As the results illustrated that under condition of high initial ferrous concentration presence, the pH value significantly drop because of the acidity was released by ferrous oxidation reaction to form ferric hydroxide (Smedley and Kinniburgh, 2002), after that the pH maybe was increased back at certain time base on oxidation reaction related to the initial concentration of ferrous iron due to the diffusion aqueous CO₂ from the solution and supplied air. In case of very low concentration of ferrous iron co-presence, the aquatic pH may directly increase due to the present of aqueous CO₂.

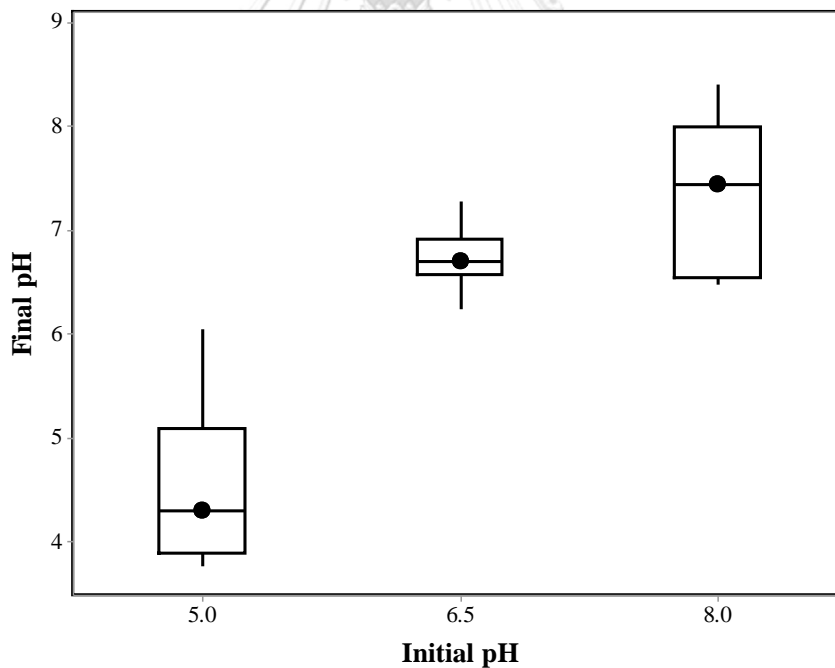


Figure 4.14 Boxplot the comparison between initial pH and final pH of ferrous oxidation performance

(B) Effect of ferrous initial concentration

As indicated in Figure 4.11, the ferrous initial concentration in synthetic groundwater between 5 and 50 mg/L showed different effect on ferrous iron removal efficiency. In order to define its exact removal performance, the boxplot of ferrous removal efficiency at different initial ferrous loading was plotted in Figure 4.15. The main effective plot of ferrous initial concentration was illustrated in term of mean value of ferrous iron removal. The removal efficiency was decreased when initial concentration of ferrous iron increased from 5 to 50mg/L. Furthermore, it found that ferrous iron removal could be achieved higher than 99% under the condition of lower ferrous initial concentration (5mg/L). This could be due to completely oxidizing of initial ferrous iron concentration with enough oxygen supply in reactor. The treatment performance dispersion at varied initial ferrous iron levels was clearly shown. At 5mg/L of initial ferrous iron loading, the removal efficiency is between 61 to 99%. However, after increasing ferrous initial concentration to 27.5 mg/L and 50 mg/L, the removal efficiency slightly decreased in range 54 to 94% and 53% to 89%, respectively. It clearly explained the limitation of dissolved oxygen in water by applying gas flow rate between 12 LPM to 16 LPM.

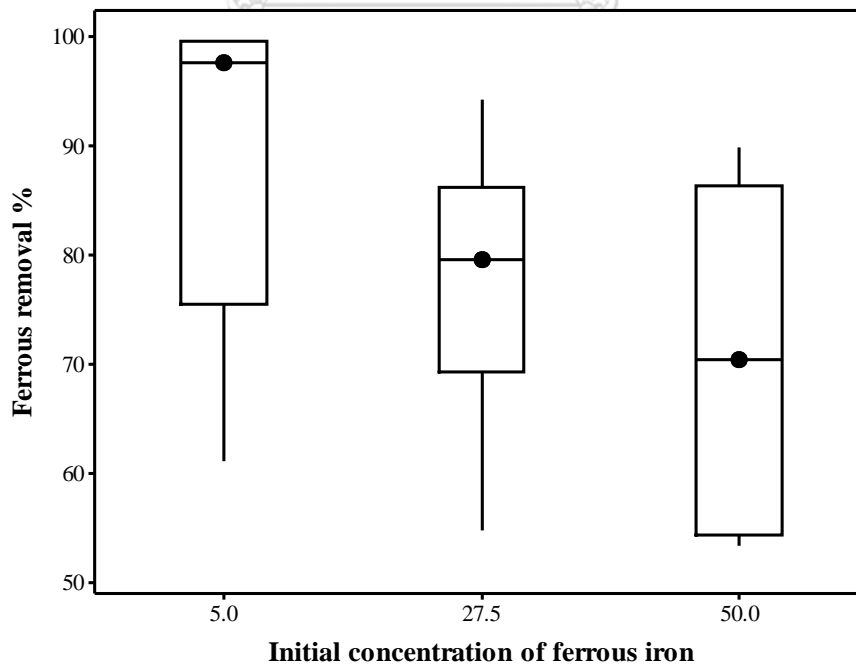


Figure 4.15 Boxplot of a relative effect of ferrous initial concentration on ferrous iron removal efficiency

Figure 4.16 reveals the impact of initial pH and initial ferrous iron concentration on ferrous removal efficiency. The removal efficiency of ferrous iron was raised with 5 mg/L of initial ferrous iron and increasing the initial pH to 8. In contrast, the removal efficiency was declined when ferrous initial loading increased at low pH 5. Therefore, it completely explained that initial pH value and initial ferrous concentration is significant influence the removal efficiency of ferrous iron.

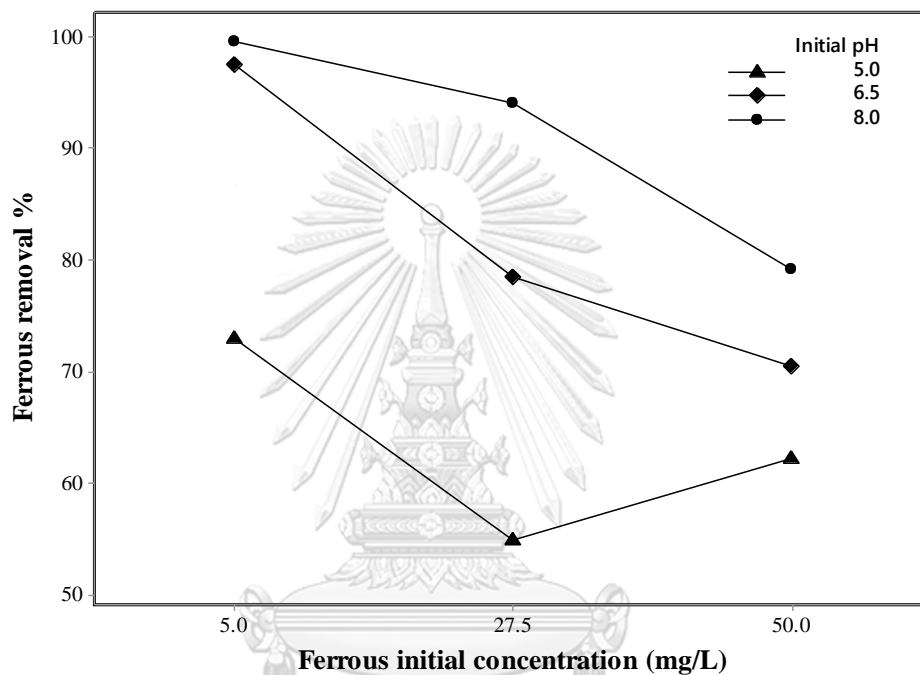


Figure 4.16 Scatter plot the relative effect of initial pH and initial ferrous concentration on ferrous iron removal efficiency

4.2.6 Summary of prediction and experimental equation

4.3 Optimization of process condition for arsenic removal

The significance of each variable and its influence on the responding variable, ferrous iron removal, were determined using factorial analysis. The variations in time (t), initial pH, gas flow rate (Q_g), initial ferrous iron concentration ($[Fe^{2+}]_0$), and additional ferric hydroxide ($[Fe(OH)^3]_0$) were observed to examine the influence of process conditions.

4.3.1 Experimental Design by CCD-RSD

The experimentation of arsenic and ferrous removal was designed by the aid of DOE. The Central Composite Design of Response Surface Methodology (CCD-RSM) was applied to find an optimization process condition. As shown in Table 4.6, three levels of five factors were designed for experiments. Furthermore, the run of 30 experimental conditions was illustrated in Table 4.7. This designed condition was used to conduct the experiment; subsequently, the results were evaluated and analyzed.

Table 4.6 Variation of three factor levels of each impact parameter

Factors	Unit	Factor levels		
		-1	0	+1
Air flow rate (Qg)	L/min	8	12	16
Initial pH	-	5	6.5	8
Initial concentration of ferrous iron ([Fe ²⁺])	mg/L	5	27.5	50
Additional ferric hydroxide ([Fe(OH) ₃])	mg/L	0	12.5	25
Time operation	min	5	23	40

Table 4.7 Experimental conditions for optimization influent factor

Run	Qg [L/min]±5	pH [-]±5	[Fe ²⁺] ₀ [mg/L] ±5	[Fe ³⁺] ₀ [mg/L] ±5	Time [minute]
1	16.00	5.0	50.00	25.00	5
2	16.00	8.0	50.00	0.00	5
3	12.00	6.5	25.00	12.50	23
4	16.00	8.0	0.00	0.00	40
5	12.00	6.5	25.00	12.50	23
6	16.00	8.0	0.00	25.00	5
7	12.00	6.5	25.00	12.50	40
8	8.00	8.0	50.00	25.00	5
9	8.00	5.0	50.00	25.00	40

10	8.00	5.0	0.00	25.00	5
11	8.00	5.0	50.00	0.00	5
12	12.00	5.0	25.00	12.50	23
13	8.00	5.0	0.00	0.00	40
14	16.00	8.0	50.00	25.00	40
15	16.00	6.5	25.00	12.50	23
16	8.00	8.0	0.00	25.00	40
17	8.00	6.5	25.00	12.50	23
18	12.00	6.5	25.00	12.50	23
19	12.00	6.5	25.00	0.00	23
20	16.00	5.0	0.00	0.00	5
21	16.00	5.0	50.00	0.00	40
22	16.00	5.0	0.00	25.00	40
23	12.00	6.5	25.00	12.50	5
24	8.00	8.0	0.00	0.00	5
25	8.00	8.0	50.00	0.00	40
26	12.00	6.5	50.00	12.50	23
27	12.00	6.5	25.00	12.50	23
28	12.00	6.5	25.00	25.00	23
29	12.00	6.5	0.00	12.50	23
30	12.00	8.0	25.00	12.50	23

4.3.2 Experimental Result

Table 4.8 demonstrates the results ferrous iron and arsenic of experiment design condition by DOE using Minitab. Initial pH, ferrous concentration and total arsenic concentration were analyzed at the time of sampling. As can be observed, the highest removal efficiency (>90%) of arsenic was found from the experimental run 9, 12, 14, 17, 18, 21, 25 and 30 while ferrous was only obtained from run number 9, 14, 18, and 30. In addition, without adding ferrous iron in the synthetic groundwater condition, the removal efficiency of ferrous iron was also given 0% from the experimental run number 4, 6, 10, 13, 16, 20, 22, 24 and 29. However, arsenic removal efficiency was defined between 29% and 56% from run number 4, 13, 20 and 24. On the other hand, under pH 6.5 performance condition, the removal efficiency of ferrous and arsenic were given around from 60-80%, including experiment number 3, 7, 15, 19, 23, 26, 27, 28, 29 (excepted number 29 for ferrous removal 0%). This outcome indicated that the presence of ferrous iron concentration in synthetic groundwater is the main influent parameter with the positive effect on arsenic removal by oxidation,

precipitation, and adsorption. Furthermore, ferrous iron loading between 25 and 50 mg/L could be represented for co-precipitating arsenic in ratio $[As]_0:[Fe^{2+}]_0 \approx 1:250 - 1:500$. The highest impact of ferric hydroxide adding on arsenic removal efficiency was found at highest pH 8 (run number 16 & 6). The condition of initial pH 5 and 6.5 operation, without ferrous iron co-presence, resulted arsenic removal efficiency 52% (run #10) & 60%(run#22), and 61% (run #29) after adding 25 and 12.5 mg/L of $Fe(OH)_3$, respectively. In contrast, without adding ferric hydroxide condition, arsenic removal efficiency was higher than 80% such as experiment run number 2, 11, 19, 21, and 25.

Table 4.8 Experimental results of ferrous iron and arsenic removal conditions

Run	Initial pH	Actual pH	% Removal Efficiency		Run	Initial pH	Actual pH	% Removal Efficiency ± 5	
			Fe	As				Fe	As
1	5.0	5.29	52	55	16	8.0	7.83	0	76
2	8.0	7.72	75	88	17	6.5	6.77	87	90
3	6.5	6.39	63	66	18	6.5	6.78	90	91
4	8.0	8.01	0	29	19	6.5	6.77	78	84
5	6.5	6.54	63	56	20	5.0	4.70	0	49
6	8.0	7.85	0	85	21	5.0	5.25	58	91
7	6.5	6.50	70	84	22	5.0	4.82	0	60
8	8.0	7.93	73	85	23	6.5	6.20	66	66
9	5.0	4.87	98	97	24	8.0	7.72	0	54
10	5.0	5.36	0	52	25	8.0	7.95	87	93
11	5.0	4.30	57	81	26	6.5	6.67	62	75
12	5.0	4.80	66	91	27	6.5	6.79	67	75
13	5.0	5.25	0	56	28	6.5	6.69	69	77
14	8.0	7.83	90	95	29	6.5	6.70	0	61
15	6.5	6.83	80	87	30	8.0	8.39	97	93

4.3.3 Empirical model for arsenic removal

The empirical correlation for arsenic removal was constructed using a comprehensive quadratic model that included square, interaction, linear, and constant components, as well as the following major influencing factors: gas flow rate (Qg), initial pH, initial ferrous iron concentration ($[Fe^{2+}]$), adding ferric hydroxide ($[Fe^{3+}]$), and operating time (Time). The experimental data from factor optimization was applied to define the

empirical correlations. Therefore, the model prediction of arsenic removal efficiency (%) provided by RSM is expressed in Equation 4.3.

$$\begin{aligned} \% \text{Arsenic Removal} = & 267 - 56.6 \text{ pH} + 1.627 [\text{Fe}^{2+}] - 1.40 [\text{Fe}^{3+}] - 10.1 \text{ Qg} + 2.69 \text{ Time} \\ & + 4.39 \text{ pH}^2 - 0.0229 [\text{Fe}^{2+}]^2 - 0.0084 [\text{Fe}^{3+}]^2 + 0.383 \text{ Qg}^2 - \\ & 0.0237 \text{ Time}^2 + 0.0204 \text{ pH} * [\text{Fe}^{2+}] + 0.294 \text{ pH} * [\text{Fe}^{3+}] + 0.211 \text{ pH} * \text{Qg} - 0.208 \text{ pH} * \text{Time} - \\ & 0.02140 [\text{Fe}^{2+}] * [\text{Fe}^{3+}] - 0.0076 [\text{Fe}^{2+}] * \text{Qg} + 0.01215 [\text{Fe}^{2+}] * \text{Time} \\ & + 0.0127 [\text{Fe}^{3+}] * \text{Qg} + 0.0149 [\text{Fe}^{3+}] * \text{Time} - 0.0455 \text{ Qg} * \text{Time} \end{aligned} \quad (\text{Eq. 4.3})$$

In addition, Table 4.9 indicated the results of statistical analysis of variance (ANOVA) analysis for ferrous iron oxidation removal. A p-value was also defined to determine the probability of difference. Based on the F-test with 95% confidence level, the lower p-value is the more statistically significant factor whereas p-value of more than 0.05 indicates insignificance. The result showed two significant single terms were initial concentration of ferrous iron (p-value <0.01) while Two-way interaction was $[\text{Fe}^{2+}] * [\text{Fe}^{2+}]$ (p-value <0.01). However, the large F-value of 17.45 and the low p-value (0.000) indicate that the model was statistically significant. This also means that the initial ferrous iron concentration is the most impact factor on ferrous oxidation operation. Figure 4.17 indicates the plot of experimental and predicted result of ferrous iron removal efficiency. The R^2 of this compared results was obtained 0.8588.

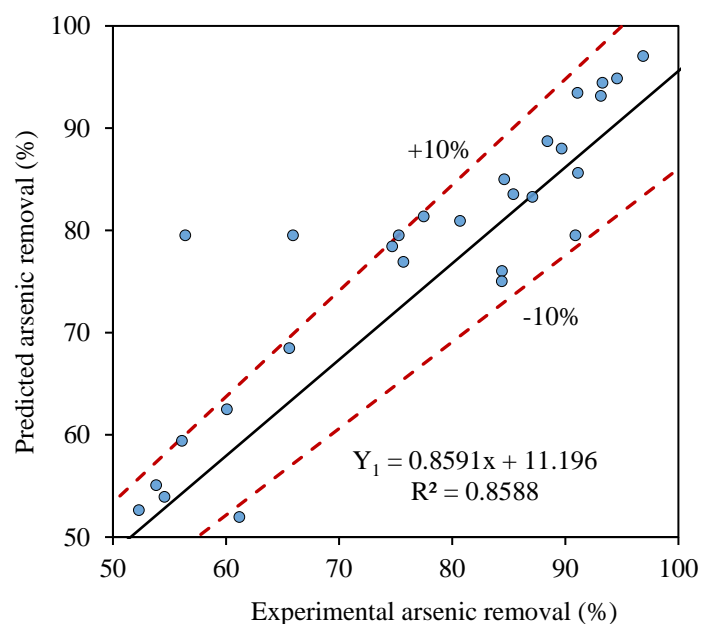


Figure 4.17 Experimental and predicted (full) ferrous removal (%)

As equation 4.1 was built using complete quadratic that consists of 21 terms such as 10 Two-Way Interaction, 5 Linear terms and 5 Square terms, and another constant value, which some factors are insignificant. Thus, deleting the inconsequential variables from the model may help to improve the expression. The new model prediction was derived via keeping the important factors which are the main parameters for optimization. The new prediction model is rewritten as following:

$$\begin{aligned} \% \text{Ferrous Removal} = & 38.5 + 2.47 \text{ pH} + 0.797 [\text{Fe}^{2+}] + 0.784 [\text{Fe}^{3+}] - 0.634 \text{ Qg} \\ & + 0.214 \text{ Time} - 0.0214 [\text{Fe}^{2+}] * [\text{Fe}^{3+}] \end{aligned} \quad (\text{Eq.4.4})$$

Furthermore, the new equation was plotted to compare with experimental results. Figure 4.18 shows the correlation of the experimental results and the predicted from Equation 4.4. The R² of this comparison result was only 0.5337. All the predicted responses were fitted to the experimental data with 20% discrepancy. The comparison of the correlation coefficient of full quadratic and new equation was represented in Table 4.10.

Table 4.9 ANOVA results of the input factors for the arsenic removal efficiency

Source	DF	Adj SS	Adj MS	F-Value	P-Value
Model	20	36806.0	1840.3	17.45	0.000
Linear	5	24649.8	4930.0	46.74	0.000
pH	1	459.5	459.5	4.36	0.066
[Fe ²⁺]	1	23667.6	23667.6	224.37	0.000
[Fe ³⁺]	1	42.7	42.7	0.40	0.541
Qg	1	121.7	121.7	1.15	0.311
Time	1	358.4	358.4	3.40	0.098
Square	5	10894.2	2178.8	20.66	0.000
pH*pH	1	104.2	104.2	0.99	0.346
[Fe ²⁺]*[Fe ²⁺]	1	4623.2	4623.2	43.83	0.000
[Fe ³⁺]*[Fe ³⁺]	1	3.7	3.7	0.04	0.855
Qg*Qg	1	180.4	180.4	1.71	0.223
Time*Time	1	108.5	108.5	1.03	0.337
2-Way Interaction	10	1261.9	126.2	1.20	0.399
pH*[Fe ²⁺]	1	224.9	224.9	2.13	0.178
pH*[Fe ³⁺]	1	71.9	71.9	0.68	0.430

pH*Qg	1	149.5	149.5	1.42	0.264
pH*Time	1	24.3	24.3	0.23	0.643
[Fe2+]*[Fe3+]	1	84.1	84.1	0.80	0.395
[Fe2+]*Qg	1	99.8	99.8	0.95	0.356
[Fe2+]*Time	1	361.7	361.7	3.43	0.097
[Fe3+]*Qg	1	24.3	24.3	0.23	0.643
[Fe3+]*Time	1	149.5	149.5	1.42	0.264
Qg*Time	1	71.9	71.9	0.68	0.430
Error	9	724.16	65.83		
Lack-of-Fit	6	443.3	73.9	0.44	0.821
Pure Error	3	143.80	168.7		
Total	29	3775.3			
Model summary					
S	R-sq	R-sq(adj)	R-sq(pred)		
10.2706	97.49%	91.90%	0.00%		

DF: Degree of freedom, Adj SS: adjust sum of squares, Adj MS: adjust mean of squares

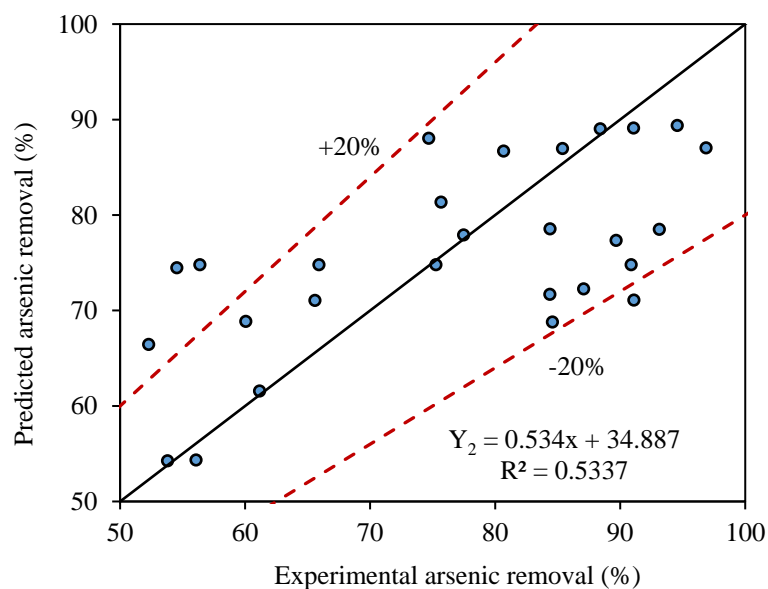


Figure 4.18 Experimental and predicted (short) ferrous removal (%)

Table 4.10 Prediction Vs Experiment of arsenic removal (%)

Equation Model	Ferrous oxidation removal	R ²
Full Equation	$267 - 56.6 \text{ pH} + 1.627 [\text{Fe}^{2+}] - 1.40 [\text{Fe}^{3+}] - 10.1 \text{ Qg}$ $+ 2.69 \text{ Time} + 4.39 \text{ pH} \cdot \text{pH} - 0.0229 [\text{Fe}^{2+}] \cdot [\text{Fe}^{2+}] -$ $0.0084 [\text{Fe}^{3+}] \cdot [\text{Fe}^{3+}] + 0.383 \text{ Qg} \cdot \text{Qg} -$ $0.0237 \text{ Time} \cdot \text{Time} + 0.0204 \text{ pH} \cdot [\text{Fe}^{2+}]$ $+ 0.294 \text{ pH} \cdot [\text{Fe}^{3+}] + 0.211 \text{ pH} \cdot \text{Qg} - 0.208 \text{ pH} \cdot \text{Time} -$ $0.02140 [\text{Fe}^{2+}] \cdot [\text{Fe}^{3+}] - 0.0076 [\text{Fe}^{2+}] \cdot \text{Qg}$ $+ 0.01215 [\text{Fe}^{2+}] \cdot \text{Time} + 0.0127 [\text{Fe}^{3+}] \cdot \text{Qg}$ $+ 0.0149 [\text{Fe}^{3+}] \cdot \text{Time} - 0.0455 \text{ Qg} \cdot \text{Time}$	0.8588
Short Equation	$38.5 + 2.47 \text{ pH} + 0.797 [\text{Fe}^{2+}] + 0.784 [\text{Fe}^{3+}] - 0.634 \text{ Qg}$ $+ 0.214 \text{ Time} - 0.0214 [\text{Fe}^{2+}] \cdot [\text{Fe}^{3+}]$	0.5337

4.3.4 Factorial Analysis

The optimal arsenic removal condition from effect factors was indicated in this part. The influential parameters on the response were plotted in Figure 4.19. This outcome is shown that initial ferrous iron concentration is the most effect factor on arsenic removal efficiency, following initial pH value factor. As can be observed, at initial pH ≥ 7 with initial ferrous iron concentration ≤ 30 mg/L could provide the highest impact the removal efficiency of arsenic.

Additionally, Figure 4.20 demonstrates the contour plots to define the correlation between each factor effect on responses. There is only relationship of $[\text{Fe}^{2+}] \cdot \text{pH}$, $[\text{Fe}^{3+}] \cdot \text{pH}$, $\text{Qg} \cdot \text{pH}$ and $\text{Time} \cdot \text{pH}$ area that could be given arsenic removal efficiency higher than 90%. Indeed, initial pH value around 7.5 and ferrous initial concentration around 30mg/L are significant influence on arsenic removal from synthetic groundwater. However, the detail discussion of the effect of initial ferrous iron and pH on arsenic removal is discussed in optimization process.

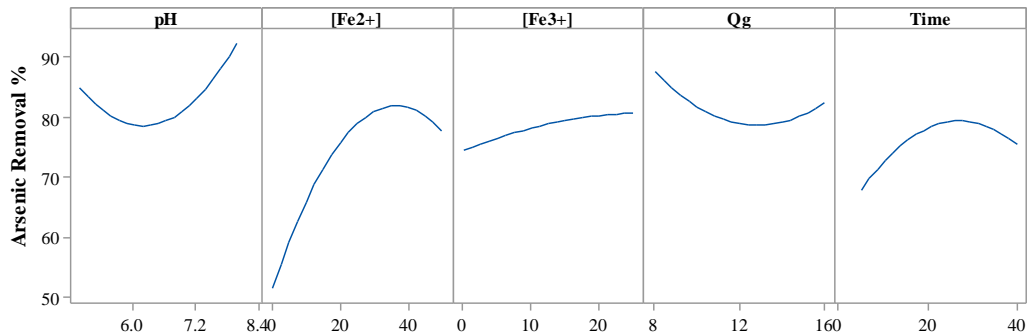


Figure 4.19 Main effect plot of arsenic removal

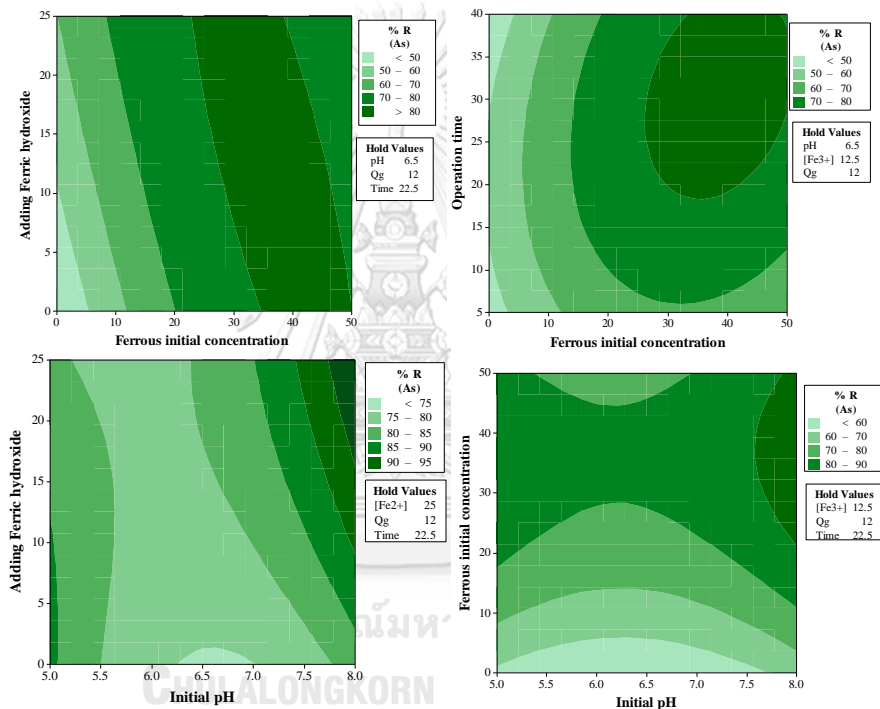


Figure 4.20 Contour plot for Arsenic removal

4.3.5 Process Optimization

The optimization process was investigated after the experimental result was obtained using complete design of response surface methods with three levels and single replication. In previous section, the main effective plot of each factor on arsenic removal illustrated the most influential factor on removal efficiency as initial pH and initial ferrous loading due to its curve shape.

(A) Effect of initial pH

Figure 4.21 demonstrated the effect of initial pH on arsenic removal efficiency. The effect of changing the initial pH from 5 to 8 provided the various range of arsenic removal efficiency. At starting pH 5, the removal efficiency was obtained from 48 to 96% while under condition of initial pH 6.5 resulted in median range of 56 to 90% of removal efficiency. However, at highest pH value 8, the result showed a low removal efficiency from 29 to 94%. As could be investigated, the result was found to get high removal of arsenic ($\geq 90\%$), the performance should be observed under initial $\text{pH} \leq 5$ and $\text{pH} \geq 6.5$. This might be due to the relative effect of initial ferrous concentration presence in groundwater. However, the different initial pH 5 and 8 could be explained the arsenic removal efficiency due to some experimental condition designed in arsenic and initial ferrous iron ratio $[\text{As}]_0:[\text{Fe}^{2+}]_0 \approx 1:1000$, i.e., run number 4, 10, 13 and 16. With experimental run number 4, the initial pH 8 could provide the arsenic removal efficiency only 29% while the removal efficiency could be given 52%, 56%, 49% under operation initial pH 5 by run number 10, 13, and 16, respectively. It can be explained that without initial ferrous iron in groundwater, arsenic can be removed around 50% under initial $\text{pH} \leq 5$.

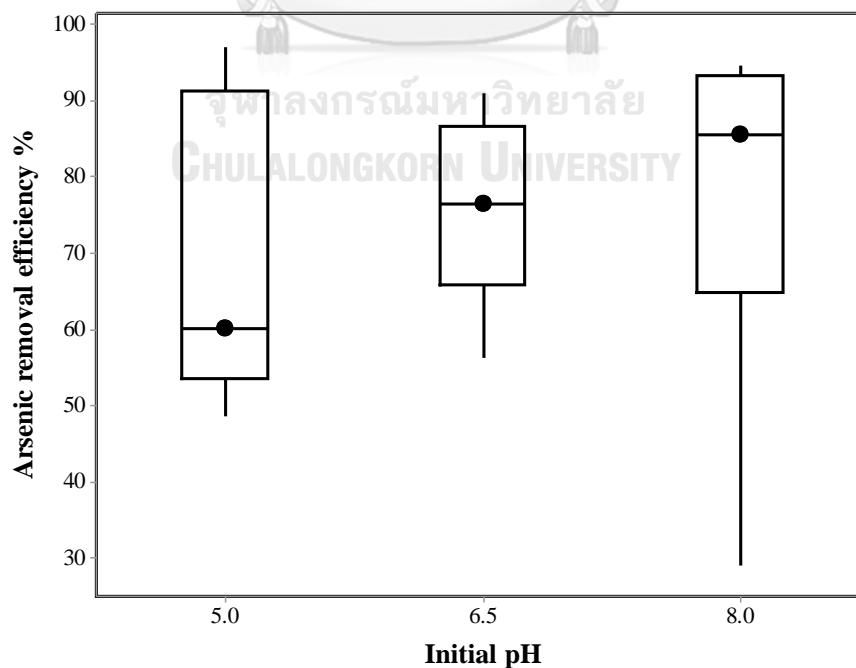
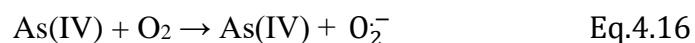
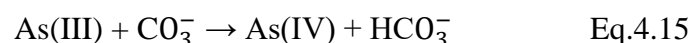
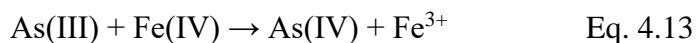
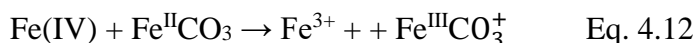
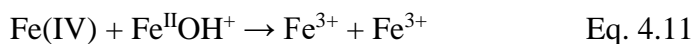
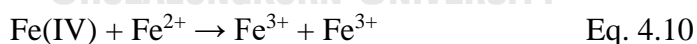
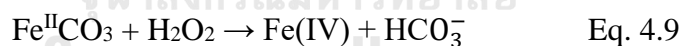
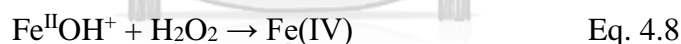
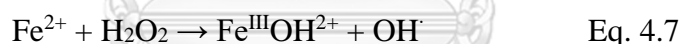
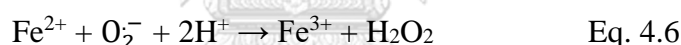


Figure 4.21 Boxplot of initial pH effect on arsenic removal efficiency

(B) Effect of initial ferrous concentration

According to Figure 4.19, the arsenic removal efficiency was achieved between 50% and 80% with the various initial concentration of ferrous iron from 0 to 50 mg/L. Indeed, after supplying a co-presence of ferrous iron 25 mg/L, the removal efficiency immediately improves from around 50% to 80%, then gradually decreases to roughly 75% after raising the ferrous starting concentration to 50 mg/L.

To understand the positive effect of ferrous iron co-presence in groundwater, the reaction of ferrous iron with H₂O₂ was revealed in Equation 4.5 and 4.6, and the formation of Fe(IV) could be seen in Equation 4.7 -4.20. Moreover, the reaction of arsenite (As(III)) adsorption on Fe(IV) to form ferric iron (Fe(III)) and As(IV) was explained in Equation 4.13-4.15. Equation 4.26 indicated the reaction of As(IV) diffusion with dissolved oxygen. In addition, Equation 4.10-4.12 showed the increasing ferrous concentration causing the interaction of Fe(IV) with Fe(Sastaravet et al.) to produce to two Fe(III) in a chain-terminating reaction (Hug et al., 2003).



After enhancing ferrous initial concentration of ferrous iron to 50 mg/L, a slightly increasing of arsenic removal was found. Figure 4.22 illustrated the boxplot of experimental conditions by various ferrous initial concentration.

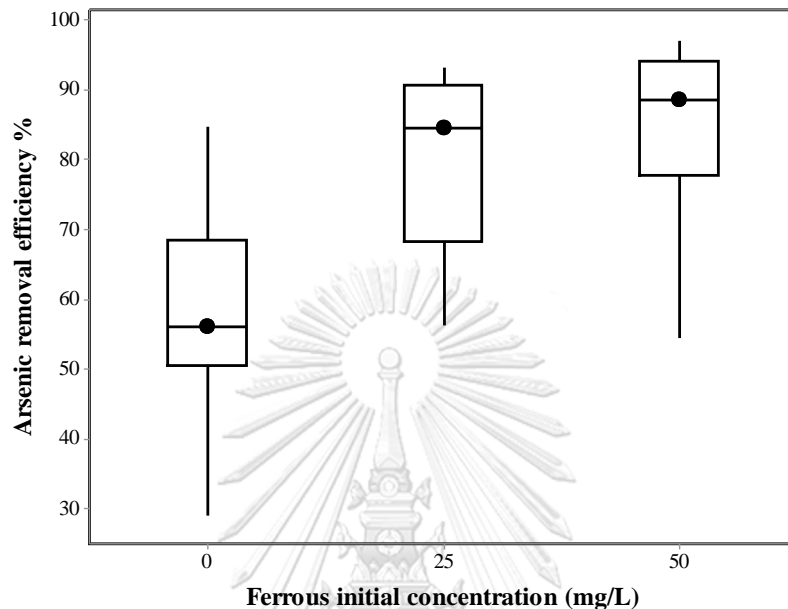


Figure 4.22 Boxplot of ferrous initial concentration effect on arsenic removal efficiency

It was obtained the removal efficiency of arsenic approximately 56% without co-presence of initial ferrous iron. However, the arsenic removal efficiency was given approximate 80% after applying initial concentration of ferrous iron (25-50mg/L). This means that ferrous initial concentration plays important role to treat arsenic from groundwater.

(C) Effect of initial pH and ferrous initial concentration

Figure 4.23 illustrated the relative effect of initial pH and ferrous iron concentration on arsenic removal efficiency. In all pH values, arsenic removal efficiency seemed to rise after increasing ferrous initial concentration to 25 mg/L, but it appeared to drop after increasing ferrous initial concentration to 50 mg/L. However, arsenic removal efficiency at initial pH 6.5 is rapidly raised by changing ferrous initial concentration to 25 mg/L, yet it speedily decreased at high ferrous initial concentration. It might be

caused by too high loading of ferrous initial concentration, which the pH value maybe dropped due to acidity product by ferrous oxidation reaction.

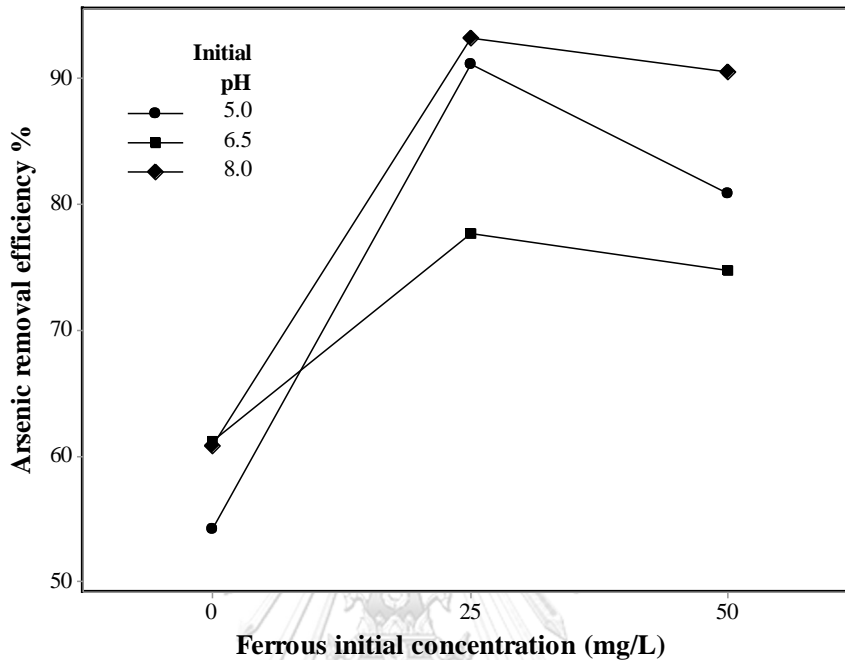


Figure 4.23 Scatter plot of relative effect of initial pH and ferrous initial concentration on arsenic removal efficiency

Furthermore, at initial pH 8, the arsenic removal efficiency performance slightly failed down after increasing ferrous concentration to 50 mg/L. This clearly proved that initial pH and initial concentration of ferrous iron is extremely impact to arsenic removal efficiency. Therefore, the optimal arsenic removal efficiency could be obtained under condition of ferrous initial concentration 25 mg/L and initial pH 8.

(D) Effect of other factors

As shown in Figure 4.19, there are three other factors (operating time, gas flow rate and adding ferric hydroxide) which also affects to arsenic removal efficiency. The result found the slightly effect of additional ferric hydroxide particles on arsenic removal efficiency. As expected, the effective trend of ferric hydroxide linearly increased with arsenite removal. The changing of arsenic removal performance is approximately 10% after adding ferric hydroxide between 0 to 25 mg/L. Although it provided small impact on arsenic removal, the positive effect on arsenate adsorption

may be still considered. Hence, arsenic adsorption on iron hydroxide might be helpful. For the effect of gas flow rate from 8 to 16 LPM, arsenic removal efficiency is slowly decreased at 12LPM, and increased with increasing gas flow rate to 16 LPM. This changing may be due to the different experiment condition such as ferrous initial concentration and operation time, as the concentration of dissolved oxygen and the mixing condition of an aquatic solution are both affected by increasing gas flow. Lastly, the operation time is also one of significant factors to observe the removal efficiency of arsenic. With operating time of 23 minutes, the removal efficiency of arsenic could be achieved 80%. In contrast, the removal efficiency of arsenic is low when the operation time is only 5 minutes. Thus, to obtain high removal efficiency of arsenic, the operation time should be ≥ 23 minutes in order to get completely oxidizing of ferrous iron and arsenite in groundwater.

4.3.6 Summary of optimum level

This section attempted to summarize the impact of process conditions on arsenic removal from aqueous solutions, as well as the optimal level of these conditions. Based on the factorial analysis using statistical analysis of variance (ANOVA) designed by CCD-RSM, initial pH and initial concentration of ferrous iron is significant factors in single term. This means that initial pH value and ferrous initial concentration are important and required factor to study and optimized for maximizing the removal efficiency of arsenic.

Firstly, initial pH value found its significant removal performance of arsenic should be higher than (≥ 6.5) in aquation solution. Furthermore, initial ferrous iron concentration was discovered in the optimal curve response, which might be due to the impact of aquatic pH. Overall, it can be stated that arsenic removal with presence of ferrous iron performance is greater at higher pH values (pH 8) under identical conditions. Based on this effective analysis, it can be summarized that ferrous iron co-presence should be lower than 50 mg/L for 100 $\mu\text{g/L}$ of arsenic or $[\text{As(III)}]_0:[\text{Fe(Sastaravet et al.)}]_0 < 1:500$ and initial pH should be around 8.

As illustrated in Figure 4.24, the optimal values were determined from the design and analysis of this part utilizing DOE's response optimizer tool. Based on the

optimization plot, the optimum levels of each factor were defined, i.e., initial pH 8, initial concentration of ferrous iron ≈ 36.85 mg/L, iron hydroxide 25 mg/L, gas flow rate 8 L/min, and operating time ≈ 33.28 minutes.

Table 4.11 summarizes the studied range (factor level) and optimum condition of each factor. Despite the fact that these conditions do not perfectly follow the effective pattern of each factor analyzed through the effect of pH, ferrous initial concentration, and other factors, the optimum conditions are still within the recommended range for successfully treating arsenic to be lower than the standard level.

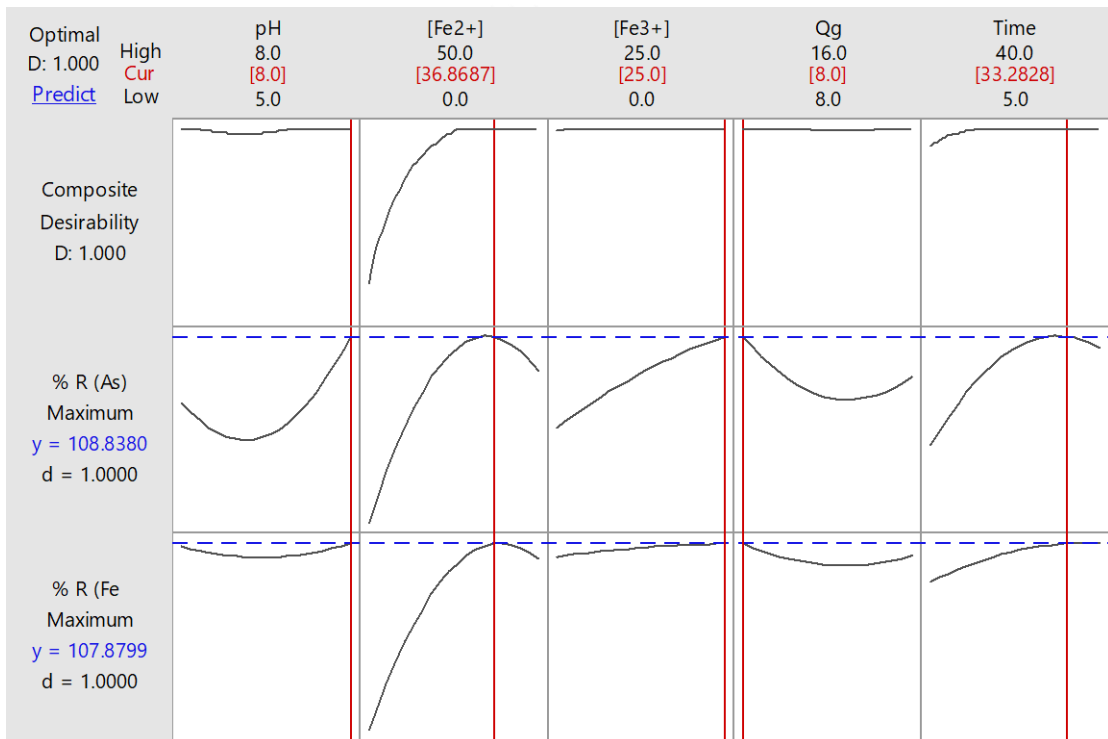


Figure 4.24 Optimization plot of each variable to maximize ferrous iron and arsenic removal

Table 4.11 Summary of factor levels studied and optimum conditions

Factors	pH	[Fe ²⁺]	[Fe(OH) ₃] ₀	Qg	Time
	[-]±5	[mg/L] ±5	[mg/L] ±5	[LPM] ±5	[min] ±5
Studied	Min. 5	0	0	8	5
ranges	Max. 8	50	25	16	40

Optimum level	8	36	25	8	33
---------------	---	----	----	---	----

4.4 Separation process

This section aimed to study insoluble ferric particles removal using the combination separation processes, i.e., sedimentation, adding solid media, and membrane filtration processes using the representative experiments and engineering parameters. The study of insoluble ferric iron removal was operated after ferrous and arsenic oxidation process in certain aeration time. One experiment condition was selected to study the separation process (Qg:12LPM, pH:8, $[\text{Fe}^{2+}]$:25mg/L, $[\text{Fe}^{3+}]$:12.5mg/L, operation Time:23min, and [As]:100 $\mu\text{g/L}$). After the performance of aeration, ferrous iron and arsenic concentration were obtained 0.8mg/L and 7 $\mu\text{g/L}$, respectively. This result shows that arsenic concentration (<10 $\mu\text{g/L}$) passed the drinking water WHO standard while ferrous iron was not (<0.3mg/L). This is because of limitation of gas flow rate supply.

4.4.1 Settling process

The settling process was performed in order to reduce the suspended solid from aeration and oxidation process of ferrous iron and arsenic removal. The turbidity was assessed in total 300 minutes period with a 30-minute sampling time-step to determine gravity separation by batch settling test. The initial turbidity at several sample ports is 180 ± 5 NTU on average. More information on the removal efficiency calculation, the iso-removal plot, and fraction removal can be found in Reynolds (1977) (Reynolds and Richards, 1995). Figure 4.25 shows the results of a batch settling test in BCR for ferric precipitation particles removal from groundwater.

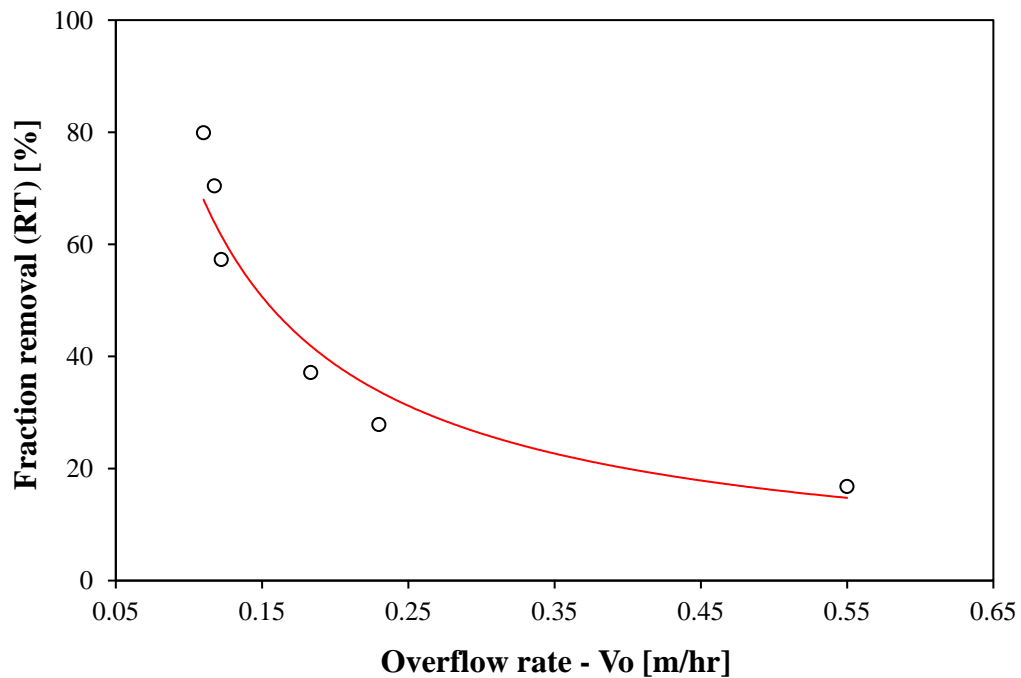


Figure 4.25 Fraction removal of insoluble ferric iron with overflow rate in BCR

The result indicated that the fraction removal (RT) reduced from 79% to 16.8% with increasing the overflow rate from 0.11 to 0.55 m/hr. As could be seen that the higher overflow provided the lower fraction removal. However, there is still more than 60 NTU turbidity in the groundwater even though five hours of settling process was experimented to remove ferric iron particles. This means that the settling process could not completely remove all turbidity to reach drinking water standard yet. It may be due to colloid particles product by insoluble ferric iron which is very difficult to settle (Kawamura, 2000). Therefore, the membrane technology is operated to treat all impurities particles and obtain completely clear and clean drinking water. Lastly, after settling process the concentration of ferrous iron was decreased to 0.02mg/L which is less than 0.3mg/L. To conclude, settling process not only removed turbidity in groundwater but also increased ferrous iron removal efficiency.

4.4.2 Solid Media effect on suspended particles

Based on the results from previous study, scouring sponge was found to be the most beneficial solid media to enhance oxygen mass transfer coefficient in tap water. Thus, in this study, scouring sponge was chosen to observe the effect on suspended solid.

Based on previous experiment, 3% of solid media was the optimal condition with gas velocity 0.7×10^{-2} m.s⁻¹ to get KLa 0.015s⁻¹, while after increasing scouring sponge from 5% to 10% loading could provide the same coefficient KLa value as 3% loading. Hence, to understand its effect on suspended solid removal, scouring sponge in all range (3-10%) were selected to study. This experiment was runed by optimal condition of arsenic and iron removal by DOE with running number 30 (Qg :12 LPM, pH: 8, [Fe²⁺] : 25mg/L, [Fe³⁺]: 12.5 mg/L and Time: 23min).

Figure 4.26 illustrates the turbidity removal efficiency of each solid media loading. As a results, adding scouring sponge media was influent to decline the turbidity, regardless increasing solid media concentration. The concentration of turbidity is represented in Table 4.12. The initial turbidity was 230 NTU. Scouring sponge 3% and 5% loading can obtained only 1% and 5% of turbidity removal, respectively. However, scouring sponge 10% loading provided 15% of turbidity removal from groundwater. This means adding high scouring sponge loading could provide higher removal of turbidity. This might be due to the surface area was enhanced to catch or attach with insoluble particles. As could be seen in Figure 4.27, which shows the picture of scouring sponge before applying to oxidation process (a), and after adding to oxidation process. The color of scouring sponge was slightly changed to a bit yellow and red because of the small particles from insoluble of ferric iron attached on its surface area. To conclude, scouring sponge 10% loading could be recommended to apply in experiment to improve oxygen mass transfer in BCR, as well as suspended solid removal.

Table 4.12 Turbidity of treated groundwater with various scouring sponge loading

Scouring sponge addition	Turbidity [NTU ± 5]
0%	230
3%	228
5%	220
10%	195

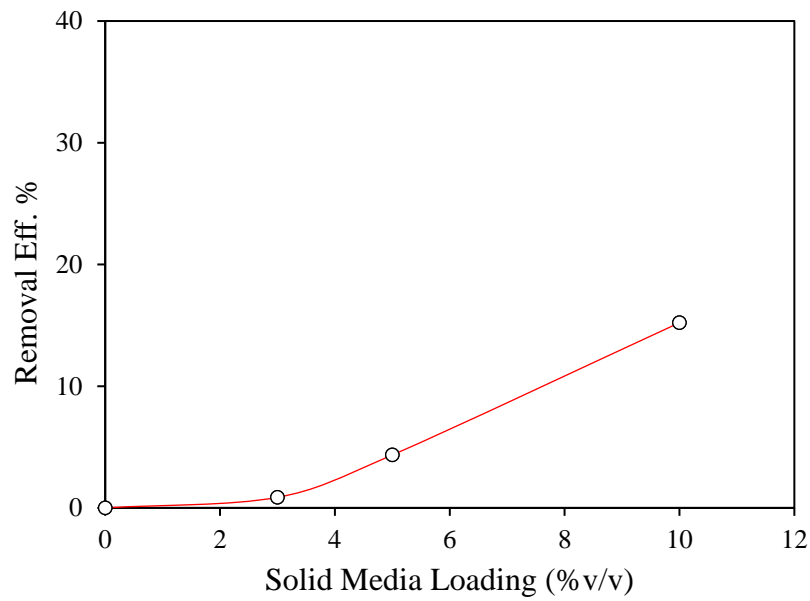


Figure 4.26 Effect of solid media adding on turbidity removal

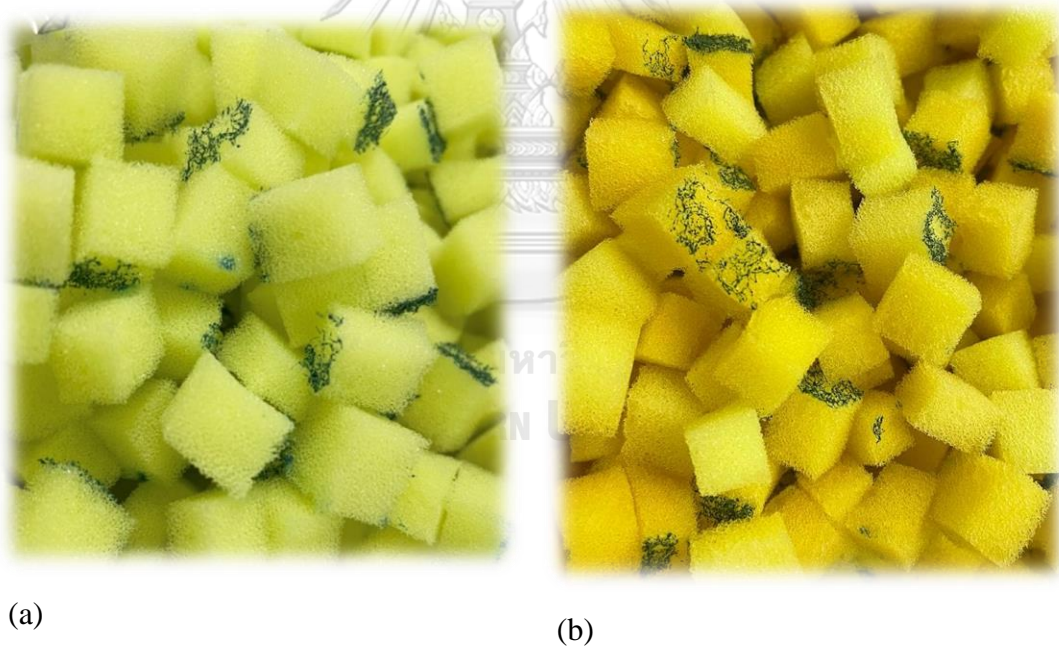


Figure 4.27 Scouring sponge before process in treatment (a), scouring sponge after process in treatment (b)

4.4.3 Membrane filtration

This part ultrafiltration membrane sheet was chosen to treat suspended solid and bacteria and virus in pretreated groundwater, which settling process was unable pass

the drinking water WHO standard. Water samples including raw groundwater, before settling water, after settling water was filtrated by UF membrane with pressure of 5 bars for 2 hours, and Tap water was used as controlled condition. Figure 4.28 indicates the normalized flux (J/J_0) versus with operation time. This result found that the water flux of raw groundwater and before settling process was rapidly declined compared to tap water. This could be because ferrous iron of raw groundwater was oxidized during membrane filtration operation and cause to precipitated particles. This solution contains high concentration of suspended solid which could foul on the membrane surface, resulting in flux decline. Furthermore, before sedimentation process (aerated groundwater), ferrous iron was all most oxidized by dissolved oxygen in water to form ferric iron particles and co-precipitated with arsenic. Therefore, the water flux of before sedimentation solution (after BCR) shows the greater flux decline. However, after sedimentation process some suspended solid was settled and removed from solution. As a result, treating the solution using sedimentation could reduce the fouling, leading to the increase of water flux. Therefore, sedimentation process was suggested to construct before membrane filtration in order to reduce membrane fouling.

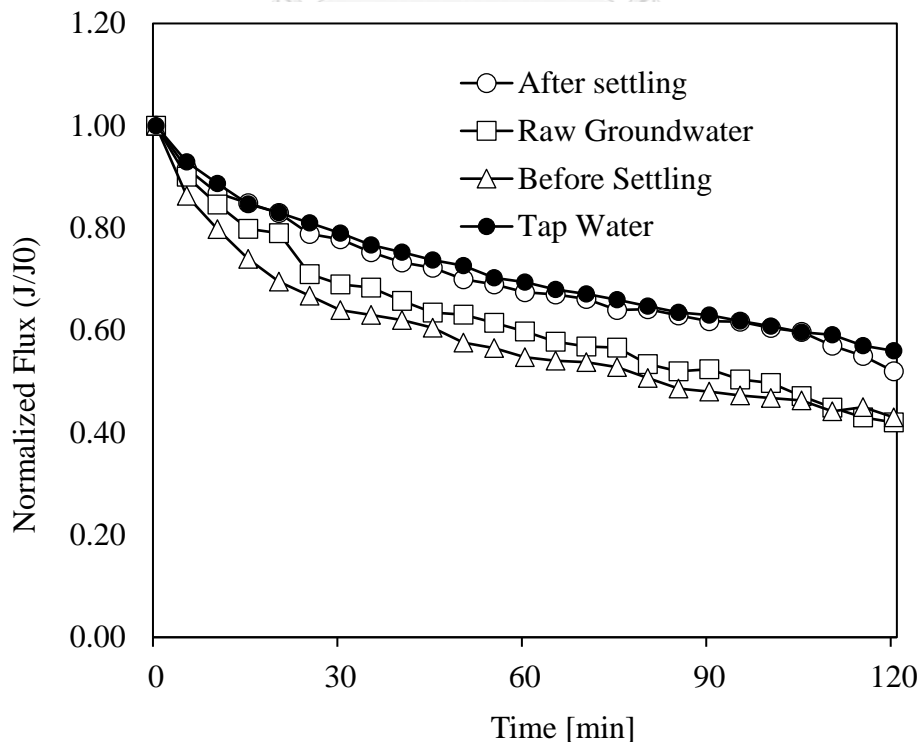


Figure 4.28 Water flux in comparison of tap water, raw groundwater, before settling process and after settling process

In addition, Figure 4.29 demonstrated the different thickness of ultrafiltration membrane after performance. As could be seen, before sedimentation, the sheet membrane became dark red due to the thickness of particles on surface membrane.



Figure 4.29 Images of filtered membrane sheet in different condition operation

4.4.4 Summary work

The significant value of this research is completely proved the co-presence of ferrous iron in groundwater could help improve arsenic removal. Therefore, the principle of this work is the combination of aeration process, sedimentation process and membrane filtration to treat arsenic and ferrous iron in groundwater and get completely clear and clean drinking water. The study works in both conventional process and new technology membrane filtration. This process could be simply understood in three main steps. First, groundwater is poured into aeration tank for oxidation process and adsorption process. Since the ferrous iron needs dissolved oxygen in water for oxidizing, thus, the adding solid media is applied to enhance oxygen mass transfer rate without extra electric consumption. Furthermore, after ferrous iron oxidizes to insoluble particles of ferric iron, the precipitation process occurs and appears as colloid particles. This colloid particle could be precipitated on

surface solid media which could be beneficial as adsorbate place for arsenic adsorption. Second, after aerated groundwater, the effluent water has a dark orange color due to high concentration of suspended solid particles. Thus, sedimentation process is required. The sedimentation process allows all large particles to settle down as physical water treatment process by gravity force. This process can reduce turbidity loading to 60 NTU for operated time 5 hours. The sedimentation process is not only to remove suspended solid, but also could be collection place to the sludge after settling to reapply in aeration tank because this sludge has found an advantage to activate as adsorbent particles for improving arsenic removal. Lastly, the effluent water passes through membrane filtration to treat all impurities particles, bacterial and virus, then obtain clear and clean drinking water. To sum up of this process, groundwater flows into aeration tank and operation in certain time, then sedimentation process, through the membrane filtration and comes out of the spout. As can be seen in Figure 4.30, and Figure 4.31 which indicates the diagram of this process system.

However, this process also has a limitation as it may not be able to treat arsenic in groundwater if that groundwater has no ferrous initial concentration at least 5 mg/L up, and under initial pH range in 5-8. Moreover, the most concern is the effect of other pollutant (fluoride, manganese etc.) in real groundwater and monsoon condition which could affect to arsenic removal efficiency.

In Cambodia, during the dry season, Cambodian household (53%) mainly relies on groundwater resources to overcome water shortages and drinking water supply source. It is estimated about 270,000 tube-wells (hand pump) are currently used for drinking water purpose, especially in rural area. The main issues and challenges, the groundwater contents high level of arsenic and iron (Ha et al., 2015), which have been exposed to harmful health effects when consumed daily. Nowadays, most people commonly use Kanchan Arsenic Filtration (KAF), which is a household drinking water treatment device for removing arsenic in drinking water (T. K. Ngai et al., 2007). The conventional KAF is to combine the slow sand filtration and iron hydroxide adsorption principles. However, this conventional process may not be able to completely remove all bacteria and some agricultural chemical contamination (T. Ngai et al., 2006), regularly replacement of both nails and sand (yearly replacement)

(Mueller, 2020) that was complained by user. The brick chip and iron nails could be dispersed easily if water does not pour slowly into tank (T. Ngai et al., 2006). This challenge is lead to study a new process of combination of conventional process with membrane filtration process in this research.

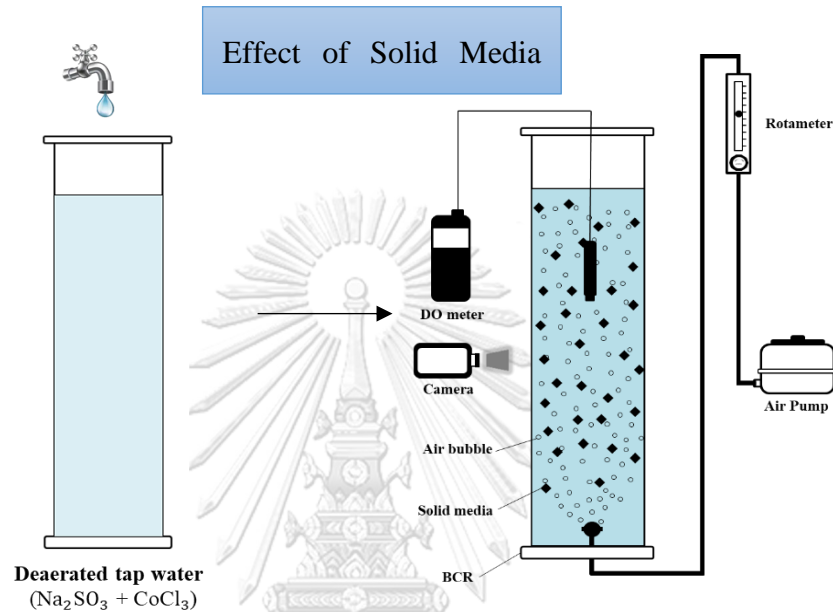
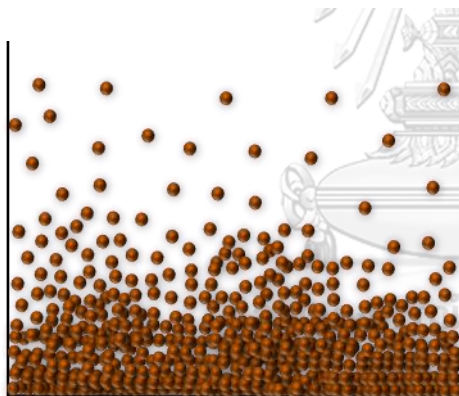
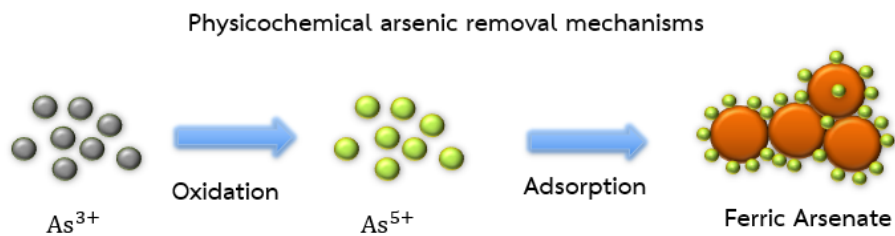
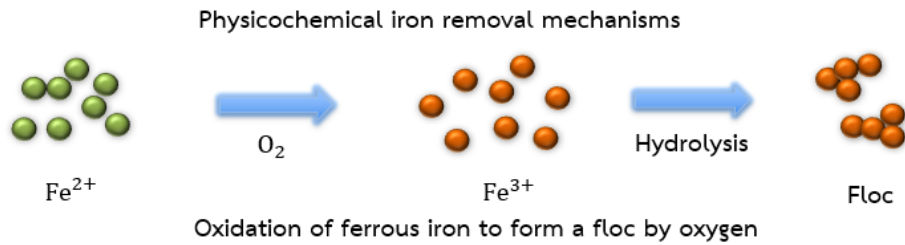


Figure 4.30 Performance of adding solid media to increase oxygen mass transfer in BCR

According to the results of this study, this process is applicable to apply in Cambodia to treat arsenic in groundwater because it has found that all most experiment condition resulted in the arsenic removal efficiency below 50 ppb, which is Cambodia drinking water quality standard (Ha et al., 2015), excepts some experiment condition without the presence of ferrous iron. However, this process is recommended to work in real groundwater under the presence of ferrous iron and arsenic together, and pH condition could be ranged in 5-8 (better performance at 8).

Lastly, the mechanism of arsenic and iron removal from groundwater could be understood by co-precipitation and adsorption process as indicated in diagram below. Ferrous iron was oxidized by oxygen to form ferric species and started to co-precipitated. Arsenate (As^{5+}) species, is oxidizing form of arsenite (As^{3+}), could be adsorbed on ferric precipitated particles to form ferric arsenate, and removed by

separation process as sludge. In separation process, large particles are fouled down by gravity force. Finally, remaining particles could be completely removed by membrane filtration process.



Sedimentation mechanism



Membrane fouling mechanism

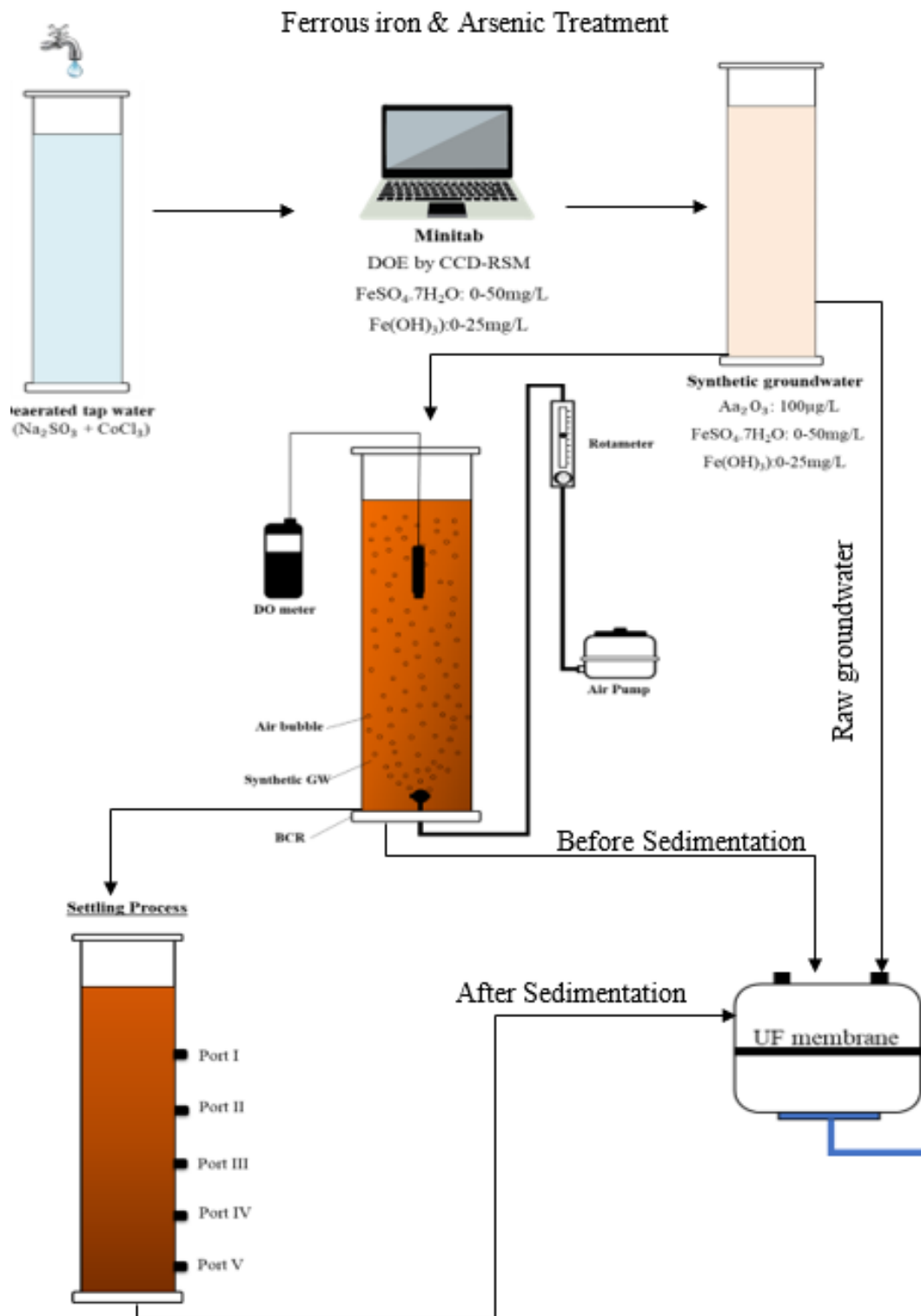


Figure 4.31 Performance of combination process of aeration process, sedimentation process and membrane filtration process

CHAPTER 5

CONCLUSION AND RECOMMENDATION

5.1 Conclusion

This study aimed to treat contaminated groundwater with arsenic and ferrous iron pollutants to obtain the drinking water quality following the regulation/recommendation from WHO by co-precipitation process and membrane separation process. Therefore, the result was concluded to four objectives as follows:

- (1) To investigate the relative effect of different solid media types on oxygen mass transfer and bubble hydrodynamic characteristic, and its physical mechanism:

Four type of solid media was studied in this research including scouring sponge, scouring pad, activated carbon foam and plastic ring. Adding solid media could enhance the oxygen mass transfer coefficient in BCR around 9% – 80% compared to without solid media adding due to its effect on bubble increasing velocity more than bubble break-up. The scouring sponge could provide the highest enhancement of K_{La} because of the effect of reducing bubble rising velocity, resulting in increased bubble retention time, not bubble break-up rate. The optimum condition of applying the scouring sponge is 3% loading with $V_g 0.7 \times 10^{-2}$ m/s.

Overall, this part concludes that a scouring sponge is recommended as the most effective solid media for improving oxygen mass transfer by enhancing bubble retention time in BCR.

- (2) To investigate the effect of the initial concentration of ferrous iron, ferric iron addition, pH, and gas flow rate (Q_g) on ferrous iron-oxidizing:

The Central Composite Design of Response Surface Methodology (CCD-RSM) was used to fine the optimization process of ferrous oxidation removal. The results found that ferrous oxidation removal efficiency could be obtained higher than 80% under optimal condition, i.e., initial pH value ≥ 6.5 , ferrous initial concentration ≤ 25 mg/L, adding ferric hydroxide < 10 mg/L, gas flow rate 12 LPM, and operation time 25 minutes. Among of five influent factor, initial pH and ferrous initial concentration

was defined as the most effective parameter to get high removal efficiency of ferrous iron in groundwater.

(3) To study the impact of the initial concentration of ferrous iron, ferric iron, and pH on arsenic treatment in the bubble column reactor (BCR):

The Central Composite Design of Response Surface Methodology (CCD-RSM) was also applied to fine the optimization process of arsenic removal in groundwater. Optimum condition for arsenic removal with ferrous iron was defined, i.e., initial pH 8, initial concentration of ferrous iron ≈ 36.85 mg/L, iron hydroxide 25 mg/L, gas flow rate 8 L/min, and operating time ≈ 33.28 minutes. Under the optimum conditions for arsenic removal, it can be observed that the total arsenic could be removed to lower than 10 $\mu\text{g/L}$ within > 30 minutes treatment with a recommended ratio, $[\text{As(III)}]_0:[\text{Fe}]_0 < 1:500$ and $[\text{As(III)}]_0:[\text{Fe(OH)}_3]_0 \geq 1:200$.

(4) To perform the separation process by combination of sedimentation and membrane filtration to remove suspended solid particles from the co-precipitation process:

- Sedimentation process was operated to remove suspended solid of ferric iron particles product by ferrous iron oxidation. However, after settling, the turbidity is remaining more than 60 NTU even though five hours was experimented.
- Scouring sponge 3% and 5% loading can obtained only 1% and 5% of turbidity removal, respectively. However, scouring sponge 10% loading provided 15% of turbidity removal from groundwater. This means adding high scouring sponge loading could provide higher removal of turbidity.
- Turbidity was completely removed from solution by ultra-filtration membrane, and the sedimentation process before membrane filtration was found the effect of decrease membrane fouling.

5.2 Recommendation

Overall, the current study suggests that adding scouring sponge in ferrous iron and arsenic treatment system could be beneficial in term of enhancement oxygen mass transfer and turbidity removal in bubble column reactor without extra charge on

electricity. Furthermore, membrane filtration followed by sedimentation process could have an advantage in reducing membrane fouling.

However, there are some recommendations for future studies as the following:

- For solid media addition, the bubble hydrodynamic characteristic should be studied in term of all solid media loading range (3%, 5% and 10%)
- The optimal condition for ferrous and arsenic removal should be tested in the actual groundwater which contaminates with other pollutants
- The combination of all process should be experimented including applying scouring sponge in real treatment system.

For further research, co-precipitate particles should be recommended to analyze by XRD or SEM in order to understand arsenic species that adsorbed on ferric iron particles and chemical form of precipitated particles. Furthermore, the minimal risk level (MRLs) is recommended for inorganic arsenic acute disease is 0.005 mg As/Kg/day in period of 14 days or less, and for chronic disease is 0.0003 mg As/Kg/day in period of 365 days or more (C.-H. Chou and Harper, 2007), and iron is 0.3mg/L.

REFERENCES

- Abufalgha, A. A., Pott, R. W., Cloete, J. C., Clarke, K. G. J. J. o. C. T., and Biotechnology. Gas-Liquid Interfacial Area and its Influence on Oxygen Transfer Coefficients in a Simulated Hydrocarbon Bioprocess in a Bubble Column Reactor. (2020).
- Appelo, C., Drijver, B., Hekkenberg, R., and De Jonge, M. J. G. Modeling in situ iron removal from ground water. *37(6)* (1999): 811-817.
- Baker, R. W. Membrane technology and applications. John Wiley & Sons, 2012.
- Banisi, S., Finch, J., Laplante, A., and Weber, M. J. C. E. S. Effect of solid particles on gas holdup in flotation columns—I. Measurement. *50(14)* (1995): 2329-2334.
- Bennett, H., et al. Characterisation of the water quality from open and rope-pump shallow wells in rural Cambodia. *61(2)* (2010): 473-479.
- Berg, M., et al. Magnitude of arsenic pollution in the Mekong and Red River Deltas — Cambodia and Vietnam. Science of The Total Environment *372(2)* (2007): 413-425. doi: <https://doi.org/10.1016/j.scitotenv.2006.09.010>.
- Brite, S. (2021). Float Test. Scotch-Brite Brand.
- Bun, S. Development of novel Bubble Column Reactor (BCR) for iron removal in groundwater. Chulalongkorn University. 2015.
- Bun, S., et al. Experimental and empirical investigation of mass transfer enhancement in multi-scale modified airlift reactors. (2019): 1-13.
- Buschmann, J., et al. Contamination of drinking water resources in the Mekong delta floodplains: Arsenic and other trace metals pose serious health risks to population. Environment International *34(6)* (2008): 756-764. doi: <https://doi.org/10.1016/j.envint.2007.12.025>.
- CDIC. Groundwater Arsenic in Cambodia. Resource Development International Cambodia (2012).
- Chaturvedi, S., and Dave, P. N. Removal of iron for safe drinking water. Desalination *303* (2012): 1-11. doi: <https://doi.org/10.1016/j.desal.2012.07.003>.
- Chaturvedi, S., and Dave, P. N. J. D. Removal of iron for safe drinking water. *303* (2012): 1-11.
- Chen, J. P., Kim, S., and Ting, Y. J. J. o. m. S. Optimization of membrane physical and chemical cleaning by a statistically designed approach. *219(1-2)* (2003): 27-45.
- Cho, K. H., Sthiannopkao, S., Pachepsky, Y. A., Kim, K.-W., and Kim, J. H. Prediction of contamination potential of groundwater arsenic in Cambodia, Laos, and Thailand using artificial neural network. Water Research *45(17)* (2011): 5535-5544. doi: <https://doi.org/10.1016/j.watres.2011.08.010>.

- Chou, C.-H., and Harper, C. Toxicological profile for arsenic. (2007).
- Chou, C.-H. S. J., Holler, J., and De Rosa, C. T. J. J. C. T. E. T. O. M. Minimal risk levels (MRLs) for hazardous substances. 7(1) (1998): 1-24.
- Chua, H., Arnot, T., and Howell, J. J. D. Controlling fouling in membrane bioreactors operated with a variable throughput. 149(1-3) (2002): 225-229.
- Crittenden, J. C., Trussell, R. R., Hand, D. W., Howe, K. J., and Tchobanoglous, G. MWH's water treatment: principles and design. John Wiley & Sons, 2012.
- Cundy, A. B., Hopkinson, L., and Whitby, R. L. D. Use of iron-based technologies in contaminated land and groundwater remediation: A review. Science of The Total Environment 400(1) (2008): 42-51. doi: <https://doi.org/10.1016/j.scitotenv.2008.07.002>.
- Dangar, S., Asoka, A., and Mishra, V. Causes and implications of groundwater depletion in India: A review. Journal of Hydrology (2021): 126103. doi: <https://doi.org/10.1016/j.jhydrol.2021.126103>.
- Ding, W., et al. Co-oxidation of As(III) and Fe(II) by oxygen through complexation between As(III) and Fe(II)/Fe(III) species. Water Research 143 (2018): 599-607. doi: <https://doi.org/10.1016/j.watres.2018.06.072>.
- Du, X., et al. Removal of manganese, ferrous and antibiotics from groundwater simultaneously using peroxydisulfate-assisted in-situ oxidation/coagulation integrated with ceramic membrane process. Separation and Purification Technology 252 (2020): 117492. doi: <https://doi.org/10.1016/j.seppur.2020.117492>.
- Edzwald, J., and Association, A. W. W. Water quality & treatment: a handbook on drinking water. McGraw-Hill Education, 2011.
- El Azher, N., Gourich, B., Vial, C., Soulam, M. B., and Ziyad, M. Study of ferrous iron oxidation in Morocco drinking water in an airlift reactor. Chemical Engineering and Processing: Process Intensification 47(9) (2008): 1877-1886. doi: <https://doi.org/10.1016/j.cep.2007.10.013>.
- Ellis, D., Bouchard, C., and Lantagne, G. Removal of iron and manganese from groundwater by oxidation and microfiltration. Desalination 130(3) (2000): 255-264. doi: [https://doi.org/10.1016/S0011-9164\(00\)00090-4](https://doi.org/10.1016/S0011-9164(00)00090-4).
- Ferreira, A., Ferreira, C., Teixeira, J. A., and Rocha, F. Temperature and solid properties effects on gas-liquid mass transfer. Chemical Engineering Journal 162(2) (2010): 743-752. doi: <https://doi.org/10.1016/j.cej.2010.05.064>.
- Garcia-Ochoa, F., and Gomez, E. J. B. a. Bioreactor scale-up and oxygen transfer rate in microbial processes: an overview. 27(2) (2009): 153-176.
- Guerra, K., Pellegrino, J., and Drewes, J. E. Impact of operating conditions on permeate flux and process economics for cross flow ceramic membrane ultrafiltration of surface water. Separation and Purification Technology 87 (2012): 47-53. doi: <https://doi.org/10.1016/j.seppur.2011.11.019>.
- Guppy, L., and Shantz, A. J. G. R. Groundwater quality in rural Cambodia: Measures

- and perceptions. 49(4) (2011): 384-394.
- Ha, K., Ngoc, N. T. M., Lee, E., and Jayakumar, R. Current status and issues of groundwater in the Mekong River basin. Korea Institute of Geoscience and Mineral Resources (KIGAM), 2015.
- Haldar, D., Duarah, P., and Purkait, M. K. MOFs for the treatment of arsenic, fluoride and iron contaminated drinking water: A review. Chemosphere 251 (2020): 126388. doi: <https://doi.org/10.1016/j.chemosphere.2020.126388>.
- He, Z., Petiraksakul, A., and Meesapya, W. J. J. K. Oxygen-transfer measurement in clean water. 13(1) (2003): 14-19.
- Hug, S. J., Leupin, O. J. E. s., and technology. Iron-catalyzed oxidation of arsenic (III) by oxygen and by hydrogen peroxide: pH-dependent formation of oxidants in the Fenton reaction. 37(12) (2003): 2734-2742.
- IWMI. Groundwater for Irrigation in Cambodia. (#3) (2013). doi: http://www.iwmi.cgiar.org/Publications/issue_briefs/cambodia/issue_brief_03-groundwater_for_irrigation_in_cambodia.pdf.
- Karakochuk, C. D., et al. Elevated levels of iron in groundwater in Prey Veng province in Cambodia: a possible factor contributing to high iron stores in women. 13(2) (2015): 575-586.
- Kawamura, S. Integrated design and operation of water treatment facilities. John Wiley & Sons, 2000.
- Khatri, N., Tyagi, S., and Rawtani, D. Recent strategies for the removal of iron from water: A review. Journal of Water Process Engineering 19 (2017): 291-304. doi: <https://doi.org/10.1016/j.jwpe.2017.08.015>.
- Kim, J. O., and Kim, S. D. J. T. C. J. o. C. E. Gas-Liquid mass transfer in a three-phase fluidized bed with floating bubble breakers. 68(3) (1990): 368-375.
- Kratochvil, M. J., Manna, U., and Lynn, D. M. J. J. o. P. S. P. A. P. C. Superhydrophobic polymer multilayers for the filtration-and absorption-based separation of oil/water mixtures. 55(18) (2017): 3127-3136.
- Lazic, Z. R. Design of experiments in chemical engineering: a practical guide. John Wiley & Sons, 2006.
- Le-Clech, P., Chen, V., and Fane, T. A. J. J. o. m. s. Fouling in membrane bioreactors used in wastewater treatment. 284(1-2) (2006): 17-53.
- Lenntech, W. J. L. W. T., and htm, P. H. B. w. l. c. p. e. c. Chemical properties, health and environmental effects of copper. (2009).
- Luong, V. T., et al. Iron-based subsurface arsenic removal technologies by aeration: A review of the current state and future prospects. Water Research 133 (2018): 110-122. doi: <https://doi.org/10.1016/j.watres.2018.01.007>.
- Luu, T. T. G., Sthiannopkao, S., and Kim, K.-W. J. E. I. Arsenic and other trace elements contamination in groundwater and a risk assessment study for the residents in the Kandal Province of Cambodia. 35(3) (2009): 455-460.

- Ma, Z., Shu, G., and Lu, X. Preparation of an antifouling and easy cleaning membrane based on amphiphobic fluorine island structure and chemical cleaning responsiveness. Journal of Membrane Science 611 (2020): 118403. doi: <https://doi.org/10.1016/j.memsci.2020.118403>.
- Maddah, H. A., et al. Determination of the treatment efficiency of different commercial membrane modules for the treatment of groundwater. 8(6) (2017): 2006-2012.
- Magara, Y., Kunikane, S., and Itoh, M. Advanced membrane technology for application to water treatment. Water Science and Technology 37(10) (1998): 91-99. doi: [https://doi.org/10.1016/S0273-1223\(98\)00307-2](https://doi.org/10.1016/S0273-1223(98)00307-2).
- Margat, J., and Van der Gun, J. Groundwater around the world: a geographic synopsis. Crc Press, 2013.
- Marsidi, N., Abu Hasan, H., and Sheikh Abdullah, S. R. A review of biological aerated filters for iron and manganese ions removal in water treatment. Journal of Water Process Engineering 23 (2018): 1-12. doi: <https://doi.org/10.1016/j.jwpe.2018.01.010>.
- Metcalf, E., and Eddy, E. J. I., New York. Wastewater engineering: treatment and reuse, McGrawHill. (2003).
- Mo/MAE. Drinking Water Quality Standards. Ministry of Industry Mines and Energy, Cambodia (2004).
- Montgomery, D. C. Design and analysis of experiments. John wiley & sons, 2017.
- Mueller, B. J. J. C. A. First step concerning improvement of arsenic removal by adapted Kanchan filters in the lowlands of Nepal. 2 (2020): 1-9.
- Ngai, T., et al. Kanchan arsenic filter. 66 (2006).
- Ngai, T. K., et al. Design for sustainable development—Household drinking water filter for arsenic and pathogen treatment in Nepal. 42(12) (2007): 1879-1888.
- Nguyen, V. T., Vigneswaran, S., Ngo, H. H., Shon, H. K., and Kandasamy, J. Arsenic removal by a membrane hybrid filtration system. Desalination 236(1) (2009): 363-369. doi: <https://doi.org/10.1016/j.desal.2007.10.088>.
- Nidheesh, P. V., and Singh, T. S. A. Arsenic removal by electrocoagulation process: Recent trends and removal mechanism. Chemosphere 181 (2017): 418-432. doi: <https://doi.org/10.1016/j.chemosphere.2017.04.082>.
- Nielsen, E., and Larsen, J. C. Arsenic, inorganic and soluble salts. (2014).
- Nur, T., et al. Removing arsenic from water by coprecipitation with iron: Effect of arsenic and iron concentrations and adsorbent incorporation. Chemosphere 226 (2019): 431-438. doi: <https://doi.org/10.1016/j.chemosphere.2019.03.142>.
- Oberli, L., et al. Condensation and freezing of droplets on superhydrophobic surfaces. Advances in Colloid and Interface Science 210 (2014): 47-57. doi: <https://doi.org/10.1016/j.cis.2013.10.018>.
- ODC. OpenDevelopment Cambodia: Groundwater. (2016). doi: <https://opendevlopmentcambodia.net/topics/groundwater/>.

- Painmanakul, P., Loubiere, K., Hebrard, G., Buffière, P. J. C. E., and Intensification, P. P. Study of different membrane spargers used in waste water treatment: characterisation and performance. *43(11)* (2004): 1347-1359.
- Pangarkar, B. L., Sane, M. G., and Guddad, M. J. I. S. R. N. Reverse osmosis and membrane distillation for desalination of groundwater: a review. 2011 (2011).
- Pierce, M. L., and Moore, C. B. J. W. R. Adsorption of arsenite and arsenate on amorphous iron hydroxide. *16(7)* (1982): 1247-1253.
- Psoch, C., and Schiewer, S. Direct filtration of natural and simulated river water with air sparging and sponge ball application for fouling control. *Desalination* *197(1)* (2006): 190-204. doi: <https://doi.org/10.1016/j.desal.2005.11.027>.
- Rahmanian, N., et al. Analysis of Physiochemical Parameters to Evaluate the Drinking Water Quality in the State of Perak, Malaysia. *Journal of Chemistry* *2015* (2015): 716125. doi: [10.1155/2015/716125](https://doi.org/10.1155/2015/716125).
- Ratha, P., Nandalal, K., Pitawala, H., Dharmagunawardhane, H., and Weerakoon, S. Arsenic Contamination in Cambodia: A Status Review. (2017).
- RDI. Summary of Groundwater Data. *Resource Development International* (2008). doi: <http://rdic.org/groundwater-summary-data/>.
- Reynolds, T. D., and Richards, P. A. C. *Unit operations and processes in environmental engineering*. PWS Publishing Company, 1995.
- Sampson, M. L., Bostick, B., Chiew, H., Hagan, J. M., and Shantz, A. Arsenicosis in Cambodia: Case studies and policy response. *Applied Geochemistry* *23(11)* (2008): 2977-2986. doi: <https://doi.org/10.1016/j.apgeochem.2008.06.022>.
- Sastaravet, P., et al. Relative Effect of Additional Solid Media on Bubble Hydrodynamics in Bubble Column and Airlift Reactors towards Mass Transfer Enhancement. *8(6)* (2020): 713.
- Sen, M., Manna, A., and Pal, P. Removal of arsenic from contaminated groundwater by membrane-integrated hybrid treatment system. *Journal of Membrane Science* *354(1)* (2010): 108-113. doi: <https://doi.org/10.1016/j.memsci.2010.02.063>.
- Shaji, E., et al. Arsenic contamination of groundwater: A global synopsis with focus on the Indian Peninsula. *Geoscience Frontiers* *12(3)* (2021): 101079. doi: <https://doi.org/10.1016/j.gsf.2020.08.015>.
- Shankar, S., and Shanker, U. J. T. s. w. j. Arsenic contamination of groundwater: a review of sources, prevalence, health risks, and strategies for mitigation. 2014 (2014).
- Sharma, S. K., Petrusevski, B., Schippers, J. C. J. J. o. W. S. R., and Technology—AQUA. Biological iron removal from groundwater: a review. *54(4)* (2005): 239-247.
- Shi, Q., et al. Formation of Fe (iii)–As (v) complexes: effect on the solubility of ferric hydroxide precipitates and molecular structural identification. *7(5)* (2020): 1388-1398.

- Shi, X., Tal, G., Hankins, N. P., and Gitis, V. Fouling and cleaning of ultrafiltration membranes: A review. Journal of Water Process Engineering 1 (2014): 121-138. doi: <https://doi.org/10.1016/j.jwpe.2014.04.003>.
- Smedley, P. L., and Kinniburgh, D. G. J. A. g. A review of the source, behaviour and distribution of arsenic in natural waters. 17(5) (2002): 517-568.
- Sophally, S. J. K. I. f. G. E. S. Groundwater resources in Cambodia. (2011).
- Stenstrom, M. K., Leu, S.-Y. B., and Jiang, P. J. P. o. t. W. E. F. Theory to practice: Oxygen transfer and the new ASCE standard. 2006(7) (2006): 4838-4852.
- Sthiannopkao, S., et al. Arsenic levels in human hair, Kandal Province, Cambodia: The influences of groundwater arsenic, consumption period, age and gender. Applied Geochemistry 25(1) (2010): 81-90. doi: <https://doi.org/10.1016/j.apgeochem.2009.10.003>.
- Tang, X., et al. Can ultrafiltration singly treat the iron- and manganese-containing groundwater? Journal of Hazardous Materials 409 (2021): 124983. doi: <https://doi.org/10.1016/j.jhazmat.2020.124983>.
- Timalsina, H., Mainali, B., Angove, M. J., Komai, T., and Paudel, S. R. Potential modification of groundwater arsenic removal filter commonly used in Nepal: A review. Groundwater for Sustainable Development 12 (2021): 100549. doi: <https://doi.org/10.1016/j.gsd.2021.100549>.
- Tweed, S., et al. Seasonal influences on groundwater arsenic concentrations in the irrigated region of the Cambodian Mekong Delta. Science of The Total Environment 728 (2020): 138598. doi: <https://doi.org/10.1016/j.scitotenv.2020.138598>.
- van der Gun, J. Chapter 24 - Groundwater resources sustainability. In A. Mukherjee, B. R. Scanlon, A. Aureli, S. Langan, H. Guo & A. A. McKenzie (Eds.), Global Groundwater (pp. 331-345): Elsevier. 2021.
- Vang, S., et al. Identification of irrigation by pumping groundwater in Cambodia. (2009).
- Verberk, J., Van Dijk, H. J. W. S., and Supply, T. W. Research on AirFlush®: distribution of water and air in tubular and capillary membrane modules. 3(5-6) (2003): 409-414.
- Wang, G., et al. Three-dimensional structured sponge with high oil wettability for the clean-up of oil contaminations and separation of oil–water mixtures. 5(20) (2014): 5942-5948.
- WHO. Guidelines for drinking-water quality: second addendum. Vol. 1, Recommendations. (2008).
- Wongwailikhit, K., et al. Gas Sparger orifice sizes and solid particle characteristics in a bubble column–relative effect on hydrodynamics and mass transfer. 41(3) (2018): 461-468.
- Xiu, W., et al. Arsenic removal and transformation by *Pseudomonas* sp. strain GE-1-induced ferrihydrite: co-precipitation versus adsorption. 226(6) (2015): 1-14.

- YANN, T., MIYANAGA, K., and TAN, R. The Effectiveness of Different Types of Polyaluminum Chloride (PAC) and Aluminum Sulfate (alum) with Ca (OCl) 2 Dosing for Treatment of Surface Water of Tonle Sap River. (2020).
- Zainab, S. M., Junaid, M., Xu, N., and Malik, R. N. Antibiotics and antibiotic resistant genes (ARGs) in groundwater: A global review on dissemination, sources, interactions, environmental and human health risks. Water Research 187 (2020): 116455. doi: <https://doi.org/10.1016/j.watres.2020.116455>.
- Zheng, Z., Chen, Y., Zhan, X., Gao, M., and Wang, Z. Mass transfer intensification in a novel airlift reactor assembly with helical sieve plates. Chemical Engineering Journal 342 (2018): 61-70. doi: <https://doi.org/10.1016/j.cej.2018.01.039>.



APPENDIXES

Appendix 1: Summary of all methods (S. Chaturvedi and P. N. Dave, 2012)

Method	Removal efficiency (%)	Operating condition	Advantage	Disadvantage	Cost	Uses
EC	95–99	Current density 0.01 to 0.04 A/m ² pH should be slightly basic approx 7.5 EC found to be very fast and effective method for the water containing iron from low to very high concentrations.	EC requires simple equipment and is easy to operate with sufficient operational latitude to handle most problems encountered on running. Wastewater treated by EC gives palatable, clear, colorless and odorless water. EC technique can be conveniently used in rural areas where electricity is not available, since a solar panel attached to the unit may be sufficient to carry out the process	The sacrificial electrodes are dissolved into wastewater streams as a result of oxidation, and need to be regularly replaced.	Approx. 6.05 US\$/m ³	adaptable for household use
Oxidation/ filtration method	80–90	pH should be in range of 7.5 to 8.5. Quality of water that used	The majority of iron treatment systems employ the processes of oxidation/ filtration. The oxidant chemically oxidizes the iron (forming a particle), and kills iron bacteria and any other diseasecausing bacteria that may be present. A low-cost method of providing oxidation is to use the oxygen in air as the oxidizing agent.	The oxidant is difficult to store or transport safely and system parts can be degraded by corrosion. The oxidation reaction results in a solid manganese compound that may interfere with system operation.	Approx. 4.05 US\$/m ³	In rural areas
IE	~90	Effective for water containing less than 25 mg/L of dissolved Fe/ Mn	Can remove iron that bound with organics. Softener resin can be rejuvenated and reused. Water quality such as pH or alkalinity are not important in the operation of IE	Used only for small quantities of iron and manganese because there is a risk of rapid clogging if any oxidation occurs during the process, the resulting precipitate can coat and foul	\$0.05 to \$0.20 per barrel	Use for ground and surface water Adaptable where use of water is minimum

				the media. Cleaning would then be required using acid or sodium bisulfate		
Adsorption	84-92	Operated under anoxic condition suppressing the oxidation of ferrous iron and iron is removed by adsorptive filtration	Longer filtration runs due to slower head loss development. Better filtrate quality. Shorter ripening time and less backwash water requirement.	Ferrous ion adsorbed at filter media which is cleaned by oxygen-rich water or by oxidant.	Low cost	Useful for surface water like well
Activated carbon and other filtration materials	75-90	Chemical nature of the carbon source, or the amount of oxygen and hydrogen associated with it. Chemical composition and concentration of the contaminant	Its multifunctional nature and the fact that it adds nothing detrimental to treat water. Some filtration materials not required any chemicals	cannot significantly reduce bacterial contamination	Low cost	Used in municipal region
Subsurface iron removal	>50	Periodically injection of aerated water is required.	No costly filter media and maintenance is needed. The tube well is the 1st preferred option for drinking water in rural areas; and available to a majority of the rural poor in their household; Additional hardware beyond the existing hand pump is affordable and locally available/repairable.	Low removal efficiency.	Low cost	Provide safe drinking water in rural areas.
Aerated granular filter	70	pH 7.5-8.0 Temperature of water in between 15-30 °C	It is a catalytic reaction rather than biological. Filtration rate is fast.	Back washing required. Process effective at low temperature.	Higher than biological process.	Can use at laboratory scale
UF/MF	80-90	Low pressure or vacuum membrane filtration processes	Can control small pathogenic microorganisms such as viruses. No need for chemicals. Size-exclusion filtration as opposed to media depth filtration.	UF alone, however, is still unable to fully eliminate dissolved inorganic constituents such as iron and manganese that can deteriorate the	As advancements are made in membrane production and module design, capital	Adaptable for household use

				quality of water with respect to taste and color.	and operating costs continue to decline	
Bioremediation	70	Anaerobic condition is more suitable	Addition of matched microbe strains to the medium to enhance the resident microbe population's ability to break down contaminants. No need of chemicals.	Heavy metals such as cadmium and lead are not readily absorbed or captured by microorganisms	Low cost	Use for ground water treatment.
Supercritical fluid extraction	~80	Increased contact between the chelating agent and metal ions increased extraction efficiency of Fe	Increased contact between the chelating agent and metal ions increases the rate of metal chelate formation and is the principal factor in increased extraction efficiency. Heavy metal can also be removed.	Limited by the complexity of the process and the cost of ligands suitable for effective metal extraction	High cost	Remove metals from sludge to levels suitable for land application.

Appendix 2: Dissolved-oxygen concentration in water as a function of temperature and barometric pressure

(salinity = 0 part per thousand (ppt)) (Metcalf and Eddy, 2003)

Temp (°C)	Dissolved-oxygen concentration, mg/L									
	Barometric pressure, millimeters of mercury									
	735	740	745	745	745	745	745	770	775	780
10	10.90	10.98	11.05	11.13	11.20	11.28	11.35	11.43	11.50	11.58
11	10.65	10.72	10.80	10.87	10.94	11.02	11.09	11.16	11.24	11.31
12	10.41	10.48	10.55	10.62	10.69	10.77	10.84	10.91	10.98	11.05
13	10.17	10.24	10.31	10.38	10.46	10.53	10.60	10.67	10.74	10.81
14	9.95	10.02	10.09	10.16	10.23	10.29	10.36	10.43	10.50	10.57
15	9.73	9.80	9.87	9.94	10.00	10.07	10.14	10.21	10.27	10.34
16	9.53	9.59	9.66	9.73	9.79	9.86	9.92	9.99	10.06	10.12
17	9.33	9.39	9.46	9.52	9.59	9.65	9.72	9.78	9.85	9.91
18	9.14	9.20	9.26	9.33	9.39	9.45	9.52	9.58	9.64	9.71
19	8.95	9.01	9.07	9.14	9.20	9.26	9.32	9.39	9.45	9.51
20	8.77	8.83	8.89	8.95	9.02	9.08	9.14	9.20	9.26	9.32
21	8.60	8.66	8.72	8.78	8.84	8.90	8.89	9.02	9.08	9.14
22	8.63	8.49	8.55	8.61	8.67	8.73	8.79	8.84	8.90	8.96
23	8.27	8.33	8.39	8.44	8.50	8.56	8.62	8.68	8.73	8.79
24	8.11	8.17	8.23	8.29	8.34	8.40	8.46	8.51	8.57	8.63
25	7.96	8.02	8.08	8.13	8.19	8.24	8.30	8.36	8.41	8.47
26	7.82	7.87	7.93	7.98	8.04	8.09	8.15	8.20	8.26	8.31
27	7.68	7.73	7.79	7.84	7.89	7.95	8.00	8.06	8.11	8.17
28	7.54	7.59	7.65	7.70	7.75	7.81	7.86	7.91	7.97	8.02
29	7.41	7.46	7.51	7.57	7.62	7.67	7.72	7.78	7.83	7.88
30	7.28	7.33	7.38	7.44	7.49	7.54	7.59	7.64	7.69	7.75

Appendix 3: Detail Experimental Design and Result of Factorial Trial Ferrous Analysis

StdOrder	RunOrder	PtType	Blocks	Qg	pH	[Fe ²⁺]	[Fe ³⁺]	Time	%Removal
5	1	1	1	8	5.0	50.0	0.0	5	86.96
7	2	1	1	8	8.0	50.0	0.0	25	85.75
32	3	0	1	12	6.5	27.5	12.5	15	79.41
24	4	-1	1	12	6.5	27.5	25.0	15	72.86
21	5	-1	1	12	6.5	5.0	12.5	15	97.56
23	6	-1	1	12	6.5	27.5	0.0	15	89.87
13	7	1	1	8	5.0	50.0	25.0	25	53.40
19	8	-1	1	12	5.0	27.5	12.5	15	54.90
14	9	1	1	16	5.0	50.0	25.0	5	53.65
22	10	-1	1	12	6.5	50.0	12.5	15	70.51
17	11	-1	1	8	6.5	27.5	12.5	15	67.41
2	12	1	1	16	5.0	5.0	0.0	5	61.19
18	13	-1	1	16	6.5	27.5	12.5	15	71.85
31	14	0	1	12	6.5	27.5	12.5	15	69.44
20	15	-1	1	12	8.0	27.5	12.5	15	94.17
16	16	1	1	16	8.0	50.0	25.0	25	89.83
12	17	1	1	16	8.0	5.0	25.0	5	99.59
6	18	1	1	16	5.0	50.0	0.0	25	55.13
9	19	1	1	8	5.0	5.0	25.0	5	79.73
15	20	1	1	8	8.0	50.0	25.0	5	67.97
10	21	1	1	16	5.0	5.0	25.0	25	74.33
26	22	-1	1	12	6.5	27.5	12.5	25	93.85
1	23	1	1	8	5.0	5.0	0.0	25	76.78
28	24	0	1	12	6.5	27.5	12.5	15	84.93
27	25	0	1	12	6.5	27.5	12.5	15	81.80
29	26	0	1	12	6.5	27.5	12.5	15	82.30

3	27	1	1	8	8.0	5.0	0.0	5	99.59
4	28	1	1	16	8.0	5.0	0.0	25	99.49
8	29	1	1	16	8.0	50.0	0.0	5	73.47
30	30	0	1	12	6.5	27.5	12.5	15	79.63
25	31	-1	1	12	6.5	27.5	12.5	5	68.98
11	32	1	1	8	8.0	5.0	25.0	25	99.59



Appendix 4: Detail Experimental Design and Result of Factorial Trial Arsenic Co-presence with Ferrous Iron Analysis

Std Order	Run Order	PtType	Blocks	pH	[Fe ²⁺]	[Fe ³⁺]	Qg	Time	% R (Fe ²⁺)	% R (As)
15	1	1	1	5.0	50	25.0	16	5.0	52	55
12	2	1	1	8.0	50	0.0	16	5.0	75	88
32	3	0	1	6.5	25	12.5	12	22.5	63	66
10	5	1	1	8.0	0	0.0	16	40.0	0	29
28	6	0	1	6.5	25	12.5	12	22.5	63	56
14	7	1	1	8.0	0	25.0	16	5.0	0	85
26	8	-1	1	6.5	25	12.5	12	40.0	70	84
8	9	1	1	8.0	50	25.0	8	5.0	73	85
7	10	1	1	5.0	50	25.0	8	40.0	98	97
5	11	1	1	5.0	0	25.0	8	5.0	0	52
3	12	1	1	5.0	50	0.0	8	5.0	57	81
17	13	-1	1	5.0	25	12.5	12	22.5	66	91
1	14	1	1	5.0	0	0.0	8	40.0	0	56
16	15	1	1	8.0	50	25.0	16	40.0	90	95
24	16	-1	1	6.5	25	12.5	16	22.5	80	87
6	17	1	1	8.0	0	25.0	8	40.0	0	76
23	18	-1	1	6.5	25	12.5	8	22.5	87	90
27	19	0	1	6.5	25	12.5	12	22.5	90	91
21	20	-1	1	6.5	25	0.0	12	22.5	78	84
9	21	1	1	5.0	0	0.0	16	5.0	0	49
11	22	1	1	5.0	50	0.0	16	40.0	58	91
13	23	1	1	5.0	0	25.0	16	40.0	0	60
25	24	-1	1	6.5	25	12.5	12	5.0	66	66
2	25	1	1	8.0	0	0.0	8	5.0	0	54

4	26	1	1	8.0	50	0.0	8	40.0	87	93
20	27	-1	1	6.5	50	12.5	12	22.5	62	75
31	28	0	1	6.5	25	12.5	12	22.5	67	75
22	29	-1	1	6.5	25	25.0	12	22.5	69	77
19	30	-1	1	6.5	0	12.5	12	22.5	0	61
18	31	-1	1	8.0	25	12.5	12	22.5	97	93



VITA

NAME	Bonita Pen
DATE OF BIRTH	12 August 1996
PLACE OF BIRTH	Cambodia
INSTITUTIONS ATTENDED	Chulalongkorn University
HOME ADDRESS	#488 Ratchathewi apartment, Room 307, soi 18 Phetchaburi, Thanon Phetchaburi, Ratchathewi amphur, Bangkok 10400



จุฬาลงกรณ์มหาวิทยาลัย
CHULALONGKORN UNIVERSITY